Non-Iterative Data-Driven Model Reference Control

THÈSE N^{O} 4658 (2010)

PRÉSENTÉE LE 9 AVRIL 2010

À LA FACULTÉ SCIENCES ET TECHNIQUES DE L'INGÉNIEUR

LABORATOIRE D'AUTOMATIQUE

PROGRAMME DOCTORAL EN INFORMATIQUE, COMMUNICATIONS ET INFORMATION

ÉCOLE POLYTECHNIQUE FÉDÉRALE DE LAUSANNE

POUR L'OBTENTION DU GRADE DE DOCTEUR ÈS SCIENCES

PAR

Klaske VAN HEUSDEN

acceptée sur proposition du jury:

Prof. R. Longchamp, président du jury
Prof. D. Bonvin, Dr A. Karimi, directeurs de thèse
Prof. H. Hjalmarsson, rapporteur
Dr L. Miskovic, rapporteur
Prof. P. M. J. Van den Hof, rapporteur

ÉCOLE POLYTECHNIQUE
FÉDÉRALE DE LAUSANNE

Suisse
2010

Acknowledgements

First of all I would like to thank Dr. Alireza Karimi. This thesis is the result of many of our short, long and even longer discussions. Thank you for always being available to answer my questions, for your calmness and for your capability of putting things in perspective. Thanks also to professor Dominique Bonvin for the valuable feedback and support.

Several other people have contributed to this thesis, either directly or indirectly. Many thanks to professor Torsten Söderström, professor Maarten Steinbuch and Arjen den Hamer for their collaboration. Thanks to professor Robert Bitmead, who's remarks indirectly led to some of the results in this thesis. I would also like to thank the members of my thesis committee for their thorough reading of this thesis.

Thanks to professor Roland Longchamp, professor Dominique Bonvin and Dr. Denis Gillet for having accepted me as a PhD student in the Automatic Control laboratory. Thanks to my colleagues at the LA for contributing to the enjoyable atmosphere in the lab. Thanks to the LA secretaries and technical staff, for facilitating life in many ways. A special thanks goes to my office mates Yvan, Damien and Basile. Sorry I had to cut down on the breaks lately.

The years spent in Lausanne working on this thesis were very enjoyable, for which many of the people I got to know here are responsible. Thanks to Karin, for everything (but obviously mainly the cooking), Chloe (for the ironing), Antoine (the perfect flatmate),

Nino (no it really wasn't him), Annabelle (for the funny stories at sat), Seb, Davor, Jo, Andrea and all the others that I do not mention here for some unexplainable reason. Thanks to my friends at the ski school for the entertainment in winter and to my friends of the Kayak Club Lausanne for the distraction in summer. Thanks also to Mike and Fleur for taking the brilliant decision of moving to Geneva and to Maaike, Marije, Sarah, Imme and Maja, cause some things will never change. Last but not least, I cannot think of a better way to describe my appreciation of the support of my parents than to say: *'t kon minder*.

Abstract

In model reference control, the objective is to design a controller such that the closed-loop system resembles a reference model. In the standard model-based solution, a plant model replaces the unknown plant in the design phase. The norm of the error between the controlled plant model and the reference model is minimized. The order of the resulting controller depends on the order of the plant model. Furthermore, since the plant model is not exact, the achieved closed-loop performance is limited by the quality of the model.

In recent years, several data-driven techniques have been proposed as an alternative to this model-based approach. In these approaches, the order of the controller can be fixed. Since no model is used, the problem of undermodeling is avoided. However, closed-loop stability cannot, in general, be guaranteed. Furthermore, these techniques are sensitive to measurement noise.

This thesis treats non-iterative data-driven controller tuning. This controller tuning approach leads to an identification problem where the input is affected by noise, and not the output as in standard identification problems. A straightforward data-driven tuning scheme is proposed, and the correlation approach is used to deal with measurement noise. For linearly parameterized controllers, this leads to a convex optimization problem. The accuracy of the correlation approach is compared to that of several solutions proposed in the literature. It is shown that, if the order of the controller is fixed, both

the correlation approach and a specific errors-in-variables approach can be used.

The model reference controller-tuning problem is extended with a constraint that ensures closed-loop stability. This constraint is derived from stability conditions based on the small-gain theorem. For linearly parameterized controllers, the resulting optimization problem is convex. The proposed constraint for stability is conservative. As an alternative, a non-conservative a posteriori stability test is developed based on similar stability conditions.

The proposed methods are applied to several numerical and experimental examples.

Keywords: Data-driven controller tuning, convex optimization, closed-loop stability, bias error, variance error

Résumé

L'objectif de la commande par modèle de référence est de dimensionner un régulateur afin que le système en boucle fermée se comporte comme le modèle de référence (ou modèle de poursuite). La solution classique utilise un modèle du système pour minimiser la norme de l'erreur entre ce modèle du système en boucle fermée et le modèle de poursuite. L'ordre du régulateur dépend ainsi de l'ordre du modèle. La performance en boucle fermée est limitée par la qualité du modèle.

Plusieurs techniques pour la synthèse d'un régulateur à partir de données expérimentales ont été proposées récemment. Ces techniques offrent une alternative aux techniques basées sur un modèle. L'ordre du régulateur peut être fixé à l'avance. Puisque aucun modèle du système n'est utilisé, le problème de sous-modélisation est évité. Pourtant, la stabilité du système en boucle fermée ne peut généralement pas être garantie. De plus, ces techniques sont sensibles au bruit de mesure.

Dans cette thèse on étudie la synthèse non-itérative d'un régulateur basée sur les données. Cette approche directe mène à un problème d'identification, où contrairement aux problèmes d'identification standards, l'entrée, et non pas la sortie, est affectée par le bruit de mesure. Un schéma simple est proposé pour la synthèse des régulateurs et l'approche de corrélation est utilisés pour éliminer l'effet du bruit de mesure. Le problème d'optimisation résultant est convexe si la paramétrisation du régulateur est linéaire. La précision

de l'approche de corrélation est comparée à la précision d'autres solutions proposées dans la littérature. Si l'ordre du régulateur est fixe, l'approche de corrélation ainsi qu'une approche spécifique pour des problèmes EIV (*errors-in-variables*) peuvent être utilisés.

Afin de garantir la stabilité du système en boucle fermée, une contrainte est ajoutée au problème de la commande par modèle de référence. Le problème d'optimisation sous contrainte est convexe si la paramétrisation du régulateur est linéaire. La contrainte de stabilité est basée sur le théorème des petits gains et est par conséquent conservatrice. Une alternative consiste à vérifier la stabilité a posteriori. Un test de stabilité non-conservatrice est développé basée sur les mêmes conditions.

Les méthodes proposées sont appliquées à plusieurs exemples numériques et expérimentaux.

Mots-clés : Synthèse d'un régulateur à partir de données expérimentales, optimisation convexe, stabilité en boucle fermée, erreur de biais, erreur de variance

Contents

Notation

Abbreviations and acronyms

DFT	Discrete Fourier transform
ETFE	Empirical transfer function estimate
EIV	Errors-in-variables
FIR	Finite impulse response
FRF	Frequency response function
ICbT	Iterative Correlation-based Tuning
IFT	Iterative Feedback Tuning
IV	Instrumental variable
LMI	Linear matrix inequality
LTI	Linear time invariant
MIMO	Multi-input multi-output
ML	Maximum likelihood
MRAC	Model Reference Adaptive Control
PEM	Prediction error method
PRBS	Pseudo random binary sequence
SISO	Single-input single-output
SNR	Signal-to-noise ratio
STR	Self-Tuning Regulation
VRFT	Virtual Reference Feedback Tuning

1

Introduction

1.1 Motivation

The robot shown in Figure 1.1 is designed to perform pick-and-place tasks with high accuracy. The structure is designed such that these tasks can be performed with high velocity. This hardware is the necessary basis to achieve the performance required in modern robotics. To actually achieve the required performance, a feedback controller needs to be designed that ensures both safe operation and precision of movements with high velocity.

The control engineer has a large choice of possible control strategies to achieve the required task. He or she can decide to develop a model of the system based on the geometry of the robot and physical laws (known as first-principle modeling). This model can then be used to design a controller and to evaluate the performance specifications for the feedback loop of the controller and the model. If this design is performed carefully, the controller achieves the required performance when applied to the model. However, this does not guarantee that the controller achieves the required performance when applied to the robot. The model is necessarily a simplification of the real plant. Furthermore, variables such as the inertia of the robot arm are not known exactly. The achieved performance depends on the mismatch between the plant and the model. Besides limited performance due to limited model accuracy, first-principle modeling is in general time-consuming and therefore expensive.

Fig. 1.1. Pick-and-place robot.

The control engineer can also decide to use system identification techniques, where a mathematical model is derived from observed data from the plant. In this case, identification experiments need to be designed and performed and an appropriate model structure needs to be chosen. The collected set of data is then used to identify the parameters of this model structure and the identified model can be used to design a controller. This approach thus uses two optimizations, one in the identification step and a second one in the controller design. As for first-principle modeling, the identification step introduces in general a mismatch between the model and the plant, and the performance of the controller is limited by this mismatch.

An additional difficulty of model-based approaches is that the complexity of the resulting controller depends, in general, on the complexity of the model. The order of the controller might actually be too high to be implemented, and a controller-order reduction step might be needed before implementation.

In recent years, several data-driven techniques have been proposed as an alternative to the model-based approaches described above. In a data-driven approach, the data are used directly to minimize a control criterion. The identification and controller design steps are thus lumped together, resulting in a direct "data-to-

controller" algorithm. Compared to a model-based approach, the modeling step is omitted and the problem of undermodeling of the plant is avoided. Furthermore, since there is no intermediate model, the structure of the designed controller does not depend on the structure of this model, and the order and structure of the controller can be fixed.

Even though these data-driven techniques have been shown effective on various application examples, the control engineer is not likely to choose such a method, mainly because it cannot ensure safe operation of the robot. Since measured data are used directly to compute the controller that minimizes a control objective, no model of the plant is needed for controller design. Consequently, no model is available to verify the robustness margins either, and stability cannot be guaranteed before actual controller implementation. Another difficulty, related to the stability problem, is that without a model it is difficult to verify whether the defined control objectives are actually achievable. Furthermore, the effectiveness of data-driven approaches is strongly affected by measurement noise.

Development of a method that guarantees closed-loop stability for data-driven controller tuning is a necessary step towards a serious alternative to model-based approaches. Furthermore, solutions are needed that deal with the effect of noise. Ideally, a data-driven approach comprises a complete controller design recipe that includes experiment design and an approach to define adequate control objectives.

1.2 State of the art

This thesis studies data-driven controller tuning. Such techniques are often compared to or even opposed to model-based techniques. However, both terms are ambiguous. Many techniques can be referred to as model-based, and their characteristics differ considerably. Methods that use identification techniques to estimate a model from data, and then use this model to calculate a controller are sometimes referred to as model-based, but have also been named data-driven. The following definition clarifies which techniques are referred to by the term *model-based approach* in this thesis.

Definition 1.1 (Model-based approach) *Two distinct steps are used to calculate the controller. In a first step a model of the plant is defined. In a second step the controller is calculated using the model, algebraically or by optimization.*

Methods that use first-principle modeling to define a plant model, and then use this model to calculate a controller are an example of such model-based techniques. Methods that use identification techniques (an optimization) to define a model of the plant, and then use the model parameters in a second optimization for controller design are another example.

In contrast to these model-based approaches, the term *data-driven approach* refers to techniques with the following property.

Definition 1.2 (Data-driven approach) *Measured data are used directly to minimize a control criterion. Only one optimization in which the controller parameters are the optimization variables is used to calculate the controller.*

In these definitions model-based approaches can be regarded as *indirect*, whereas data-driven approaches are *direct*. Note that a method that identifies a plant model parameterized directly in terms of the controller parameters is also an example of a direct approach. In this case no intermediate model parameters are involved and the controller parameters are estimated directly from the data.

Various data-driven controller tuning methods have been proposed in the literature. A non-exhaustive overview is given in Section 1.2.1. Two adaptive control schemes are treated, but the main focus is on more recent approaches, like Iterative Feedback Tuning (IFT), Iterative Correlation-based Tuning (ICbT), unfalsified control, and Virtual Reference Feedback Tuning (VRFT). Controller tuning methods that use non-parametric frequency domain models are also discussed.

In non-iterative data-driven controller tuning, a set of measured data from one single experiment is used to calculate a fixed-order controller. The exact same data set could be used to identify a model of the plant, which can then be used to calculate a controller. In model-based techniques, the order of the resulting controller is in general related to the order of the model. Identification of models

that can be used for fixed- or low-order controller design is treated in Section 1.2.2.

One of the main challenges in data-driven controller tuning is closed-loop stability. In Section 1.2.3, ideas to incorporate conditions for closed-loop stability in the controller design are discussed, as well as a posteriori stability tests.

1.2.1 Data-driven controller tuning

Adaptive control

In the 1950's, extensive research on adaptive control was triggered by the development of autopilots for aircrafts [6]. These systems function over a wide range of operating conditions, related to the speed and altitude of the aircraft. Adaptive schemes were developed to deal with changing conditions. Measured data are used in feedback to adapt the controller continuously.

The literature on adaptive control is extensive, see for example [6] and [48]. In the following, two specific schemes are summarized, Model Reference Adaptive Control (MRAC) and Self-Tuning Regulation (STR).

In MRAC, the control objective is given as a reference model, which generates an ideal plant output for the applied reference signal. The parameters of the controller are then adjusted such that the error between this ideal output and the measured output of the plant is minimized. This approach is *direct*, since the parameters of the controller are adjusted without the use of an intermediate model. In the original MRAC, the MIT rule was used to update the controller parameters [60]. The parameter update is based on a steepest descend approach, where the update is proportional to the derivative of the objective function with respect to the parameters. The gradient can, for example, be estimated using a model of the plant. Other update rules have been proposed, for example based on stability theory [6].

STR is an *indirect* adaptive approach. The measured data are used to identify a plant model. The controller is then calculated online, using this updated plant model. This scheme is very flexible as different identification approaches and different controller design

methods can be combined. Because the design calculations can be time consuming, the model can be reparameterized to simplify the design step. A model that is parameterized using the controller parameters is called a direct parameterization. It can be shown that, in some specific cases, an MRAC approach is equivalent to an STR approach that uses a direct parameterization ([6], p. 182).

Stability of adaptive control methods cannot be guaranteed in general [4]. One of the problems due to the continuous controller updates is related to persistence of excitation. If the controlled plant functions at steady state, the ideal controller achieves a constant error. Consequently, the measured signals are not rich enough to identify a correct model, resulting in a parameter update that drives the controller away from the ideal controller. As a result, the error increases and a correct model can, again, be identified. This phenomenon is called bursting [2].

In the adaptive control approaches described above, the controller or model parameters are estimated. These estimates are then used as if they represent the true system. This is called the "certainty equivalence principle" [6]. Unmodeled dynamics and estimation uncertainties are not taken into account.

Iterative Feedback Tuning

In practice, the "certainty equivalence principle" is not realistic. Since the order of the controller is limited and modeling errors cannot be avoided, the controller performance is limited by the quality of the model. Iterative Feedback Tuning (IFT) can be used to overcome these problems. IFT was initially not intended to deal with time-varying systems. It is a fine tuning approach that optimizes an initial fixed-order controller that does not meet the performance specifications. Experiments are performed with one fixed controller. A new controller is then calculated off-line.

The approach was first proposed in [30]. The control objective is formulated as a desired trajectory for the given reference signal, which can for example be generated using a reference model. The control objective is then minimized using a gradient approach to find a (local) optimum, with the initial controller as a starting point. At each iteration, closed-loop experiments are performed and the re-

sponse of the plant is used directly to estimate the gradient. No plant model is needed and the estimate of the gradient is unbiased. The controller parameters are updated using a stochastic approximation procedure. Convergence of the method to a local optimum is shown in [30], provided the measured signals remain bounded. The optimization thus converges, if the successive controllers are all stabilizing.

IFT was initially developed for LTI SISO systems. The method was then extended to LTI MIMO systems [27]. Analysis of the method for nonlinear systems is provided in [26]. Performance of the method has been shown in several application examples, see [28] for an overview. A gradient approach that is similar to IFT is proposed in [37]. In this method, the gradients are calculated using non-parametric frequency domain descriptions of the current closed-loop system.

The controller parameters converge to a local minimum, provided the successive controllers all stabilize the system. Unfortunately, guaranteeing stability is not straightforward and it is in general not known whether this condition is satisfied. In [33], it is proposed to minimize an H_∞ criterion that ensures robust stability. A robust H_2 criterion is also proposed. In [66], a robust criterion is proposed, where a second term that represents robustness is added to the original performance criterion. The optimal controller that minimizes these criteria is robust, but stability cannot be guaranteed throughout the iterations. The choice of an adequate control criterion for nonminimum-phase plants is discussed in [52], where a degree of freedom in the reference model is introduced to avoid cancelation of the unstable zero.

IFT can also be used for disturbance rejection, where the norm of the system output due to noise is minimized. For each iteration, one experiment is performed in the standard operating conditions, without excitation of the reference signal. A second experiment is performed to estimate the gradient, with excitation of the reference. The convergence rate of the algorithm depends on the quality of the gradient estimate, which is analyzed in [25]. The excitation in the first experiment is the noise, which cannot be adjusted to improve the accuracy. In [24], the reference signal used in the second experiment

is shaped using a prefilter to improve the convergence rate. In [35], addition of external excitation is proposed to improve convergence.

Iterative Correlation-based Tuning

In Iterative Correlation-based Tuning (ICbT), the control criterion is defined as a reference model. Instead of minimizing the norm of an error signal related to the model reference criterion, the correlation between the known reference signal and the error signal is minimized. The resulting controller is asymptotically insensitive to noise [57].

A correlation function is defined as the mathematical expectation of the multiplication of an instrumental variable and the model reference error. If the complexity of the controller is sufficient to achieve the model-reference objective, decorrelation of the instrumental variables and the error signal can be achieved using the iterative Robbins-Monro stochastic approximation algorithm [43]. If a large number of data is available, the Newton-Raphson algorithm for deterministic optimization can be used to improve the convergence speed [42]. The accuracy of the controller parameters is analyzed in [43], where conditions for convergence are also given. Compared to IFT, fewer experiments are needed per iteration, but a model is used to calculate the gradient. The effect of undermodeling on the convergence is studied.

If the complexity of the controller is not sufficient to match the model-reference criterion, complete decorrelation cannot be achieved. In this case, a norm of the correlation can be minimized. For a specific choice of extended instrumental variables, the optimal controller minimizes the model reference criterion weighted by the square of the power spectrum of the reference signal [41]. Specifications on the input sensitivity can be added to the approach [58]. In [57], the approach is adapted for disturbance rejection.

The method has been extended to MIMO controllers [59]. The procedure decouples the system by decorrelating the reference from the non-corresponding outputs. A single experiment is sufficient per iteration, in contrast to other data-driven methods, where the number of experiments increases with the number of inputs and outputs. The variance of the controller parameters is analyzed for simultaneous excitation of the different reference signals and for separated

excitation. It is shown that the variance is smaller is the reference signals are excited separately.

The correlation approach has also been applied to precompensator tuning [38].

Unfalsified control

Unfalsified control, introduced in [70], uses the philosophical principle that a scientific theory cannot be proven to be true, but that the best one can do is to show that a hypothesis is wrong, i.e. a false hypothesis can be falsified by observations. In unfalsified control, a set of controllers is considered and the control specifications are defined as a function of a time-domain reference signal, input to the plant and output of the system controlled by each controller in the set. These signals can be computed 'virtually', for each controller in the set, using only one set of measured data. If the virtual signals do not satisfy the control specifications, the controller is falsified and discarded. The algorithm can be implemented recursively or in batch adaptation.

The control specifications need to be verified for each controller in the set. In the early publications on unfalsified control, the controller set was therefore discrete, and for fixed-order controllers the parameter spaces were gridded. In ellipsoidal unfalsified control [81], the parameter space is continuous and the parameters can be updated analytically, which reduces the computational load considerably. Several application examples have been reported and a considerable effort has been made towards stability and convergence of the method, see [81] and [4] and the references therein. It is shown in [15] that, even though under certain hypotheses convergence to a stabilizing controller can be guaranteed, this does not prevent the system response to become arbitrarily large before convergence, and unfalsified control can therefore not be applied safely.

An H_∞ approach named iterative controller unfalsification is proposed in [47]. The approach uses time-domain data to evaluate an H_∞-norm control criterion. The approach converges as the length of an experiment tends to infinity, but neither convergence nor stability can be shown for the proposed iterative approach. Furthermore, the approach is sensitive to measurement noise [31].

Virtual Reference Feedback Tuning

The concept of virtual reference controller design was first introduced in [23]. By using a specific filtering scheme, an error signal corresponding to an approximate model reference error can be evaluated for each controller using only one experiment and no iterations are needed to minimize an approximate model reference criterion.

Several papers have treated this approach since, e.g. [9, 71]. An extension to the original method with appropriate weighting for fixed-order controllers is presented as Virtual Reference Feedback Tuning (VRFT) in [9]. If the controller is parameterized linearly, the optimization problem becomes convex and, in contrast to IFT and ICbT, convergence to the global optimum can be shown. The method is developed for noise-free measurements. For noisy measurements, the use of instrumental variables is proposed. In [71], several remarks and extensions to [9] are proposed. The use of a prediction error method (PEM) for the identification of the inverse controller is suggested to deal with measurement noise.

In [31], the use of cross-correlations is suggested for identification for control and it is shown how VRFT fits into the proposed framework. The paper discussed asymptotic properties. Many extended instrumental variable techniques as well as some frequency domain approaches fit into the proposed framework, but no detailed identification algorithm is presented.

Several examples of application of VRFT have been reported, e.g. [10, 65]. The method has been extended to 2 degree-of-freedom controllers [51] and to nonlinear plants [11]. In [46], a technique derived from VRFT is proposed, which intends to shape both the sensitivity and complementary sensitivity functions. The main difference with VRFT is that the sensitivity and complementary sensitivity do not necessarily match those of one and the same reference model. The resulting controller does not minimize an (approximate) model reference criterion, but provides a trade-off between a match of the sensitivity and a match of the complementary sensitivity function. The resulting tuning scheme is very simple.

The techniques mentioned above summarize the main results in data-driven controller tuning. Other ideas have been reported, for example the use of the behavioural approach in [56], where the measurements are assumed to be noise-free. Most of the methods discussed above use time-domain data. Approaches using frequency-domain data can also be found under the name "direct" or "data-driven". Some recent frequency-domain results are discussed next.

Frequency-domain methods

In [34], it is proposed to use frequency response function (FRF) data from a system to directly identify a controller. It is argued that, since no intermediate optimization step is used for the identification of this FRF, the problem of undermodeling of the plant is avoided and consequently the resulting performance limitation due to the plant-model mismatch is also avoided. One can argue whether such an approach is truly data-driven, since an explicit representation of the plant is used. However, this non-parametric model can be measured directly, or computed from time-domain data without any optimization step, in which case it can be seen as a representation of the measured data in the frequency domain. Furthermore, the claimed advantage that undermodeling of the plant is avoided corresponds to the main motivation for data-driven techniques.

An H_2 and an LQG scheme are proposed in [34]. The robustness issue is taken into account by adding a stability term to the cost function, which penalizes solutions that approach the critical point in the Nyquist curve. In [18], a direct approach for H_∞ controller design is proposed using FRF data.

In [40] and [39], non-parametric frequency-domain models are used to design fixed-order controllers. In [40], the open-loop transfer function is shaped using linear programming. Robustness margins are imposed as bounds in the Nyquist diagram. In [39], it is shown how the H_∞ robust performance condition can be approximated in the Nyquist diagram. For linearly parameterized controllers, the resulting constraints are convex. The approach can handle frequency-domain uncertainty as well as multimodel uncertainty.

Challenges of direct data-driven control

In a recent review of challenges encountered in adaptive control [4], model-free approaches as well as iterative identification and control are considered. It is shown that the problems encountered in these methods are similar to some of the known problems of adaptive control. A major theoretical problem is closed-loop stability. A second problem, which is closely connected to the stability problem, is the choice of the control objective. In data-driven and iterative identification and control techniques, a full description of the plant is lacking. It is therefore impossible to decide beforehand whether the defined control objective can be achieved. If the control objective is inadequate, at least, the desired performance will not be achieved and, at worst, the closed-loop might be unstable. In [31], a simple analytical example shows an unachievable control objective that leads to destabilizing optimal controllers in model-free approaches.

1.2.2 Model-based fixed-order controller design

In a model-based approach, the order of the controller typically depends on the order of the plant. In order to limit the order of the controller, it is therefore desirable to limit the order of the model. An overview of identification of restricted-complexity models can be found in [29]. In the following, identification of low-order models for controller design is discussed and some results on the accuracy of model reduction and direct identification of low-order models are given.

Identifying low-order models for controller design

If the order of the model is limited, a bias error exists between the model and the plant due to undermodeling. It has been shown that bias shaping, i.e. imposing a frequency dependent weighting on this error due to undermodeling, is essential for meeting the control performance [20]. The main idea is that the modeling error can be large in frequency zones that are not important for the resulting closed-loop performance, but the error must be limited in other frequency zones, typically around the bandwidth of the closed-loop system.

The identification criterion used to identify the plant must thus be connected to the control objective.

In [67], this idea is used for model reduction. An optimal low-order model for controller design is calculated by minimizing a criterion that reflects the control objective. The optimal weighting for identification of the plant model actually depends on the controller that is to be designed. This observation is the basis of iterative identification and control techniques, see [1] for an overview. The idea is that a first model is identified in closed-loop operation. This model is then used to calculate a new controller, which is implemented. A new model is identified with this new controller, thus resulting in an iterative approach. The quality of consecutive models should improve, because the frequency weighting approaches the optimal weighting as the controller approaches the ideal controller. However, convergence of such methods cannot be shown.

If an approximation of the ideal filter is used, bias shaping can be done by prefiltering of the data, where the approximate filter is applied to the data before identification of the plant. This approach is non-iterative. According to [29], VRFT can be seen as such a prefiltering approach, where the low-order plant is parameterized through the parameterization of the controller. This parameterization is known in adaptive control as the direct parameterization.

A statistical view on identification of low-order models

Low-order models can either be identified directly from data, or be calculated in a model-reduction step, after having identified a high-order model. An obvious question is then, which of these methods should be preferred? Should one first identify a full-order model and then use this model for further calculations or is it better to identify a reduced-order model directly? This question is treated in [29].

The discussion in [29] is based on the so-called separation principle, which uses the invariance principle of maximum-likelihood (ML) estimation (Theorem 5.1.1 [84]). Let $g : \Theta \to \Omega$ be a function mapping $\theta \in \Theta \in \mathbf{R}^n$ to an interval $\Omega \in \mathbf{R}^m$, with $m \leqslant n$. The theorem states that, if $\hat{\theta}$ is a maximum-likelihood estimator of θ, then $g(\hat{\theta})$ is a maximum-likelihood estimator of $g(\theta)$.

According to [29], *"it follows under very general conditions on g that, if $\hat{\theta}$ is asymptotically efficient, i.e. it is consistent and its asymptotic covariance matrix reaches the Cramér-Rao lower limit, then $g(\hat{\theta})$ is also asymptotically efficient."* The results of [80] on model reduction confirm this idea.

According to this separation principle, a full-order model can be identified and then used in further calculations without jeopardizing the asymptotic efficiency. However, the properties for a finite number of data of such an asymptotically efficient estimator are not necessarily optimal.

1.2.3 Ensuring closed-loop stability

Ideally, a control-design method should guarantee closed-loop stability. Attempts to incorporate a stability condition at the design stage can be found for iterative identification and control [53]. The main idea is that, if the controller change is small enough, instability cannot occur. This idea of cautious controller updates and gradual performance increase is widely accepted in iterative identification and control [3, 7]. If the design method does not include a stability guarantee, the controller can be tested before actual implementation. Several tests have been developed to verify closed-loop stability before implementation of the controller.

In [37], it is suggested to include an a posteriori stability test in an iterative controller-tuning scheme. The stability condition is based on ν-gap metrics and can be verified using spectral estimates of the current closed-loop system, which are also used in the iterative scheme. Extensions to the approach are given in [36]. In [62], the ν-gap metric is used not only to ensure stability conditions but also to ensure a certain closed-loop performance. For validation of the conditions, the H_∞-norm of a matrix of loop-transfer functions with the current controller in the loop needs to be identified.

In [83], it is shown that it is impossible to ensure stability in iterative unfalsification and control schemes, based on a finite number of data and without additional information on the plant. A priori assumptions are necessary in order to guarantee stability. An algorithm that uses an a priori assumption on the maximal derivative of the plant frequency response function is proposed.

In [50], stability of iterative identification and control methods is treated. It is pointed out that model-based methods need an accurate model of the plant in order to verify the stability of a controller based on an approximate model, which somewhat contradicts the controller design approach. This raises the important question of how much information is really needed in order to guarantee stability and how reliable is the answer. A stability test for iterative identification and control methods is presented, where the difference between two consecutive controllers is small. The needed accuracy of the nonparametric model identified in the proposed test is related to this controller change. In [16], the approach is detailed for both linear SISO and linear MIMO systems.

In [71], a scheme is proposed that generates the necessary signals to identify the closed-loop system without actually implementing the controller. The resulting stability test requires the accurate identification of a possibly unstable system in an errors-in-variables problem. Another model-based approach based on an uncertainty set that contains the true plant with a certain probability has been proposed by [21].

1.3 Contributions

This thesis presents algorithms for and analysis of non-iterative data-driven controller tuning, where an approximation of the model reference criterion is minimized. Only linear time-invariant SISO systems are considered. The contributions can be summarized as follows:

Proposition of straightforward schemes for non-iterative controller tuning
Two schemes are proposed, one for open-loop experiments and one for closed-loop experiments. The approach is therefore applicable to both open-loop stable and unstable systems.

Application of the correlation approach to deal with noise
The controller identification problem for stable systems is analyzed in detail. It is shown that, if the order of the controller is fixed, the controller parameters identified using standard PEM do not converge to the optimal values due to noise. Application of the correlation approach is proposed to deal with the noise,

and it is shown that the controller converges to the optimal controller, also for fixed-order controllers.

Proposition of a data-driven approach with integrated constraint for closed-loop stability
A sufficient condition for closed-loop stability is proposed, which can be added as a constraint to the (approximate) model reference problem. In the case of stable systems, an active constraint indicates that the control objective cannot be achieved. In a data-driven approach, the stability constraint needs to be estimated. Stability is guaranteed as the number of data tends to infinity. In order to guarantee stability for a finite number of data, the estimation error needs to be taken into account. Bounds on the error are given for periodic data. For linearly parameterized controllers, the data-driven approach for the constrained approximate model reference problem is a convex optimization problem.

Proposition of a posteriori data-driven test for stability
A non-conservative a posteriori stability test is proposed, based on a similar stability condition as used in the data-driven approach with guaranteed stability. The condition is verified using an estimate based on available open- or closed-loop data. If some a priori information on the plant and disturbances is available, error bounds can be defined and stability can be guaranteed. If no error bound can be defined, the proposed approach offers a straightforward trade-off between conservatism and reliability. Data from different closed-loop experiments can be combined, also if the data is collected with different controllers in the loop.

Analysis of the accuracy of data-driven model reference control
Various identification approaches have been proposed to deal with the measurement noise in the context of non-iterative data-driven controller tuning. The accuracy of these approaches is compared to the accuracy of the correlation approach and that of an errors-in-variables approach for periodic data. It is shown that, if the ideal controller is in the controller set, the Cramér-Rao bound can be obtained. If the order of the controller is fixed, the estimate converges to the optimal controller only for (extended) instrumental variable methods, which includes the

correlation approach. A comparison with a statistically efficient model-based approach shows that data-driven controller tuning is asymptotically equivalent to this model-based approach. For a finite number of data, the data-driven approach can be more accurate, as shown in a numerical example.

1.4 Outline

Chapter 2 introduces the approximate model reference problem. Data-driven tuning schemes for stable and unstable plants are proposed in Section 2.2. The assumptions used throughout the thesis are also given in this section. The resulting controller identification problem is analyzed in Section 2.3. Implementation of the correlation approach is discussed in Section 2.4 and application of the method to a pick-and-place robot is presented in Section 2.5.

Chapter 3 presents correlation-based controller tuning with guaranteed stability. A stability constraint for model reference control is introduced in Section 3.1. In Section 3.2 and 3.3, constraints for stability are added to the correlation approach presented in Chapter 2. The connection of the proposed approach with Toeplitz-based methods as used in model and controller unfalsification is shown in Section 3.4. Error bounds for the estimate of the stability condition for a finite number of periodic data are given in Section 3.5, and Section 3.6 illustrates the effectiveness of the proposed approach in simulation and on an experimental setup.

The non-conservative a posteriori stability test is presented in Chapter 4. In Section 4.1, conditions for closed-loop stability are given. In Section 4.2, it is shown how the signals that are necessary to verify the stability conditions can be generated. The data-driven test is presented in Section 4.3. Section 4.4 describes how to combine data from different closed-loop experiments. The effectiveness of the test is shown in a numerical example in Section 4.5.

In Chapter 5, the accuracy of non-iterative model reference controller tuning is discussed. Different identification approaches for data-driven controller tuning are analyzed in 5.1. The performance of these approaches is compared in Section 5.2. In Section 5.3, the

accuracy of the controller parameters is compared to the accuracy of a statistically efficient model-based approach.

Conclusions and perspectives are provided in Chapter 6.

2

Non-iterative data-driven controller tuning: an identification problem

The control objective used throughout this thesis is an approximation of the model reference control problem. This approximation, which has been used in model reduction and data-driven controller tuning, is defined in Section 2.1. In Section 2.2, tuning schemes for both open-loop and closed-loop experiments are proposed, which generate an error signal that can be used to directly minimize the approximate model reference criterion over a predefined set of controllers. The set of controllers, and therefore the order of the controller, is fixed. This characteristic is essential throughout this thesis.

If the order of the controller is fixed, the control objective can in general not be achieved, and a bias error exists between the ideal controller and the optimal controller in the predefined class of controllers. Due to this bias error and the effect of noise, controllers identified using prediction error methods do not converge to the optimal controller, as shown in Section 2.3. The use of the correlation approach is proposed to deal with the effect of noise in the design of fixed-order controllers. The approach has been applied to a pick-and-place robot, the results of which are presented in Section 2.5.

2.1 An approximate model reference criterion

Consider the unknown LTI SISO plant $G(q^{-1})$, where q^{-1} denotes the backward shift operator. Specifications for the controlled plant

are given as a stable strictly proper reference model $M(q^{-1})$. The objective is to design a linear, fixed-order controller $K(q^{-1}, \rho)$, with parameters ρ, for which the closed-loop system resembles the reference model $M(q^{-1})$.

This can be achieved by minimizing the (filtered) two-norm of the difference between the reference model and the achieved closed-loop system:

$$J_{mr}(\rho) = \left\| F\left[M - \frac{K(\rho)G}{1 + K(\rho)G} \right] \right\|_2^2 \tag{2.1}$$

with F a weighting filter. Note that the objective is to design a fixed-order controller and $J_{mr}(\rho) = 0$ can in general not be achieved.

The model reference criterion (2.1) is non-convex with respect to the controller parameters ρ. An approximation that is convex for linearly parameterized controllers can be defined using the reference model M as illustrated next. M can be represented as:

$$M = \frac{K^*G}{1 + K^*G}. \tag{2.2}$$

The backward shift operator is omitted here and in the sequel. K^* is the ideal controller, which is defined indirectly by G and M:

$$K^* = \frac{M}{G(1 - M)}. \tag{2.3}$$

This controller K^* exists because $M \neq 1$, since M is strictly proper. K^* might be of very high order since it depends on the unknown and possibly high-order plant G. Furthermore, K^* might not stabilize the plant internally and might be non-causal. However, the unknown ideal controller will only be used for analysis and the results will be valid also for a non-causal K^*. Furthermore, since M is strictly proper, $K^*G = M(1 - M)^{-1}$ is causal.

The ideal sensitivity function is given by

$$\frac{1}{1 + K^*G} = 1 - M. \tag{2.4}$$

Using (2.2), the model reference criterion (2.1) can be expressed as:

$$J_{mr}(\rho) = \left\| F\left[\frac{K^*G - K(\rho)G}{(1 + K^*G)(1 + K(\rho)G)} \right] \right\|_2^2 \tag{2.5}$$

Approximation of $\frac{1}{1+K(\rho)G}$ by the ideal sensitivity function (2.4) leads to the following approximation of the model reference criterion:

$$J(\rho) = \left\| F\left[\frac{K^*G - K(\rho)G}{(1+K^*G)^2}\right]\right\|_2^2 = \left\| F(1-M)[M - K(\rho)(1-M)G]\right\|_2^2. \quad (2.6)$$

Let the controller be linearly parametrized

$$K(q^{-1},\rho) = \beta^T(q^{-1})\rho, \quad \rho \in \mathcal{D}_K \quad (2.7)$$

where the set $\mathcal{D}_K$ is compact and $\beta(q^{-1})$ is a vector of stable linear discrete-time transfer operators:

$$\beta(q^{-1}) = [\beta_1(q^{-1}), \beta_2(q^{-1}), \ldots, \beta_{n_\rho}(q^{-1})]^T. \quad (2.8)$$

Note that orthogonal basis functions can be chosen. n_ρ is the number of controller parameters. With this structure of $K(\rho)$, the approximate model reference criterion $J(\rho)$ is convex in the controller parameters ρ.

Special cases of unstable controllers can also be handled, for example if $\beta(q^{-1})$ contains an integrator. In this case, the reference model M needs correspond to the controller structure to ensure that $J(\rho)$ is bounded on $\mathcal{D}_K$, see Section 2.4 for details.

Definition 2.1 (Optimal controller) *Let the controller be parameterized as in (2.7) and $J(\rho)$ given by (2.6). The parameters ρ_0 of the optimal controller $K(\rho_0)$ are defined as the optimum of the following convex optimization:*

$$\rho_0 = \arg\min_{\rho\in\mathcal{D}_K} J(\rho). \quad (2.9)$$

Note that, if the ideal controller K^* is in the set of controllers given by $K(\rho)$, the optimal $K(\rho_0)$ is given by $K(\rho_0) = K^*$, i.e. $\rho_0 = \rho^*$. In this case, ρ^* does not depend on the frequency weighting, since $K(\rho^*)G(1-M) = M$ and therefore both $J(\rho^*) = 0$ and $J_{mr}(\rho^*) = 0$; the approximate model reference criterion $J(\rho)$ and $J_{mr}(\rho)$ have the same optimum, ρ^*.

The criterion $J(\rho)$ is a good approximation of $J_{mr}(\rho)$ if the difference between $K(\rho)$ and the ideal controller K^* can be made small. This approximation has been used in model reduction and controller reduction, see [29] for an overview. A similar approximation in the H_∞ framework is for example used in [5], an H_2 example can be found in [68]. The approximation has also been used in data-driven controller tuning [9]. The quality of the approximation is discussed in [9].

2.2 Non-iterative data-driven controller tuning schemes

In the following, two data-driven tuning schemes are presented that can be used to define a time-domain estimate of the control criterion $J(\rho)$. This criterion consists of the error transfer function $M - K(\rho)(1-M)G$, filtered by $F(1-M)$, where F is a user-defined filter. The open-loop tuning scheme proposed next, is a straightforward implementation of this error function, filtered by the filter L. This filter L should be chosen such that the data-driven controller converges to the optimal controller $K(\rho_0)$, and is discussed in detail in Section 2.4. The scheme can be used for stable systems, and the global optimum of the time-domain criterion can be found using only one set of measured data. For unstable systems, one closed-loop experiment is proposed.

2.2.1 Tuning scheme for stable plants

Let the error $\varepsilon_c(t,\rho)$ be given by the tuning scheme of Figure 2.1. $\varepsilon_c(t,\rho)$ can be expressed in terms of the exogenous signals $r(t)$ and $v(t)$ as follows:

$$\begin{aligned}\varepsilon_c(t,\rho) &= L\left[Mr(t) - K(\rho)(1-M)y(t)\right] \\ &= L\left[M - K(\rho)(1-M)G\right]r(t) - LK(\rho)(1-M)v(t) \end{aligned} \quad (2.10)$$

This error signal can be evaluated for each controller $K(\rho)$, using only one experiment. If the filter L is chosen, as discussed in Section 2.4, this scheme can be used to identify the optimal controller $K(\rho_0)$.

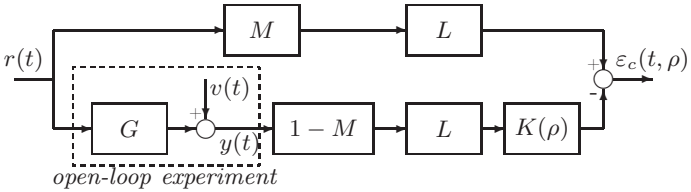

Fig. 2.1. Tuning scheme for the model reference control problem using only one open-loop experiment

However, in the resulting parameter estimation problem, the input to the function to be identified, $K(\rho)$, is affected by noise, in contrast to classical identification problems, where its output is affected by noise. For this particular identification problem, standard prediction-error methods cannot be used, as shown in Section 2.3. The correlation approach can be used to reduce the effect of noise on the estimated controller parameters.

2.2.2 Tuning scheme for unstable plants

If the plant is unstable, an initial stabilizing controller K_s is needed to perform an experiment. Data from an experiment on the plant controlled by this stabilizing controller K_s is assumed available, but K_s need not be known. Consider the tuning scheme shown in Figure 2.2. The excitation signal $r(t)$ is applied directly to the input of the plant. The data set consists of the exogenous excitation signal $r(t)$, the output of the controller $u_1(t)$, the resulting input to the plant $u_2(t) = u_1(t) + r(t)$, and the output of the controlled plant $y(t)$. The error $\varepsilon_c(t, \rho)$, which reads

$$\varepsilon_c(t, \rho) = L\left[Mu_2(t) - K(\rho)(1 - M)y(t)\right], \tag{2.11}$$

can be used to compute the optimal controller. Again, prediction-error methods cannot be used for this specific identification problem and the correlation approach will be used to reduce the effect of noise. In Section 2.4, the correlation approach is detailed for both the open-loop and the closed-loop scheme. Note that the closed-loop scheme can also be used for stable systems.

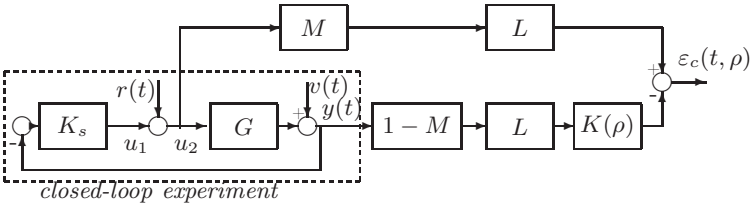

Fig. 2.2. Tuning scheme for model reference control problem using one closed-loop experiment

2.2.3 Definitions and assumptions

The following definitions and assumptions are used throughout this thesis. The auto-correlation of the signal $r(t)$ is defined as

$$R_r(\tau) = \lim_{N\to\infty} \frac{1}{N} \sum_{t=1}^{N} E\{r(t-\tau)r(t)\}. \tag{2.12}$$

The spectrum of $r(t)$ is defined as:

$$\Phi_r(\omega) = \sum_{\tau=-\infty}^{\infty} R_r(\tau) e^{-j\tau\omega}, \tag{2.13}$$

provided the infinite sum exists. The cross-correlation between the signals $r(t)$ and $v(t)$ is defined as:

$$R_{rv}(\tau) = \lim_{N\to\infty} \frac{1}{N} \sum_{t=1}^{N} E\left\{r(t-\tau)v(t)\right\}. \tag{2.14}$$

The auto-correlation of the periodic signal $r(t)$ with period N_p is defined on one period and given by:

$$R_r(\tau) = \frac{1}{N_p} \sum_{t=1}^{N_p} r(t-\tau)r(t), \tag{2.15}$$

for $\tau = 0, \ldots, N_p - 1$. The spectrum of the periodic $r(t)$ is defined as

$$\Phi_r(\omega_k) = \sum_{\tau=0}^{N_p-1} R_r(\tau)e^{-j\tau\omega_k}, \omega_k = 2\pi k/N_p, k = 0, \ldots, N_p - 1. \tag{2.16}$$

The measurement noise $v(t)$ is assumed to satisfy:

A1 The measurement noise $v(t)$ is uncorrelated with $r(t)$, i.e.

$$R_{rv}(\tau) = \lim_{N\to\infty} \frac{1}{N} \sum_{t=1}^{N} E\left\{r(t-\tau)v(t)\right\} = 0 \tag{2.17}$$

for all τ.

A2 The measurement noise can be represented as

$$v(t) = H_v(q^{-1})e(t),$$

where $e(t)$ is a zero-mean white noise signal with variance σ^2 and bounded fourth moments. H_v and H_v^{-1} are stable filters.

If non-periodic signals are considered, the reference signal is assumed to satisfy the following assumptions:

A3 $r(t)$ is quasi-stationary, i.e. $R_r(\tau)$ exists for all τ.

A4 The spectrum of $r(t)$ satisfies $\Phi_r(\omega) > 0, \forall\omega$.

Assumption **A3** includes deterministic as well as stochastic signals, i.e. $r(t)$ can be the realization of a stochastic process. In some cases, periodic input signals will be considered:

A5 The reference signal is periodic with period N_p, i.e. $r(t+nN_p) = r(t)$ for any integer n. The signal $r(t)$ includes an integer number of periods, i.e. $N = n_pN_p$, with n_p the number of periods. If $r(t)$ is used to excite a plant, the output of the plant is also assumed to be periodic, i.e. there are no transients present in the response of the system.

A6 The spectrum of the periodic reference signal $r(t)$ satisfies $\Phi_r(\omega_k) > 0, \omega_k = 2\pi k/N_p, k = 0, \ldots, N_p - 1$.

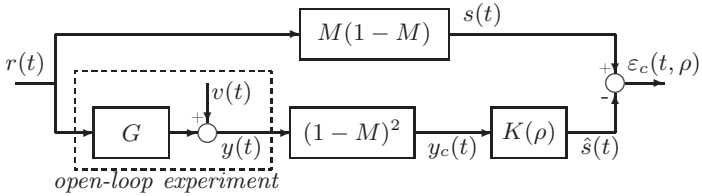

Fig. 2.3. Tuning scheme for model-reference problem, with $L = 1 - M$.

2.3 Analysis of the controller identification problem

In the following, the nature of the controller identification problem is analyzed using well-known prediction-error methods (PEM). Only stable plants and open-loop measurement data are considered here. Assume that the user-defined filter $F = 1$ and the filter L is fixed as $L = 1 - M$. The controller tuning scheme of Figure 2.1 is now given by Figure 2.3.

2.3.1 Controller identification in the prediction error framework

The scheme of Figure 2.3 can be rearranged as depicted in Figure 2.4, to show clearly the nature of the identification problem. The input $y_c(t)$ of the controller to be identified $K(\rho)$ is affected by the noise term $\tilde{y}_c(t)$. The output of the ideal controller K^* is not affected by noise. Its input, $y_c^*(t)$ is also noise-free. The unknown signals in this scheme are $v(t), y_c^*$ and the noise signal $\tilde{y}_c(t)$ given by:

$$\tilde{y}_c(t) = (1 - M)^2 v(t) = H_{\tilde{y}} e(t). \tag{2.18}$$

The known signals are $r(t), y_c(t) = (1 - M)^2 y(t)$ and $s(t)$ given by:

$$s(t) = (1 - M)^2 G K^* r(t) = (1 - M) M r(t).$$

In contrast to errors-in-variables problems, there is no fundamental identifiability problem since the output $s(t)$ is not affected by noise and the reference signal $r(t)$ is available.

Two cases are considered:

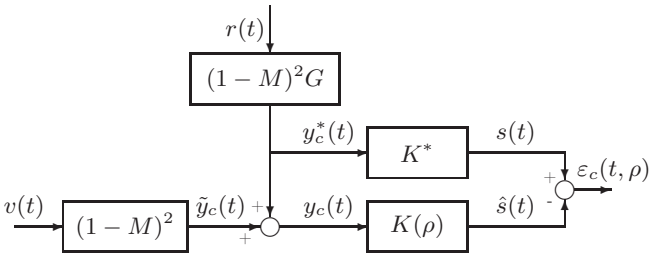

Fig. 2.4. Alternative representation of data-driven controller tuning scheme

C1 The objective can be achieved, i.e. $K^* \in \{K(\rho)\}$. Therefore $K(\rho_0) = K^*$ and $J(\rho_0) = 0$

C2 The objective cannot be achieved, i.e. $K^* \notin \{K(\rho)\}$, $K(\rho_0) \neq K^*$ and $J(\rho_0) > 0$.

Case **C1** is often assumed in system identification. However, since one of the main advantages of data-driven controller design is that the order of the controller can be fixed, this assumption does not necessarily hold and **C2**, the case of undermodeling of the controller, needs to be considered.

Assume that **A1** and **A2** are satisfied and that, in Case **C1**:

A7 The input $r(t) = 0, \forall t \leqslant 0$. $r(t)$ is persistently exciting of order n_ρ and $L(1-M)G$ has no zero on the imaginary axis.

In case **C2**, the control objective is formulated as minimization of $J(\rho)$, the 2-norm of an error function. Because the 2-norm is considered, i.e. the integral of the error function over all frequencies, and $J(\rho) \neq 0, \forall \rho$, the system must be excited at all frequencies. The assumption that the spectrum of $r(t)$, $\Phi_r(\omega) > 0$, $\forall \omega$ is sufficient for the analysis of convergence of the estimate in case **C2**. However, for the ease of notation, the following stronger assumption will be used.

A8 The input $r(t)$ is a zero-mean white noise with unit variance and $L(1-M)G$ has no zero on the imaginary axis.

Consider the scheme of Figure 2.4. Using (2.7), the error can be calculated as

$$\varepsilon_c(t,\rho) = s(t) - \hat{s}(t) = s(t) - K(\rho)y_c(t) = s(t) - \phi^T(t)\rho, \quad (2.19)$$

where the regression vector $\phi(t)$ is given by:

$$\phi(t) = \beta y_c(t) = \beta y_c^*(t) + \beta\tilde{y}_c(t) \triangleq \phi_0(t) + \tilde{\phi}(t), \quad (2.20)$$

with $\beta(q^{-1})$ defined in (2.8). The error signal can be written as

$$\begin{aligned}\varepsilon_c(t) &= K^* y_c^*(t) - K(\rho)y_c^*(t) - K(\rho)\tilde{y}_c(t)\\ &= [K^* - K(\rho)]y_c^*(t) - K(\rho)H_{\tilde{y}}e(t)\end{aligned} \quad (2.21)$$

Note that the noise filter is given by $K(\rho)H_{\tilde{y}}$, which corresponds to a parameterization of the noise model $H(\eta,\rho)$, where the noise model depends on the controller parameters ρ as well as on the parameters η. In the prediction error framework, the corresponding prediction error is then given by:

$$\begin{aligned}&\varepsilon_p(t,\eta,\rho) = H^{-1}(\eta,\rho)\varepsilon_c(t)\\ &= H^{-1}(\eta,\rho)\left(K^* y_c^*(t) - K(\rho)y_c^*(t) - K(\rho)\tilde{y}_c(t)\right)\\ &= H^{-1}(\eta,\rho)\left([K^* - K(\rho)]y_c^*(t) + [H(\eta,\rho) - K(\rho)H_{\tilde{y}}]e(t)\right) - e(t),\end{aligned} \quad (2.22)$$

Non-iterative data-driven controller tuning thus corresponds to an identification problem with a specific parameterization of the noise model, given by $H(\eta,\rho) = K(\rho)H_p(\eta)$, where $H_p(\eta)$ is the part of the noise model independent of the controller parameters.

2.3.2 Full-order controllers: no undermodeling

In the standard identification framework, the system to be identified is usually assumed to be contained in the model set, i.e. no undermodeling is present. A well-known result in this case is that, if the noise model and the plant model are independently parameterized, the noise model does not affect the consistency of the estimate of the plant [54]. However, non-iterative data-driven controller tuning leads to a structure where the controller parameters appear in the noise model. Consequently, the estimate of the controller is consistent only if the noise model is identified correctly.

The PEM estimate with a fixed noise model, i.e. the output error structure with $H(\eta, \rho) = 1$, is now used to illustrate the differences with a standard identification problem. If $H(\eta, \rho) = 1$ and the controller is parameterized as in (2.7), the PEM criterion $\frac{1}{N}\sum_{t=1}^{N} \varepsilon_p^2(t, \rho)$ is a quadratic function of ρ. The optimizer is given by the least-squares solution:

$$\hat{\rho} = \left[\frac{1}{N}\sum_{t=1}^{N} \phi(t)\phi(t)^T\right]^{-1} \frac{1}{N}\sum_{t=1}^{N} \phi(t)s(t). \tag{2.23}$$

In Case **C1**, it follows from (2.20) that

$$s(t) = \phi_0^T(t)\rho_0 = \phi^T(t)\rho_0 - K(\rho_0)\tilde{y}_c(t).$$

The estimation error is then given by

$$\hat{\rho} - \rho_0 = \left[\frac{1}{N}\sum_{t=1}^{N} \phi(t)\phi(t)^T\right]^{-1} \frac{1}{N}\sum_{t=1}^{N} \phi(t)K(\rho_0)\tilde{y}_c(t). \tag{2.24}$$

The regressor $\phi(t)$ is correlated with the noise $\tilde{y}_c(t)$, and consequently the estimate is not consistent.

In contrast to the standard identification problem, the PEM estimate is not consistent here, unless the noise model is identified correctly. Similar to the case of closed-loop identification [19], a tailor-made parameterization can be used to find a consistent estimate.

To summarize:

- In the prediction error framework, the controller tuning problem requires a tailor-made parametrization, where the noise model is parameterized as $K(\rho)H_p(\eta)$. If the noise model is not estimated correctly, the estimate is not consistent, contrary to the standard Box-Jenkins identification problem.
- $(H_p(\eta)K(\rho))^{-1}$ needs to be stable.
- The identification problem becomes a non-convex optimization problem, also for the linearly parameterized controllers (2.7).

2.3.3 Fixed-order controllers: undermodeling of the controller

If, in practice, the order of the controller is fixed, Case **C1** typically does not apply. In Case **C2**, $K^* \notin \{K(\rho)\}$, the criterion $J(\rho) > 0$ and the frequency weighting of the error becomes critical for the quality of the controller. This *bias shaping* is well known in the context of iterative identification and control [20].

Asymptotic convergence of the estimate is analyzed next, under Assumption **A8**. The optimal controller $K(\rho_0)$ is defined in Definition 2.1. The estimate converges asymptotically if

$$\lim_{N\to\infty} \hat{\rho} = \rho_0 = \arg\min_{\rho\in\mathcal{D}_K} J(\rho).$$

Using (2.22), the prediction error estimate is given by

$$\hat{\rho} = \arg\min_{\rho\in\mathcal{D}_K} \frac{1}{N}\sum_{t=1}^{N} \varepsilon_p^2(t,\eta,\rho) = \arg\min_{\rho\in\mathcal{D}_K} J_p(\rho). \tag{2.25}$$

Then

$$\hat{\rho} = \arg\min_{\rho\in\mathcal{D}_K} \frac{1}{N}\sum_{t=1}^{N} \big[H^{-1}(\eta,\rho)\big([K^* - K(\rho)]y_c^*(t) + [H(\eta,\rho) - K(\rho)H_{\tilde{y}}]e(t)\big)\big]^2 \tag{2.26}$$

If no measurement noise is present, the estimate is given by

$$\hat{\rho} = \arg\min_{\rho\in\mathcal{D}_K} \frac{1}{N}\sum_{t=1}^{N} \big[H^{-1}(\eta,\rho)(1-M)\big(M - K(\rho)(1-M)G\big)r(t)\big]^2$$

The estimate converges asymptotically to ρ_0, the minimizer of (2.6), only if the noise model is chosen as $H(\eta,\rho) = 1$ (output error structure). In this case, $\lim_{N\to\infty} J_p(\rho) = J(\rho)$ and consequently $\lim_{N\to\infty} \hat{\rho} = \rho_0$. However, if the measurements are affected by noise and $e(t) \neq 0$, the controller parameters appear in the noise term

$$\hat{\rho} = \arg\min_{\rho\in\mathcal{D}_K} \frac{1}{N}\sum_{t=1}^{N} \big[H^{-1}(\eta,\rho)\big((1-M)\big(M - K(\rho)(1-M)G\big)r(t) + [H(\eta,\rho) - K(\rho)H_{\tilde{y}}]e(t)\big)\big]^2. \tag{2.27}$$

The noise model $H(\eta, \rho)$ should thus be equal to $K(\rho)H_{\tilde{y}}$ to eliminate the effect of noise, and equal to 1 for bias shaping. Since these two objectives are in general conflicting, $\lim_{N\to\infty} \hat{\rho} \neq \rho_0$.

To summarize: In case **C1**, the PEM gives a consistent estimate, when a tailor-made parametrization is used. However, the PEM cannot be used for bias shaping in case **C2**. Since the possibility to fix the order of the controller is one of the main advantages of data-driven controller tuning approaches, case **C2** needs to be considered in practice. A PEM is therefore not an adequate identification method for this specific problem.

2.4 Application of the correlation approach

The correlation approach can be used to deal with the effect of noise in direct controller tuning. The use of cross-correlations is well-known in identification, for example in instrumental variable techniques [74] and in spectral analysis. The use of cross-correlations for identification for control is proposed in [31], but no details for implementation are given. In ICbT, a specific choice of extended instrumental variables is proposed. Because this specific choice of instrumental variables permits bias shaping, also in Case **C2** [41], this approach is applied here to the non-iterative data-driven model reference problem. The proposed approach is therefore applicable in both Case **C1** and Case **C2**.

Consider the open-loop tuning scheme of Figure 2.1. The ideal controller $K(\rho^*)$ achieves $M = K(\rho^*)G(1 - M)$. As a result, the error signal (2.10) becomes filtered noise:

$$\varepsilon_c(t, \rho^*) = -K(\rho^*)L(1 - M)v(t) \tag{2.28}$$

Since according to Assumption **A1** $v(t)$ is not correlated with the reference $r(t)$, the ideal error $\varepsilon_c(t, \rho^*)$ will not be correlated with $r(t)$ either. In the correlation approach, the objective is to tune the controller parameters ρ such that $\varepsilon_c(t, \rho)$ and $r(t)$ become uncorrelated. In the following, the correlation approach is detailed for the open-loop scheme of Figure 2.1 and the closed-loop scheme of Figure 2.2, both for periodic and non-periodic data.

2.4.1 Use of open-loop experiments

Let the plant G be excited by $r(t)$ as illustrated in Figure 2.1. The output of the plant is affected by noise, $y(t) = Gr(t) + v(t)$. Assume that the signals $r(t)$ and $y(t)$ of length N are available, that **A1-A4** are satisfied and that $L(1 - M)G$ has no zero on the imaginary axis. The error $\varepsilon_c(t, \rho)$ is calculated according to the tuning scheme of Figure 2.1 and is given by (2.10). The vector of instrumental variables $\zeta(t)$, correlated with $r(t)$ and uncorrelated with $v(t)$, is defined as:

$$\zeta(t) = [r(t + l_1), r(t + l_1 - 1), \dots r(t), r(t - 1), \dots, r(t - l_1)]^T \quad (2.29)$$

where l_1 is a sufficiently large integer. A discussion on the choice of l_1 can be found in Section 2.4.3. The correlation function is defined as

$$f_{N,l_1}(\rho) = \frac{1}{N} \sum_{t=1}^{N} \zeta(t)\varepsilon_c(t, \rho) \quad (2.30)$$

and the correlation criterion $J_{N,l_1}(\rho)$ as

$$J_{N,l_1}(\rho) = f^T_{N,l_1}(\rho) f_{N,l_1}(\rho). \quad (2.31)$$

The optimizer $\hat{\rho}$ of the data-driven problem is defined as:

$$\hat{\rho} = \arg \min_{\rho \in \mathcal{D}_K} J_{N,l_1}(\rho). \quad (2.32)$$

Since $J_{N,l_1}(\rho)$ is a quadratic function of ρ, the global optimum can be found analytically.

Theorem 2.1 *Consider the controller structure defined in (2.7). Let the stable filter L be defined as:*

$$L(e^{-j\omega}) = \frac{F(e^{-j\omega})(1 - M(e^{-j\omega}))}{\Phi_r(\omega)} \quad (2.33)$$

This filter might be non-causal. Then, as $N, l_1 \to \infty$ and $l_1/N \to 0$, the optimizer $\hat{\rho}$ in (2.32) converges w.p.1 to ρ_0, the optimizer of $J(\rho)$ as defined in Definition 2.1:

$$\lim_{N,l_1 \to \infty, l_1/N \to 0} \hat{\rho} = \rho_0 \quad (2.34)$$

Proof: Firstly stochastic convergence is established. We have [54]:

$$\lim_{N\to\infty} f_{N,l_1}(\rho) = [R_{r\varepsilon_c}(-l_1,\rho),\ldots,R_{r\varepsilon_c}(l_1,\rho)]^T, \quad \text{w.p. } 1$$

The correlation criterion is a continuous function of this variable, which leads to ([63], page 450):

$$\lim_{N\to\infty} J_{N,l_1}(\rho) = \sum_{\tau=-l_1}^{l_1} R^2_{r\varepsilon_c}(\tau,\rho), \text{ w.p. } 1. \tag{2.35}$$

Note that this result holds for finite l_1. In this case the correlation criterion converges because $N\to\infty$ implies $l_1/N\to 0$.

Secondly, convergence of this deterministic variable to $J(\rho)$ is established as $l_1\to\infty$. Since $K(\rho)$ is stable, $L(M-K(\rho)(1-M)G)$ is stable and $\sum_{\tau=-l_1}^{l_1} R^2_{r\varepsilon_c}(\tau,\rho)$ and the limit $\sum_{\tau=-\infty}^{\infty} R^2_{r\varepsilon_c}(\tau,\rho)$ are bounded on $\mathcal{D}_K$. The sequence of deterministic convex functions $\sum_{\tau=-l_1}^{l_1} R^2_{r\varepsilon_c}(\tau,\rho)$ then converges uniformly to $\sum_{\tau=-\infty}^{\infty} R^2_{r\varepsilon_c}(\tau,\rho)$ on the compact set $\mathcal{D}_K$ as $l_1\to\infty$. This follows from Theorem 10.8 from [69], which states that pointwise convergence of a series of convex functions to a convex limit function implies uniform convergence on a compact set.

It then follows that as $N, l_1\to\infty, l_1/N\to 0$ the correlation criterion converges uniformly:

$$\lim_{N,l_1\to\infty,l_1/N\to 0} J_{N,l_1}(\rho) = \sum_{\tau=-\infty}^{\infty} R^2_{r\varepsilon_c}(\tau,\rho), \text{ w.p. } 1. \tag{2.36}$$

Using Parseval's theorem, this is equivalent to:

$$\begin{aligned}\sum_{\tau=-\infty}^{\infty} R^2_{r\varepsilon_c}(\tau,\rho) &= \frac{1}{2\pi}\int_{-\pi}^{\pi} |\Phi_{r\varepsilon_c}(\omega,\rho)|^2 d\omega \\ &= \frac{1}{2\pi}\int_{-\pi}^{\pi} |L\big(M-K(\rho)(1-M)G\big)|^2 \Phi_r^2(\omega) d\omega\end{aligned}$$

With the expression of L given in (2.33), (2.36) becomes:

$$\lim_{N,l_1\to\infty,l_1/N\to 0} J_{N,l_1}(\rho) = J(\rho), \text{w.p.1.} \tag{2.37}$$

Because convergence is uniform, this implies that the minimizing argument $\hat{\rho}$ converges to the minimizing argument ρ_0 of $J(\rho)$. ■

Remark: $J_{N,l_1}(\rho)$ converges uniformly to $J(\rho)$ on $\mathcal{D}_K$ if $J(\rho)$ is bounded. This is the case if $L(M - K(\rho)(1 - M)G)$ is stable. If $K(\rho)$ is unstable, for example when the controller contains an integrator, and the unstable poles of $K(\rho)$ are zeros of $(1 - M)G$, then $L(M - K(\rho)(1 - M)G)$ is stable and $J(\rho)$ is bounded. If M is chosen with care such that $L(M - K(\rho)(1 - M)G)$ is stable, the convergence result holds also for unstable controllers.

Note that the error signal $\varepsilon_c(t, \rho)$ is filtered by L in the above implementation. This filtering can also be applied to the instrumental variables, as proposed in [44]. As the number of data tends to infinity, the estimates are equivalent.

2.4.2 Use of closed-loop experiments

Assume that data from the system stabilized by K_s are available. The closed-loop system of this controller and the plant G is given by M_s, i.e.

$$M_s = \frac{K_s G}{1 + K_s G}.$$

Let the unstable plant G be excited by $r(t)$ in closed loop according to the scheme of Figure 2.2. The output of the plant is affected by the noise $v(t)$. The discrete-time signals $r(t)$, $y(t)$, $u_1(t)$ and $u_2(t)$ of length N are available and are assumed to satisfy **A1-A4**. It is assumed that $L(1 - M)G/(1 + K_s G)$ has no zero on the imaginary axis. The error $\varepsilon_c(t, \rho)$ is given by (2.11). The vector of instrumental variables $\zeta(t)$ is given by (2.29). The correlation function $f_{N,l_1}(\rho)$ is given by (2.30), the correlation criterion $J_{N,l_1}(\rho)$ is defined in (2.31). The optimizer $\hat{\rho}$ is defined in (2.32).

Theorem 2.2 *Consider the controller structure defined in (2.7). Let the stable filter L be defined as:*

$$L(e^{-j\omega}) = \frac{F(e^{-j\omega})(1 - M(e^{-j\omega}))}{\big(1 - M_s(e^{-j\omega})\big)\Phi_r(\omega)}. \tag{2.38}$$

Then, as $N, l_1 \to \infty$ and $l_1/N \to 0$, the optimizer $\hat{\rho}$ in (2.32) converges w.p.1 to ρ_0, the optimizer of $J(\rho)$ as defined in Definition 2.1:

$$\lim_{N,l_1\to\infty, l_1/N\to 0} \hat{\rho} = \rho_0 \tag{2.39}$$

Proof: The proof is similar to that of Theorem 2.1. As $N, l_1 \to \infty$ and $l_1/N \to 0$, the correlation function $f_{N,l_1}(\rho)$ converges w.p.1 to the cross-correlation between $r(t)$ and $\varepsilon_c(t,\rho)$;

$$\begin{aligned} R_{r\varepsilon_c}(\tau,\rho) &= \lim_{N\to\infty} \frac{1}{N}\sum_{t=1}^{N} E\left\{r(t-\tau)\varepsilon_c(t,\rho)\right\} \\ &= \lim_{N\to\infty} \frac{1}{N}\sum_{t=1}^{N} r(t-\tau)L(1-M_s)\big[M-K(\rho)(1-M)G\big]r(t). \end{aligned}$$

Using Parseval's theorem, the correlation criterion converges to:

$$\begin{aligned} \sum_{\tau=-\infty}^{\infty} R^2_{r\varepsilon_c}(\tau,\rho) &= \frac{1}{2\pi}\int_{-\pi}^{\pi} |\Phi_{r\varepsilon_c}(\omega,\rho)|^2 d\omega \\ &= \frac{1}{2\pi}\int_{-\pi}^{\pi} |L(1-M_s)\big[M-K(\rho)(1-M)G\big]|^2 \Phi_r^2(\omega) d\omega \end{aligned}$$

Using the expression of L in (2.38) leads to

$$\lim_{N,l_1\to\infty, l_1/N\to 0} J_{N,l_1}(\rho) = J(\rho) \tag{2.40}$$

Even though G is unstable, the initial closed loop is stable and so is $L(1-M_s)(M-K(\rho)(1-M)G)$. The rest of the proof follows from the proof of Theorem 2.1. ■

Remark: The filter L depends on the unknown plant G and thus cannot be implemented. However,

$$\big(1-M_s(e^{-j\omega})\big)\Phi_r(\omega) = \frac{1}{1+K_s(e^{-j\omega})G(e^{-j\omega})}\Phi_r(\omega) = \Phi_{ru_2}(\omega),$$

where $\Phi_{ru_2}(\omega)$ is the cross-spectrum between $r(t)$ and $u_2(t)$, which can be estimated using the measured data. The weighting filter is then given by:

$$L(e^{-j\omega}) = \frac{F(e^{-j\omega})(1-M(e^{-j\omega}))}{\Phi_{ru_2}(\omega)}. \tag{2.41}$$

2.4.3 Use of a finite number of data

The following analysis is detailed for the scheme for stable plants. Analysis for the case of unstable plants is similar and therefore omitted here.

According to Theorem 2.1, as the number of data tends to infinity, the estimate $\hat{\rho}$ of (2.32) converges to ρ_0, the optimum of the approximate model reference problem as defined in Definition 2.1. In practice, only a finite number of data is available and an approximation of the criterion $J(\rho)$ is used. The quality of this approximation is analyzed next.

Using assumption **A2**, the error $\varepsilon_c(t,\rho)$ can be written as:

$$\begin{aligned}\varepsilon_c(t,\rho) &= L\big[M - K(\rho)(1-M)G\big]r(t) - LK(\rho)(1-M)H_v e(t)\\ &= D_d r(t) - D_s e(t) = r_{D_d}(t) - e_{D_s}(t) \quad (2.42)\end{aligned}$$

with obvious definitions for the filters D_d and D_s. The filter L for stable plants is given by (2.33). $r_{D_d}(t)$ represents the deterministic part of the error that stems from the reference signal $r(t)$, $e_{D_s}(t)$ results from the stochastic noise $v(t) = H_v e(t)$. The correlation function $f_{N,l_1}(\rho)$ can be expressed as:

$$f_{N,l_1}(\rho) = \frac{1}{N}\sum_{t=1}^{N}\zeta(t)\big[r_{D_d}(t) - e_{D_s}(t)\big] \quad (2.43)$$

In the absence of noise, the correlation criterion is given by:

$$\tilde{J}_{N,l_1}(\rho) = \frac{1}{N^2}\sum_{t=1}^{N}\zeta^T(t)r_{D_d}(t)\sum_{t=1}^{N}\zeta(t)r_{D_d}(t) = \sum_{\tau=-l_1}^{l_1}\hat{R}^2_{rr_{D_d}}(\tau)$$

where $\hat{R}_{rr_{D_d}}(\tau) = \frac{1}{N}\sum_{t=1}^{N} r(t-\tau)r_{D_d}(t)$ is an estimate of the cross-correlation between $r(t)$ and $r_{D_d}(t)$ given by

$$R_{rr_{D_d}}(\tau) = \lim_{N\to\infty}\frac{1}{N}\sum_{t=1}^{N}E\{r(t-\tau)r_{D_d}(t)\}.$$

The length of $\zeta(t)$ defines the size of the rectangular window.

The expected value of the correlation criterion $J_{N,l_1}(\rho)$ based on a finite number of data can then be expressed as:

$$E\{J_{N,l_1}(\rho)\} \approx \tilde{J}_{N,l_1}(\rho) + \frac{\sigma^2(2l_1+1)}{2\pi N}\int_{-\pi}^{\pi}\frac{|1-M|^4|K(\rho)|^2|H_v|^2|F|^2}{\Phi_r(\omega)}d\omega, \quad (2.44)$$

where the expected value is taken with respect to the noise $e(t)$. Consequently, the minimizer $\hat{\rho}$ of $J_{N,l_1}(\rho)$ based on a finite number of data is biased with respect to noise. Derivation of (2.44) is shown in Appendix A.1.

Asymptotically, $\tilde{J}_{N,l_1}(\rho)$ converges to $J(\rho)$ and the second term becomes zero, thus corresponding to the result of Theorem 2.1. However, for a finite number of data, the deterministic $\tilde{J}_{N,l_1}(\rho)$ corresponds to a windowed estimate of $J(\rho)$ and the second term adds a bias to the minimizer of this estimate.

Remarks:

- The controller that minimizes the biased criterion $J_{N,l_1}(\rho)$ will have a low gain wherever $|1-M|^2|H_v||F|$ is large. $(1-M)$ is the sensitivity function of the reference model and H_v represents the frequency contents of the noise. Hence, the controller gain is reduced at frequencies where both the sensitivity and the noise are high. This will in general increase the robustness of the closed-loop system.
- The controller gain is reduced in the frequency ranges where the input spectrum is weak. This is an interesting characteristic in the sense that, if the data are not informative in a frequency region, the controller gain in this region is decreased, which again increases the robustness of the closed-loop system.
- The bias in $J_{N,l_1}(\rho)$ decreases as the number of data N increases. It increases as the number of lags l_1 used in the instrumental variable vector $\zeta(t)$ increases.

Practical issues

The choice of l_1 determines the quality of the estimate $\tilde{J}_{N,l_1}(\rho)$. Assume that $R_{rr_{D_d}}(\tau) \approx 0$ for $|\tau| > \tau_0$, where τ_0 is an integer that depends on the length of the impulse response of D_d and the length of $R_r(\tau)$. In order to find a good estimate of $J(\rho)$, the length l_1 of

$\zeta(t)$ should be chosen as $l_1 \geqslant \tau_0$. However, (2.44) states that the bias increases as l_1 increases. With the choice of l_1, a trade-off is made between accuracy and bias.

2.4.4 Use of periodic data

The correlation function $f_{N,l_1}(\rho)$ as defined in (2.30) is an estimate of the cross-correlation between $r(t)$ and $\varepsilon_c(t,\rho)$, which is, in the noise-free case, given by $\hat{R}_{rr_{D_d}}(\tau)$ defined in Section 2.4.3. For non-periodic signals, this estimate is not exact, i.e. $\hat{R}_{rr_{D_d}}(\tau) \neq R_{rr_{D_d}}(\tau)$. If on the other hand periodic signals are considered, the deterministic part of the correlations can be calculated exactly. Periodic excitation should therefore be used whenever possible. In the following, the use of periodic data is discussed in detail for the open-loop scheme of Figure 2.1. Implementation for the closed-loop scheme is similar and is therefore not detailed here.

Let the plant G be excited in open loop by the periodic signal $r(t)$ of length N satisfying **A5** and **A6**. Assume that $L(1-M)G$ has no zero on the imaginary axis and that the noise satisfies **A1** and **A2**. For the periodic reference signal $r(t)$, the vector of instrumental variables defined in (2.29) is also periodic. The length of the instrumental variable vector $\zeta(t)$ satisfies $l_1 \leqslant (N_p - 1)/2$. The correlation function $f_{N,l_1}(\rho)$ is defined in (2.30) and the correlation criterion $J_{N,l_1}(\rho)$ in (2.31). The optimizer $\hat{\rho}$ is defined in (2.32).

Theorem 2.3 *Consider the controller structure defined in (2.7). Let the stable weighting filter L be defined for the frequencies ω_k where the spectrum $\Phi_r(\omega_k)$ is nonzero:*

$$L(e^{-j\omega_k}) = \frac{F(e^{-j\omega_k})(1 - M(e^{-j\omega_k}))}{\Phi_r(\omega_k)}. \tag{2.45}$$

Then, as $N, l_1 \to \infty$ and $l_1/N \to 0$, the optimizer $\hat{\rho}$ in (2.32) converges w.p.1 to ρ_0, the optimizer of $J(\rho)$ as defined in Definition 2.1:

$$\lim_{N,l_1\to\infty,l_1/N\to 0} \hat{\rho} = \rho_0 \tag{2.46}$$

Proof: The correlation function $f_{N,l_1}(\rho)$ converges to the cross-correlation between $r(t)$ and $\varepsilon_c(t,\rho)$, which is unaffected by noise due to **A1**:

$$\lim_{N\to\infty} f_{N,l_1}(\rho) = [R_{r\varepsilon_c}(-l_1,\rho),\ldots,R_{r\varepsilon_c}(l_1,\rho)]^T, \text{w.p.1.} \qquad (2.47)$$

The proof of Theorem 2.1 then holds as $N, l_1 \to \infty, l_1/N \to 0$. ■

This theorem states that the estimate converges to ρ_0 as the number of data tends to infinity. This result is equivalent to the non-periodic case of Theorem 2.1. However, because the deterministic part of the correlations can be calculated exactly for periodic data, the quality of the estimate is better for a finite number of data.

Remark: If a parametric representation of $\Phi_r(\omega_k)$ is available, the filter L can be implemented in the time domain since $F(q^{-1})$ and $M(q^{-1})$ are known. If such a representation is not available, the exact filter (2.45) can be applied in the frequency domain. The deterministic part of the periodic cross-correlation can therefore be found without any approximation, which is not the case for non-periodic reference signals. If a parametric representation is not available, the spectrum of a non-periodic signal needs to be estimated. Estimation of the spectrum leads to an approximation of L and consequently to an approximation of $R_{rr_{D_d}}(\tau)$.

A bias expression similar to (2.44) can be found for the periodic case. In general, the bias increases the robustness of the controller (see 2.4.3). The bias decreases as N increases, but it increases with the length of the instrumental variables. As for the non-periodic case, a trade-off between accuracy and bias is made through the choice of l_1.

2.5 Application to a double SCARA robot

In the previous sections, non-iterative correlation-based controller tuning is proposed to calculate the optimal controller parameters ρ_0 as defined in Definition 2.1. These parameters minimize the approximate model reference criterion for a given reference model M and a given controller structure. The designed controller achieves good performance if both M and the structure of $K(\rho)$ are appropriate for

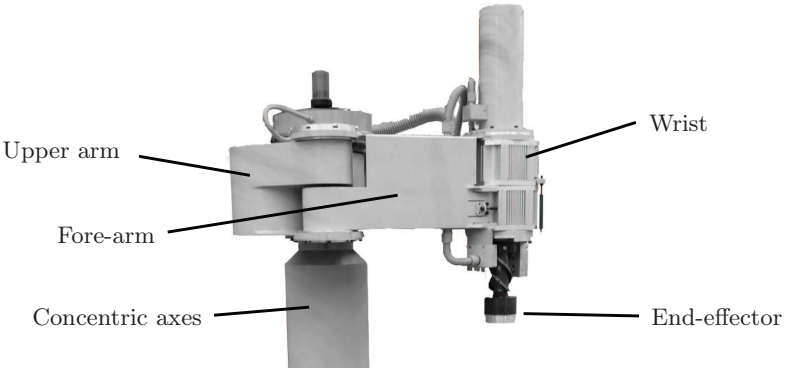

Fig. 2.5. FAMMDD double SCARA pick-and-place robot.

the plant. In practice, M and $K(\rho)$ are defined by the user and it is not straightforward how to choose either of them.

In this section, application of the proposed approach to a pick-and-place robot is discussed. It is shown how the approach can be used to systematically design low-order controllers, starting with the design of a high-order FIR controller. An orthogonal basis is then chosen to approximate the high-order FIR controller by a controller that can actually be implemented. If the order of the controller needs to be reduced further, the main characteristics of the high-order controllers can be used to define an appropriate structure for $K(\rho)$. In this example, all controllers are implemented, but the iterations can also be performed off-line. An iterative procedure is used to define the reference model, based on the windsurfing approach for iterative control design [3], where the required performance is increased gradually by increasing the bandwidth of the reference model.

Experimental setup

The pick-and-place robot considered is known as the FAMMDD, Fast and Accurate Manipulator Modules, Direct Drive. This robot is developed at Philips CFT [76]. The main design specification is that, for relatively simple assembly operations, the robot should be

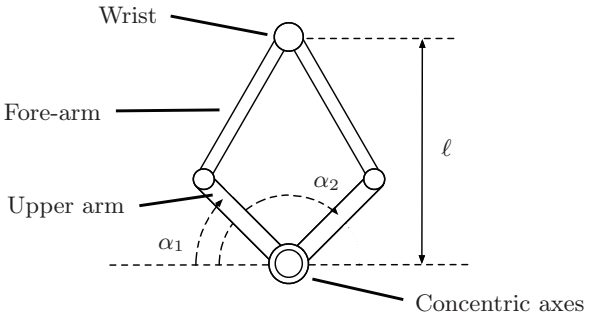

Fig. 2.6. Schematic representation of FAMMDD.

able to compete with a manual station. The version of the robot in the laboratory of the Control Systems Technology group at the Eindhoven University of Technology uses no transmission, hence the name Direct Drive.

The FAMM consists of two SCARAs (Selective Compliant Assembly Robot Arms), see Figures 2.5 and 2.6. The upper arms are fixed to two concentric axes, and the end-effector is situated at the wrist. The robot is driven by four AC motors, two in the wrist and two on the main axis. Only displacements in the horizontal plane will be considered in the experiments, the position of the end-effector in the wrist is fixed.

Both SCARAs are driven by a servomotor integrated in the axis. Permanent magnets are fixed to the axis, which acts as the rotor of the motor. The base of the robot contains the stator coils. An advantage compared to a single SCARA robot is that the mass of the main actuators does not move as the end-effector is displaced. The arms are designed such that the moving mass is minimized, while the required stiffness is maintained. The transmission-free actuation avoids play and other transmission disadvantages, but the load dynamics are dominant since they are not reduced by a transmission either.

The first motor drives the left arm, and affects the angle α_1, as shown in Figure 2.6. The second motor drives the right arm, affecting the angle α_2. If both motors are moving in the same direction,

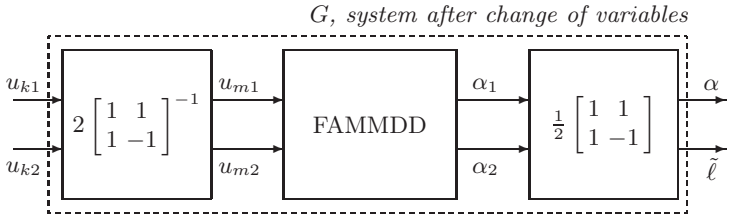

Fig. 2.7. Controlled variables as implemented on the FAMMDD.

$\alpha_1 - \alpha_2 = 0$ and the end-effector rotates around the main axis. If the motors move in opposite directions, the distance ℓ of the end-effector from the main axis changes. The load dynamics depend on the position ℓ of the end-effector, thereby resulting in nonlinear behavior.

Both angles α_1 and α_2 are measured. The objective is to position the end-effector, and the controlled variables are the rotation angle $\alpha = (\alpha_1 + \alpha_2)/2$ and $\tilde{\ell} = (\alpha_1 - \alpha_2)/2$. Note that ℓ is a nonlinear function of the controlled variable $\tilde{\ell}$. The implementation of this change of variables is shown in Figure 2.7. Outputs of the system are α and $\tilde{\ell}$, inputs are u_{k1} and u_{k2}, and u_{m1} and u_{m2} are the resulting inputs to the first and second motor respectively.

If the distance of the wrist from the main axis, ℓ, is constant, and only small rotations α around the axes are considered, the system is approximately linear. In the following experiments, the distance of the wrist from the main axis is controlled by $K_{\tilde{\ell}}$, a PD controller with a low-pass filter. The controller for the resulting SISO system with input u_{k1} and output α is designed using the approach of Section 2.4.2.

Experiments

An initial stabilizing controller, K_α, is available and the experiments are performed in closed loop, according to the scheme of Figure 2.8. Because there is no friction compensation, the experiments are performed on the robot in movement. The system is sampled with a sampling time of 1 ms. $r(t)$ is a PRBS with a period length of

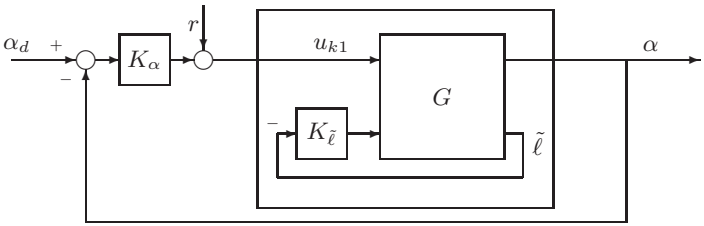

Fig. 2.8. Closed-loop setup used for controller tuning.

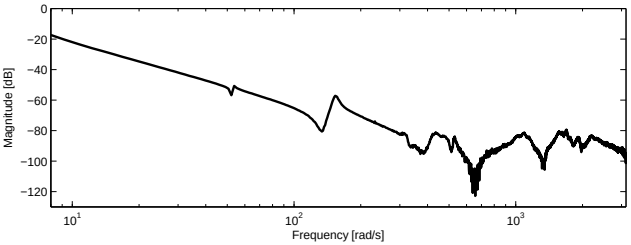

Fig. 2.9. Measured frequency response function from u_{k1} to α.

$N_p = 4095$ and amplitude 0.24. A sinusoid of ≈ 0.25 Hz with amplitude 0.6 radians is applied to $\alpha_d(t)$, where the exact frequency is chosen such that the excitation and its harmonics due to nonlinearities are located at frequencies in between the frequencies ω_k excited by $r(t)$.

A set of data of length $N = 150N_p$ is collected according to the scheme of Figure 2.2. The DFT of these signals is used to calculate a frequency response function of the transfer function from u_{k1} to α, see Figure 2.9. The first anti-resonance and resonance are situated around 150 rad/s.

Correlation-based non-iterative data-driven controller design

At low frequencies, the system behaves as a double integrator. The first reference model M_1 is chosen accordingly, such that $1 - M_1$ has

two zeros at 1:

$$M_1 = \frac{0.00137q^{-4} - 0.00135q^{-5}}{1 - 3.75q^{-1} + 5.32q^{-2} - 3.42q^{-3} + 0.898q^{-4} - 0.037q^{-5}}.$$

The bandwidth of M_1 lies below the first anti-resonance of the plant and it is expected that this objective can be achieved. Due to the anti-resonances in the system, the ideal controller (2.3) is expected to show resonant behaviour. In an FIR structure, such resonant behaviour can only be described if the order of the FIR filter is high. An FIR controller of order 1500 is therefore designed using the approach of Section 2.4.2. It is assumed that the distance between K^* and this high-order FIR controller $K(\rho)$ can be made very small, and that $K(\rho)$ approximates the characteristics of K^*. Since $r(t)$ is a PRBS signal, the extended instruments of (2.29) can be taken as,

$$\zeta(t) = [r(t), r(t-1), \ldots, r(t-l_1)]^T. \tag{2.48}$$

$F = 1$ and $l_1 = (N_p - 1)/2$. Note that, since $\hat{\rho}$ can be determined analytically, and $N_p = 4095$, no computational problems are encountered for the calculation of 1500 parameters.

The Bode diagram of the 1500th-order FIR controller is shown in Figure 2.10. The controller contains two poorly damped resonances, one that cancels the first anti-resonance of the plant and a second one at a higher frequency. This controller cannot be implemented, first of all because the order of the controller is too large. Secondly, even though this controller may achieve perfect model matching for the measured output α, it is not necessarily a good controller for the plant. For systems that contain an anti-resonance, cancelation of this anti-resonance may cause oscillations in other (not necessarily measured) parts of the system.

A second controller of order 30 is therefore calculated, with an orthogonal basis of Laguerre functions with poles in 0.8. This orthogonal basis offers many degrees of freedom at low frequencies, and thus permits model matching at the frequencies that are important for closed-loop performance. However, the match at high frequencies is expected to be limited. The Bode diagram of the resulting controller is shown in Figure 2.10. The damping of the low-frequency resonance is larger than that of the FIR controller. As expected, the

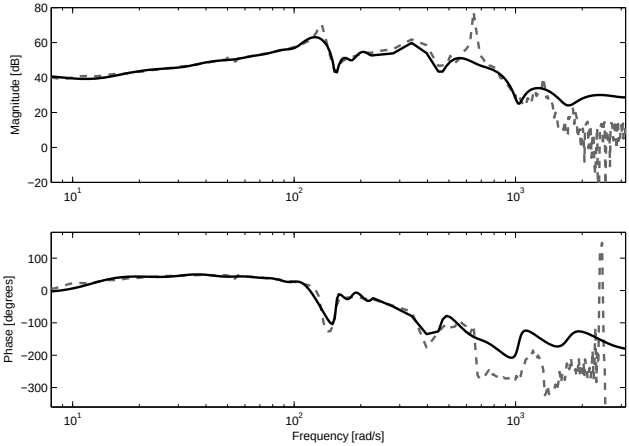

Fig. 2.10. Calculated controllers for M_1. Grey dashed: FIR of order 1500. Black: Laguerre basis functions of order 30.

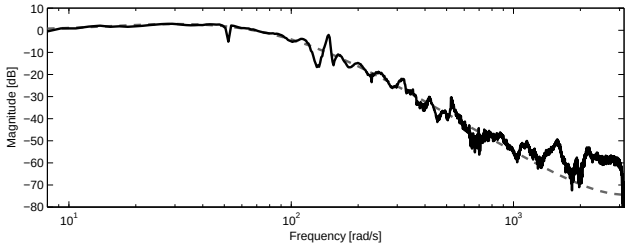

Fig. 2.11. Achieved closed-loop performance. Grey dashed: reference model M_1. Black: measured FRF of the complementary sensitivity with 30th-order controller.

controller resembles the FIR controller at low frequencies, but the fit at higher frequencies is limited.

The 30th-order controller is implemented and the same experiment as described above is performed with this controller in the loop. The measured response is used to estimate the complementary sensitivity function. The achieved closed-loop performance is shown in

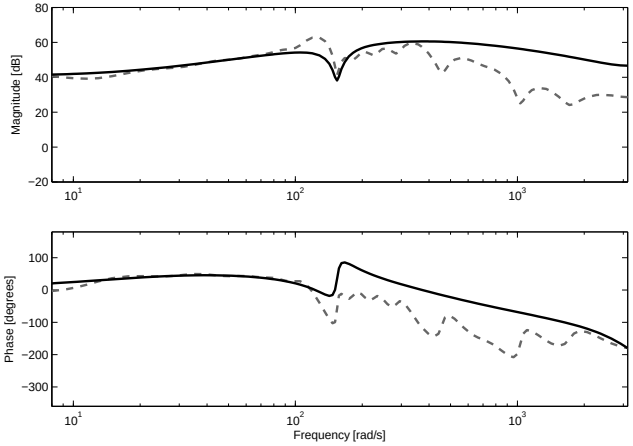

Fig. 2.12. Calculated controllers for M_1. Grey dashed: Laguerre basis of order 30. Black: K_1 of order 4

Figure 2.11. The controller structure does not permit perfect model matching, but the error is small at all frequencies ranges.

If, for practical reasons, the order of the controller needs to be reduced further, the characteristics of the 1500th- and 30th-order controller can be used to choose an appropriate structure for the low-order controller. In this example, a controller of order 4 is designed, using the data that is measured with the 30th-order controller in the loop. The high-order FIR controller and the 30th-order controller clearly show the behaviour of a notch filter at about 160 rad/s. Some of the parameters of the low-order controller need to be fixed to reproduce this behaviour. The fixed part of the controller therefore includes a notch filter, designed using the response of the 30th-order controller. The remaining two poles are fixed at 0.7. The structure of the controller is given by:

$$K_1(\rho) = \frac{(\rho_0 + \rho_1 q^{-1} + \rho_2 q^{-1})(1 - z_1 q^{-1})(1 - z_2 q^{-1})}{(1 - p_1 q^{-1})(1 - p_2 q^{-1})(1 - p_3 q^{-1})(1 - p_4 q^{-1})},$$

where $z_1 = z_2^* = 0.98 + 0.15i$, $p_1 = p_2^* = 0.95 + 0.14i$ and $p_3 = p_4 = 0.7$. This controller structure cannot cancel the anti-resonance of the

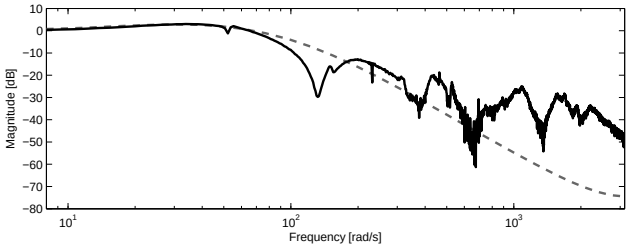

Fig. 2.13. Achieved closed-loop performance. Grey dashed: reference model M_1. Black: measured FRF of the complementary sensitivity with K_1.

system. $\zeta(t)$ is defined as (2.48), with $l_1 = 500$ and $F = 1$. The Bode diagram of the resulting controller is shown in Figure 2.12, where the Bode diagram of the 30th-order controller is given for comparison.

The achieved closed-loop performance is shown in Figure 2.13. The controlled system matches the reference model at low frequencies, up to the bandwidth of M_1. At higher frequencies, the model cannot be matched due to the limited structure of K_1. However, since the controlled system resembles the reference model up to the bandwidth, the tracking performance achieved with this low-order controller is expected to be good. The time response of the controlled system is shown in Fig. 2.14. As expected, the response of the system follows the response of the reference model reasonably well. Note that the time responses shown in this section are normalized for comparison.

Increasing the bandwidth of the controlled system

The performance requirements can be increased by increasing the bandwidth of the reference model. A second reference model is defined as

$$M_2 = \frac{0.03211q^{-4} - 0.03117q^{-5}}{1 - 3.01q^{-1} + 3.36q^{-2} - 1.68q^{-3} + 0.34q^{-4} - 0.013q^{-5}}.$$

A new set of data of length $N = 150N_p$ is collected with K_1 in the loop. A low-order controller $K_2(\rho)$ is designed, with the same

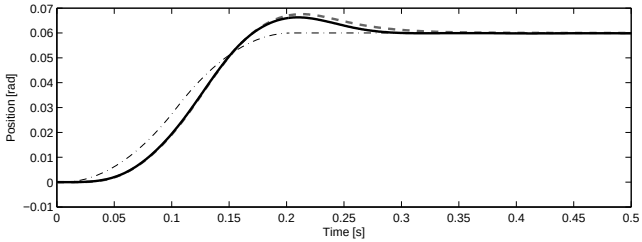

Fig. 2.14. Tracking performance. Dash-dot thin line: reference signal α_d. Black: measured response with K_1. Grey dashed: response of the reference model M_1. Note that the measured response and the response to M_1 are overlapping up to about 0.2 seconds.

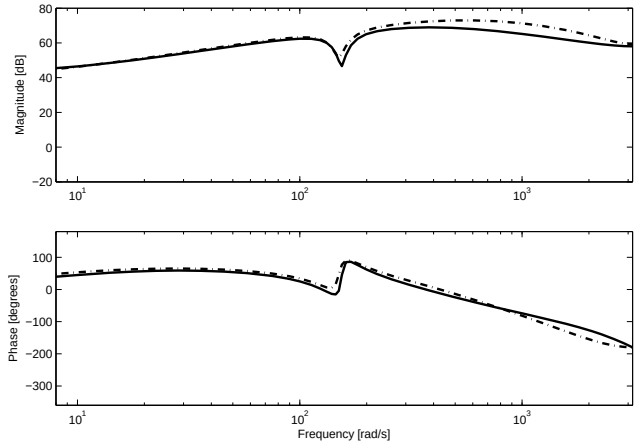

Fig. 2.15. Calculated controllers for M_2. Black: 4th-order controller K_2, calculated according to Section 2.4.2. Dash-dot: 5th-order controller K_{ls}.

structure as that of $K_1(\rho)$. $\zeta(t)$ is defined according to (2.48), $l_1 = 500$ and $F = 1$.

For comparison, another controller K_{ls} is designed using loop shaping. The non-parametric model of Figure 2.9 is used to design the controller, and the cross-over frequency is chosen similar to that

of $M/(1-M)$. A notch filter is introduced to deal with the resonance. This filter is designed using the non-parametric model and is not the same as the fixed part of K_1 and K_2. A lead filter is added for the phase margin. A second-order low-pass filter is added to limit the high-frequency gain, resulting in a 5th-order controller.

The Bode diagram of K_2 and of K_{ls} are shown in Figure 2.15. The achieved closed-loop performance is shown in Figure 2.16. Model-matching up to the bandwidth is not possible with the limited controller structure. Since the control objective for K_2 is model-matching, it is expected that the achieved model-reference criterion J_{mr} of (2.1) is smaller for K_2 than for K_{ls}. J_{mr} can be approximated by $\hat{J}_{mr}(K) = \sum_{\omega_k}[M_2(e^{-j\omega_k}) - T(e^{-j\omega_k})]^2$, where $T(e^{-j\omega_k})$ is the measured FRF as shown in Figure 2.16. As expected, $\hat{J}_{mr}(K_2) = 93.9 < \hat{J}_{mr}(K_{ls}) = 104.2$. The maximum value of the measured sensitivity function $S(e^{-j\omega_k})$ is larger for K_2 than for K_{ls} (not shown). This can be expected since there are no specifications on the robustness margins in model reference control, whereas the loop-shaping controller K_{ls} satisfies a specification on the modulus margin.

The time-domain response of the controlled plant is shown in Figure 2.17. Note that the measured response of the plant controlled by K_{ls} cannot be distinguished from the overlapping response of the plant controlled by K_2. The response of the plant controlled by K_2 is thus comparable to that of the plant controlled by K_{ls}. Note also that the reference signal α_d in Figure 2.17 is the same as α_d in Figure 2.14. The response of M_2 is much faster than the response of M_1 and the response of the reference model is almost superposed on α_d.

The achieved tracking performance of K_2 is thus comparable to the tracking achieved by the loop-shaping controller K_{ls}. The Bode diagram of K_2 and that of K_{ls} are also very similar. This result might not be surprising for such low-order controllers. However, it should be noted that the structure of K_2 is found systematically from a series of optimization problems, and the proposed approach can be used to calculate the optimal controller for any predefined controller structure and order. If a higher order controller can be implemented in practice, the achieved performance is improved, as illustrated by the results achieved with the 30th-order controller, shown in Figure 2.11.

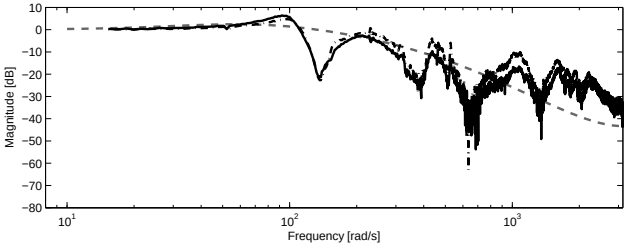

Fig. 2.16. Achieved closed-loop performance. Grey dashed: reference model M_2. Black: measured FRF of the complementary sensitivity with K_2. Black dash-dot: measured complementary sensitivity with 5th-order K_{ls}.

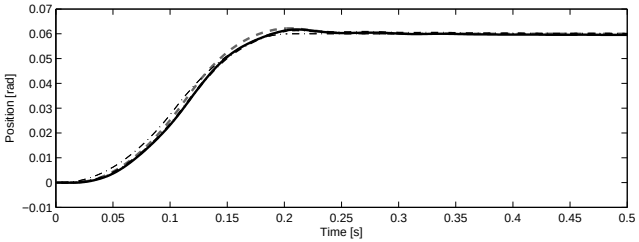

Fig. 2.17. Tracking performance. Dash-dot thin line: reference signal α_d. Black: measured response with 4th-order K_2. Black dash-dot: measured response with 5th-order K_{ls}. Grey dashed: response of the reference model M_2.

2.6 Conclusions

In this chapter, an approximate model reference criterion is defined, and straightforward schemes are proposed that can be used to identify the controller that minimizes this approximate model reference criterion. The resulting controller identification problem is analyzed. Two cases are considered. In the first case it is assumed that perfect model matching can be achieved with the predefined controller structure. It is shown that, in this case, the controller identification problem corresponds to an identification problem with a spe-

cific noise model, where the noise model depends on the controller parameters. In the second case, it is assumed that the structure of the controller does not allow perfect model matching and that a bias error exists between the ideal controller and the optimal controller. It is shown that, in the presence of measurement noise, a controller identified using prediction error methods does not converge to the optimal controller.

The use of the correlation approach is proposed to deal with the effect of noise in the controller identification problem. It is shown that the estimated controller converges to the optimal controller, also if perfect model matching cannot be achieved. Both periodic and non-periodic excitation signals are considered and the approach is applicable to both stable and unstable systems. A closed-loop experiment is proposed for unstable systems. This closed-loop approach has been applied to a pick-and-place robot.

3

Data-driven controller tuning with guaranteed stability

There is no guarantee that a controller determined by minimizing the model reference criterion $J_{mr}(\rho)$ or its approximation $J(\rho)$ actually stabilizes the plant. Instability can occur if the reference model is chosen inappropriately or if the measurements are strongly affected by noise. The ideal controller K^* is defined indirectly from G and M as shown in (2.3). Whether K^* stabilizes the plant depends on both the plant G and the choice of reference model M. If the plant is nonminimum phase, internal stability can only be guaranteed when M contains the unstable zeros of G. This clearly makes the choice of an appropriate M difficult in a data-driven approach.

Even if the ideal controller K^* stabilizes the plant, this is not necessarily the case for the optimal controller $K(\rho_0)$ (see [31] for an example where K^* was not in the controller set). Furthermore, if the optimal controller $K(\rho_0)$ stabilizes the plant, an estimate of $K(\rho_0)$ based on noisy data might not be stabilizing.

Instability due to an inappropriate reference model is not specific to data-driven methods, it is inherent to model reference control. In the following, a constraint is proposed that can be added to the model reference optimization problem, or to its approximation. The optimizer of the constrained problem is guaranteed to stabilize the plant.

Implementation of the constraint in a data-driven setting is discussed in Section 3.2 and 3.3. It is shown that, for linearly parameterized controllers, an estimate of the stability condition leads to

a set of convex constraints. These constraints can be added to any data-driven controller tuning scheme. In Sections 3.2 and 3.3, the constraints are added to the correlation approach of Section 2.4.

3.1 Model reference control with guaranteed stability

In the following, a sufficient condition is defined for closed-loop stability of the plant G controlled by the controller $K(\rho)$. This condition is based on the existence of a stabilizing controller K_s. The sensitivity and complementary sensitivity function of the plant controlled by this K_s are used to define the stability condition. However, in order to verify the condition, this K_s does not need to be known. In Section 3.2 it is shown how, for stable minimum-phase plants, the condition can be verified using the reference model and data from an open-loop experiment. For unstable or nonminimum-phase plants, data from a specific closed-loop experiment are sufficient to verify the condition, as shown in Section 3.3.

Consider the stabilizing controller K_s. The closed-loop plant for this controller is given by:

$$M_s = \frac{K_s G}{1 + K_s G} \tag{3.1}$$

The closed-loop system with controller $K(\rho)$ can be represented as illustrated in Figure 3.1.

Define $\Delta(\rho) := M_s - K(\rho)G(1 - M_s)$ and its infinity norm $\delta(\rho) := \|\Delta(\rho)\|_\infty$.

Theorem 3.1 *The controller $K(\rho)$ stabilizes the plant G if*

1. *$\Delta(\rho)$ is stable*
2. *$\exists \delta_N \in \ ]0, 1[$ such that $\delta(\rho) \leqslant \delta_N$*

Proof: If Condition 1 is satisfied, all transfer functions of the loop opened at q are stable, since K_s stabilizes the plant, i.e. the transfer functions from $r(t), v(t)$ and $q(t)$ to $e(t), y(t), u(t)$ and $q(t)$ are stable. The sufficient condition for stability of the closed-loop interconnection follows from the small-gain theorem [85] : the interconnection is stable if

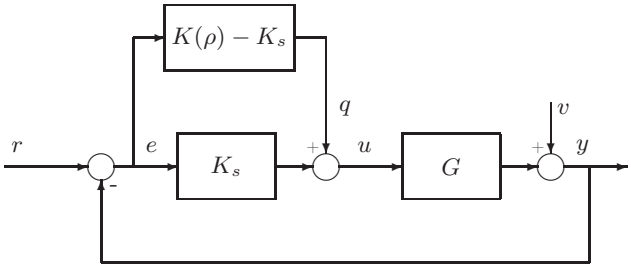

Fig. 3.1. Closed-loop system with controller $K(\rho)$ and explicit representation of the controller error $K(\rho) - K_s$

$$\left\| \frac{-(K(\rho) - K_s)G}{1 + K_s G} \right\|_\infty < 1 \tag{3.2}$$

This is the H_∞-norm of the transfer function from q back to q. Replacing $\frac{K_s G}{1+K_s G}$ by M_s and $\frac{1}{1+K_s G}$ by $1 - M_s$ gives

$$\left\| \frac{-(K(\rho) - K_s)G}{1 + K_s G} \right\|_\infty = \delta(\rho).$$

■

Theorem 3.1 thus follows from the small-gain theorem. Similar conditions for stability have been used for controller reduction (see for example [86], p. 491).

Condition 1 is satisfied if the controller $K(\rho)$ is stable, but unstable controllers can also satisfy Condition 1. Consider for example a controller with an integrator. The transfer function $\Delta(\rho) = M_s - K(\rho)G\,(1 - M_s)$ is stable if $G(1 - M_s)$ contains a zero at 1.

This sufficient condition for closed-loop stability can be used to guarantee a stabilizing solution to the model reference problem of Section 2.1.

Definition 3.1 (Stabilizing controller) *Let the controller be parameterized as in (2.7) and $J(\rho)$ given by (2.6). Let Condition 1 from Theorem 3.1 be satisfied. The parameters ρ_s of the stabilizing controller $K(\rho_s)$ are given by the optimum of the following constrained convex optimization:*

$$\begin{aligned} \rho_s &= \arg \min_{\rho \in \mathcal{D}_K} J(\rho) \\ &\text{subject to } \delta(\rho) \leqslant \delta_N \end{aligned} \tag{3.3}$$

In the following, a data-driven approach is presented that combines minimization of the estimate $J_{N,l_1}(\rho)$ and a set of constraints that estimate the bound $\delta(\rho)$. The estimation errors can be taken into account through the choice of δ_N, as shown in Section 3.5.

3.2 Data-driven approach for stable minimum-phase systems

Theorem 3.1 is based on the small-gain theorem and requires the closed-loop system M_s to be internally stable. For stable minimum-phase plants, any stable reference model M defines the ideal controller K^* according to (2.3) that internally stabilizes the system. The reference model can therefore be used to define the sufficient condition for stability.

Lemma 3.1 *Let M_s be given by M. The controller $K(\rho)$ stabilizes the stable minimum-phase plant G if $\Delta(\rho) = M_s - K(\rho)G(1-M_s) = M - K(\rho)G(1-M)$ is stable and $\exists \delta_N \in \ ]0,1[$ such that*

$$\begin{aligned} \delta(\rho) &= \|M_s - K(\rho)(1-M_s)G\|_\infty \\ &= \|M - K(\rho)(1-M)G\|_\infty \leqslant \delta_N \end{aligned} \tag{3.4}$$

Proof: Follows from Theorem 3.1 upon replacing K_s by the stabilizing ideal controller K^*. ∎

Remark: Through the definition of K^* given in (2.3), K^* might be non-causal, but K^*G is always causal. The small-gain theorem requires causality because algebraic loops will occur for non-causal functions. However, since K^*G is always causal, no algebraic loop occurs in the interconnection of Figure 3.1 and Lemma 3.1 remains valid.

If the plant G or the controller $K(\rho)$ contains one or several integrators, the above scheme remains applicable provided the reference model is chosen with care. Let n_i be the number of integrators in the loop function KG. It is then easily verified that $\Delta(\rho)$ is stable if

$1 - M$ has $n_z \geqslant n_i$ zeros at 1. The reference model M needs to be chosen such that this condition is satisfied. Note that, if $n_i = 1$, all reference models with unity static gain satisfy this condition.

For stable minimum-phase plants, the optimization in Definition 3.1 can thus be replaced by

$$\begin{aligned} \rho_s = \arg \min_{\rho \in \mathcal{D}_K} J(\rho) \\ \text{subject to} \\ \|M - K(\rho)(1-M)G\|_\infty \leqslant \delta_N \end{aligned} \tag{3.5}$$

Remark: Condition (3.4) is sufficient but not necessary and therefore conservative. The optimal controller $K(\rho_0)$ might stabilize the system but not meet condition (3.4). However, this indicates that the distance between $K(\rho)$ and K^* cannot be made small. In this case, the approximate model reference criterion (2.6) is not a good approximation of (2.1).

In a data-driven approach, the available signals from the scheme of Figure 2.1 can be used to estimate $\delta(\rho)$. Define

$$\begin{aligned} \varepsilon_s(t,\rho) &:= Mr(t) - K(\rho)(1-M)y(t) \\ &= \big[M - K(\rho)(1-M)G\big]r(t) - K(\rho)(1-M)v(t) \end{aligned} \tag{3.6}$$

Note that the transfer function between $r(t)$ and $\varepsilon_s(t,\rho)$ is equal to $\Delta(\rho)$. Hence, the available signals $r(t)$ and $\varepsilon_s(t,\rho)$ can be used to estimate $\delta(\rho)$. It will be shown that a spectral estimate leads to a set of convex constraints on the controller parameters ρ.

In Chapter 2, the open-loop scheme can be used for both minimum and nonminimum-phase stable systems. However, Lemma 3.1 is not valid for nonminimum-phase stable systems, and the closed-loop scheme of Section 3.3 needs to be used.

Implementation using spectral estimates

In the following, it is shown that a spectral estimate of $\delta(\rho)$ defines a set of convex constraints. These constraints are added to the correlation approach presented in Section 2.4.1. Let the plant G be excited by $r(t)$ as illustrated in Figure 2.1. The output of the plant

is affected by noise, $y(t) = Gr(t) + v(t)$. The signals $r(t)$ and $y(t)$ of length N are available and assumed to satisfy **A1-A4**. The correlation criterion $J_{N,l_1}(\rho)$ is given by (2.31).

An estimate of $\delta(\rho)$ based on spectral estimates is given by:

$$\hat{\delta}(\rho) = \max_{\omega_k} \left| \frac{\hat{\Phi}_{r\varepsilon_s}(\omega_k, \rho)}{\hat{\Phi}_r(\omega_k)} \right|, \tag{3.7}$$

where $\hat{\Phi}_r(\omega_k)$ is an estimate of the spectrum of $r(t)$ for $\omega_k = 2\pi k/(2l_2+1)$, where $k = 0, \ldots, l_2 + 1$:

$$\hat{\Phi}_r(\omega_k) = \sum_{\tau=-l_2}^{l_2} \hat{R}_r(\tau) e^{-j\tau\omega_k},$$

and $\hat{R}_r(\tau)$ is an estimate of the auto-correlation $R_r(\tau)$ of $r(t)$:

$$\hat{R}_r(\tau) = \frac{1}{N} \sum_{t=1}^{N} r(t-\tau) r(t), \text{ for } \tau = -l_2, \ldots, l_2, \tag{3.8}$$

where l_2 defines the length of the rectangular window. $\hat{\Phi}_{r\varepsilon_s}(\omega_k, \rho)$ is an estimate of the cross-spectrum between $r(t)$ and $\varepsilon_s(t, \rho)$:

$$\hat{\Phi}_{r\varepsilon_s}(\omega_k, \rho) = \sum_{\tau=-l_2}^{l_2} \hat{R}_{r\varepsilon_s}(\tau, \rho) e^{-j\tau\omega_k},$$

using an estimate of the cross-correlation $R_{r\varepsilon_s}(\tau, \rho)$:

$$\hat{R}_{r\varepsilon_s}(\tau, \rho) = \frac{1}{N} \sum_{t=1}^{N} r(t-\tau) \varepsilon_s(t, \rho), \quad \tau = -l_2, \ldots, l_2.$$

Note that, although a rectangular window is used here, other windows can also be used.

Using the controller parameterization (2.7), $\hat{\Phi}_{r\varepsilon_s}(\omega_k, \rho)$ can be expressed as a linear combination of the controller parameters:

$$\begin{aligned} \hat{\Phi}_{r\varepsilon_s}(\omega_k, \rho) = \frac{1}{N} \sum_{\tau=-l_2}^{l_2} \sum_{t=1}^{N} \big[& r(t-\tau) M r(t) e^{-j\tau\omega_k} \\ & - r(t-\tau) \beta^T (1-M) y(t) e^{-j\tau\omega_k} \rho \big]. \end{aligned} \tag{3.9}$$

The estimate (3.7) can thus be used to define a set of convex constraints such that $\hat{\delta}(\rho) \leqslant \delta_N$. An approximation of (3.5) is given by:

$$\begin{gathered}\hat{\rho} = \arg \min_{\rho \in \mathcal{D}_K} J_{N,l_1}(\rho) \\ \text{subject to} \\ \left| \sum_{\tau=-l_2}^{l_2} \hat{R}_{r\varepsilon_s}(\tau,\rho) e^{-j\tau\omega_k} \right| \leqslant \delta_N \left| \sum_{\tau=-l_2}^{l_2} \hat{R}_r(\tau) e^{-j\tau\omega_k} \right|, \\ \omega_k = 2\pi k/(2l_2+1), \quad k = 0, \ldots, l_2+1\end{gathered} \tag{3.10}$$

Note that, in contrast to the unconstrained problem of Section 2.4, this optimization cannot be solved analytically. Both the objective function and the constraints in (3.10) are differentiable and the constrained optimization can be solved numerically. The problem can be solved for up to several thousand constraints and the solution is the global optimum.

Theorem 3.2 *Consider the controller structure defined in (2.7). Let the stable filter L be defined as:*

$$L(e^{-j\omega}) = \frac{F(e^{-j\omega})(1 - M(e^{-j\omega}))}{\Phi_r(\omega)} \tag{3.11}$$

*Assume that **A1-A4** are satisfied, that $L(1-M)G$ has no zero on the imaginary axis and that a strictly feasible solution exists for (3.10), for the series of optimization problems as $N, l_1, l_2 \to \infty$ as well as for (3.5). Then, as $N, l_1, l_2 \to \infty$ and $l_1/N, l_2/N \to 0$, the optimizer $\hat{\rho}$ in (3.10) converges w.p.1 to the stabilizing optimizer ρ_s of $J(\rho)$ defined in (3.5):*

$$\lim_{N,l_1,l_2 \to \infty, l_1/N, l_2/N \to 0} \hat{\rho} = \rho_s, \tag{3.12}$$

Proof: Convergence of the unconstrained problem w.p.1 follows from Theorem 2.1. As $N, l_1 \to \infty, l_1/N \to 0$ the correlation criterion $J_{N,l_1}(\rho) \to J(\rho)$ and the convergence is uniform on $\mathcal{D}_K$.

As $N \to \infty, l_2/N \to 0$, the estimate $\hat{R}_{r\varepsilon_s}(\tau,\rho)$ converges w.p.1 to $R_{r\varepsilon_s}(\tau,\rho)$ and $\hat{R}_r(\tau)$ converges w.p.1 to $R_r(\tau)$, for $\tau = [-l_2, \ldots, l_2]$.

Consequently $\frac{\hat{\Phi}_{r\varepsilon_s}(\omega_k,\rho)}{\hat{\Phi}_r(\omega_k)}$ converges pointwise to $\Delta(\omega_k)$, w.p.1. $\Delta(\omega_k)$ and $\delta(\rho)$ are bounded on $\mathcal{D}_K$ since Δ is stable. The series of convex functions $\max_{\omega_k} |\Delta(\omega_k)|$ then converges uniformly to the convex function $\delta(\rho)$ as $l_2 \to \infty$ (Theorem 10.8 of [69]). It follows that, with probability 1, $\max_{\omega_k} \left|\frac{\hat{\Phi}_{r\varepsilon_s}(\omega_k,\rho)}{\hat{\Phi}_r(\omega_k)}\right|$ converges uniformly to $\delta(\rho)$ as $N, l_2 \to \infty, l_2/N \to 0$.

Convergence of the constrained optimization then follows from the dual problem (Theorem 1.44 [13]): Consider the function $\mathcal{L}(\rho) := J(\rho) + \nu(\delta(\rho) - \delta_N)$, where ν is Lagrange multiplier and (ν_0, ρ_0) is a KKT (Karush-Kuhn-Tucker) point of $\mathcal{L}(\rho)$. Then ρ_0 is the global optimizer of (3.5). Since $J_{N,l_1}(\rho)$ and $\max_{\omega_k} \left|\frac{\hat{\Phi}_{r\varepsilon_s}(\omega_k,\rho)}{\hat{\Phi}_r(\omega_k)}\right|$ converge uniformly to $J(\rho)$ and $\delta(\rho)$, the dual of (3.10) converges uniformly to $\mathcal{L}(\rho)$. Since the convergence is uniform, it follows that the optimizer of (3.10) converges to the optimizer of (3.5). ∎

Implementation for periodic data

It is well known that the quality of spectral estimates can be improved when periodic data is used [54]. Periodic excitation should therefore be used whenever possible. The use of periodic data also improves the quality of the correlation criterion estimate (see Section 2.4.4). The trade-off for this improved quality is a limited frequency resolution.

Assume that **A1, A2, A5** and **A6** are satisfied. The length of the instrumental variable vector $\zeta(t)$ of (2.29) is chosen as $l_1 \leqslant (N_p - 1)/2$. The correlation criterion $J_{N,l_1}(\rho)$ is defined in (2.31).

The auto-correlation of the periodic reference $r(t)$ can be calculated using (2.15). According to assumption **A6**, the spectrum is nonzero for $\omega_k = 2\pi k/N_p, k = 0, \ldots, N_p - 1$. Due to symmetry, it is completely defined by half of the frequencies, i.e. $\omega_k = 2\pi k/N_p, k = 0, \ldots, \lfloor (N_p - 1)/2 \rfloor$. Let the error signal $\varepsilon_s(t, \rho)$ be generated periodically, i.e. no transients are present in the response. The cross-spectrum can be estimated for the same frequencies ω_k:

$$\hat{\Phi}_{r\varepsilon_s}(\omega_k, \rho) = \sum_{\tau=0}^{N_p-1} \hat{R}_{r\varepsilon_s}(\tau, \rho) e^{-j\tau\omega_k}, \tag{3.13}$$

where $\hat{R}_{r\varepsilon_s}(\tau,\rho)$ is given by:

$$\hat{R}_{r\varepsilon_s}(\tau,\rho)=\frac{1}{N}\sum_{t=1}^{N} r(t-\tau)\varepsilon_s(t,\rho),\quad \tau=0,\ldots,N_p-1. \tag{3.14}$$

The spectral estimate

$$\hat{\delta}(\rho)=\max_{\omega_k}\left|\frac{\hat{\Phi}_{r\varepsilon_s}(\omega_k,\rho)}{\Phi_r(\omega_k)}\right| \tag{3.15}$$

can be used to define a set of convex constraints. This estimate does not contain leakage errors and has a decreasing variance with increasing number of periods [54]. For periodic signals, the optimization problem (3.5) can be approximated by:

$$\begin{gathered}\hat{\rho}=\arg\min_{\rho\in\mathcal{D}_K} J_{N,l_1}(\rho)\\ \text{subject to}\\ \left|\sum_{\tau=0}^{N_p-1}\hat{R}_{r\varepsilon_s}(\tau,\rho)e^{-j\tau\omega_k}\right|\leqslant\delta_N\left|\sum_{\tau=0}^{N_p-1}R_r(\tau)e^{-j\tau\omega_k}\right|,\\ \omega_k=2\pi k/N_p,\quad k=0,\ldots,\lfloor(N_p-1)/2\rfloor\end{gathered} \tag{3.16}$$

$\lfloor\cdot\rfloor$ denotes the closest integer below.

Theorem 3.3 *Consider the controller structure defined in (2.7). Let the stable filter L be defined for the frequencies ω_k where the spectrum $\Phi_r(\omega_k)$ is nonzero:*

$$L(e^{-j\omega_k})=\frac{F(e^{-j\omega_k})(1-M(e^{-j\omega_k}))}{\Phi_r(\omega_k)} \tag{3.17}$$

*Assume that **A1, A2, A5** and **A6** are satisfied, that $L(1-M)G$ has no zero on the imaginary axis and that a strictly feasible solution exists for (3.16), for the series of optimization problems as $N,l_1,N_p\to\infty$ as well as for (3.5). Then, as $N,N_p,l_1\to\infty$ and $N_p/N\to 0$, the optimizer $\hat{\rho}$ of (3.16) converges w.p.1 to the stabilizing optimizer of $J(\rho)$ defined in (3.5):*

$$\lim_{N,N_p,l_1\to\infty,N_p/N\to 0}\hat{\rho}=\rho_s \tag{3.18}$$

Proof: Follows from Theorem 2.3 and Theorem 3.2 . ∎

3.3 Data-driven approach for nonminimum-phase or unstable systems

For nonminimum-phase or unstable plants, an arbitrary reference model M does not define a stabilizing ideal controller K^*. For such plants, Lemma 3.1 is not applicable, and the optimization of (3.3) needs to be used instead of (3.5). In (3.3), the control criterion $J(\rho)$ is defined using the (arbitrary) reference model M, whereas the constraint for stability uses M_s. If a stabilizing controller K_s is available, the closed-loop interconnection of G and K_s represents M_s given in (3.1). In order to estimate $\delta(\rho)$, a set of input-output data of the transfer function $M_s - K(\rho)(1 - M_s)G$ is sufficient.

Consider the tuning scheme of Figure 2.2. Define

$$\begin{aligned} &\varepsilon_s(t,\rho) := -u_1(t) - K(\rho)y(t) \\ &= \big(M_s - K(\rho)(1 - M_s)G\big)r(t) + (K_s - K(\rho))(1 - M_s)v(t) \end{aligned} \quad (3.19)$$

The transfer function between $r(t)$ and $\varepsilon_s(t,\rho)$ is equal to $\Delta(\rho)$, and the signals available from the scheme of Figure 2.2 can be used to estimate $\delta(\rho)$.

Remarks:

- In the case of stable minimum-phase plants, the fact that the constraint in (3.5) is active indicates that the model reference criterion was inappropriate. This is no longer the case for the closed-loop scheme of Figure 2.2, where violation of the constraint in (3.3) simply implies that closed-loop stability cannot be guaranteed, because the distance between the controller $K(\rho)$ and the stabilizing controller K_s is not small. This result agrees with ideas from iterative identification and control, e.g. [3,53]. In [53], the term "safe controller change" is used to denote an acceptable controller change that ensures a certain stability margin. The idea is that, by limiting the change in the controller, one can also limit the degradation that can occur in the actual closed-loop system.
- A test that uses experimental closed-loop data to verify whether a controller stabilizes the plant is proposed in [50]. The method uses coprime factorization and can handle unstable systems as

well as unstable controllers. In the specific case of a stable controller, the experiment proposed in [50] corresponds to the scheme of Figure 2.2. The transfer function considered in our stability criterion is the same as the transfer function considered in the stability test in [50]. However, the stability tests are different. In [50], both phase and amplitude are taken into account. The Nyquist stability criterion then leads to a non-conservative test, which corresponds to verifying whether $M_s - K(\rho)(1-M_s)G$ does not encircle the point -1 in the complex plane. A frequency-domain model of $M_s - K(\rho)(1-M_s)G$ is identified and used for verification. In this work, the stability criterion uses the small-gain theorem, which leads to a conservative result. However, the resulting H_∞-norm constraint is *convex* and can be added to a convex controller optimization. The non-conservative test using both amplitude and phase information would lead to non-convex constraints.

Implementation using spectral estimates

Let the unstable plant G be excited by $r(t)$ in closed loop according to the scheme of Figure 2.2. The output of the plant is affected by the noise $v(t)$. The discrete signals $r(t)$, $y(t)$, $u_1(t)$ and $u_2(t)$ of length N are available. The error $\varepsilon_c(t,\rho)$ is given by (2.11) and the correlation criterion $J_{N,l_1}(\rho)$ is defined in (2.31). The error signal $\varepsilon_s(t,\rho)$ used in the stability constraints is given by (3.19). Optimization problem (3.3) can be approximated by (3.10).

Theorem 3.4 *Consider the controller structure defined in (2.7). Let the stable filter L be defined as:*

$$L(e^{-j\omega}) = \frac{F(e^{-j\omega})(1 - M(e^{-j\omega}))}{\big(1 - M_s(e^{-j\omega})\big)\Phi_r(\omega)} \tag{3.20}$$

*Assume that **A1-A4** are satisfied, that $L(1-M)G/(1+K_sG)$ has no zero on the imaginary axis and that a strictly feasible solution exists for (3.3), for the series of optimization problems as $N, l_1, l_2 \to \infty$ as well as for (3.10). Then, as $N, l_1, l_2 \to \infty$ and $l_1/N, l_2/N \to 0$, the optimizer $\hat{\rho}$ in (3.10) converges w.p.1 to the stabilizing optimizer $J(\rho)$ as defined in (3.3):*

$$\lim_{N,l_1,l_2\to\infty,l_1/N,l_2/N\to 0} \hat{\rho} = \rho_s. \tag{3.21}$$

Proof: Even though G might be unstable, the filter $(1 - M_s)G$ is stable and consequently all filters involved are stable and all signals are bounded. The proof then follows from the proof of Theorem 2.2 and Theorem 3.2. ∎

As discussed in Section 2.4.2, the filter L depends on the unknown plant G and cannot be implemented. However, it can be approximated by (2.41). As for the scheme for stable minimum-phase systems, the quality of the estimates can be improved by using periodic data. The implementation for the closed-loop scheme is similar to the implementation for the open-loop scheme and therefore not detailed here.

3.4 Alternative implementation using Toeplitz matrices

In the method proposed in this thesis, an H_∞ specification is added to the controller tuning using the DFT. Similar H_∞ specifications have been used in system identification [64] and data-driven controller tuning [47] as well as in the stability test introduced in [82]. In these methods, non-periodic signals are considered, and the constraint on the H_∞-norm is defined using Toeplitz matrices, which leads to a Linear Matrix Inequality (LMI).

The method proposed here is closely related to Toeplitz-based methods. In the case of periodic signals, the method is equivalent to using circulant matrices, and constraints (3.16) can be imposed as an LMI. In order to show this, some results on circulant matrices are summarized first.

A circulant matrix is defined for $x(t)$ as

$$C(x) = \begin{bmatrix} x(1) & x(2) & \dots & x(N-1) & x(N) \\ x(N) & x(1) & \dots & x(N-2) & x(N-1) \\ \vdots & \vdots & \ddots & \vdots & \vdots \\ x(3) & x(4) & \dots & x(1) & x(2) \\ x(2) & x(3) & \dots & x(N) & x(1) \end{bmatrix}$$

where each row is a cyclic shift of the row above it. Some characteristics of circulant matrices are as follows [22]:

1. Consider two circulant matrices $C(x)$ and $C(z)$, then $C(x)C(z) = C(z)C(x)$, $C(x)+C(z)$, $C^{-1}(\cdot)$ and $C^T(\cdot)$ are also circulant matrices.
2. The eigenvalues of a circulant matrix of size N are given by :

$$\lambda_k(C(x)) = \sum_{t=1}^{N} x(t)e^{-it\omega_k}, \omega_k = 2\pi k/N, \quad k = 0, \ldots, N-1 \tag{3.22}$$

3. The eigenvectors of a circulant matrix of size N are given by:

$$U_k = \frac{1}{\sqrt{N}}\left(1, e^{-i\omega_k}, e^{-i2\omega_k}, \ldots, e^{-i(N-1)\omega_k}\right) \tag{3.23}$$

   Note that the eigenvectors are independent of the elements of the matrix.
4. Define the matrix U, which has the eigenvectors U_k, $k = 0, \ldots, N-1$, as columns, and define $\Lambda(\cdot) = \text{diag}(\lambda_k(C(\cdot))$. Then, U is full rank and unitary, i.e. $UU^* = I$ and $U^*U = I$. For each circulant matrix $C(\cdot)$:

$$\Lambda(\cdot) = U^*C(\cdot)U \tag{3.24}$$

Lemma 3.2 *For two $N \times N$ circulant matrices $C(x)$ and $C(z)$:*

$$\begin{aligned} C^T(x)C(x) - C^T(z)C(z) \leqslant 0 \iff \\ |\lambda_k(C(x))| - |\lambda_k(C(z))| \leqslant 0, \quad k = 0, \ldots, N-1 \end{aligned} \tag{3.25}$$

Proof: The proof follows from U being full rank:

$$\begin{aligned} &C^T(x)C(x) - C^T(z)C(z) \leqslant 0 \iff \\ &U^*\big(C^T(x)C(x) - C^T(z)C(z)\big)U \leqslant 0 \iff \\ &\Lambda(x)^*\Lambda(x) - \Lambda(z)^*\Lambda(z) \leqslant 0 \iff \\ &|\lambda_k(C(x))| - |\lambda_k(C(z))| \leqslant 0, \quad k = 0, \ldots, N-1 \end{aligned}$$

The third expression follows from (3.24) and the last one from the definition of $\Lambda(\cdot)$. ■

$C_t(\cdot)$ is defined as a truncated circulant matrix of size $N \times T$. The multiplication of two truncated matrices $C_t^T(\cdot)C_t(\cdot)$ is a circulant matrix of size $T \times T$.

The main result is now presented in the following theorem.

Theorem 3.5 *The convex constraints in (3.16) are equivalent to the following LMI:*

$$\begin{bmatrix} -\delta_N^2 C_t^T(r)C_t(r)C_t^T(r)C_t(r) & C_t^T(r)C_t(\varepsilon_s(\rho)) \\ C_t^T(\varepsilon_s(\rho))C_t(r) & -I \end{bmatrix} \leqslant 0 \qquad (3.26)$$

Proof:

$$C_t^T(\varepsilon_s(\rho))C_t(r) = C(N\hat{R}_{r\varepsilon_s}(\tau,\rho)) \qquad (3.27)$$

where $\hat{R}_{r\varepsilon_s}(\tau,\rho)$ is given by (3.15) for $\tau = 0,\ldots,N_p-1$. Its eigenvalues are given by:

$$\lambda_k\big(C(N\hat{R}_{r\varepsilon_s}(\tau,\rho))\big) = N\hat{\Phi}_{r\varepsilon_s}(\omega_k,\rho) \qquad (3.28)$$

Equivalently,

$$\lambda_k\big(C_t^T(r)C_t(r)\big) = N\Phi_r(\omega_k) \qquad (3.29)$$

Then, using Lemma 3.2, one can write:

$$\begin{aligned} C_t^T(\varepsilon_s(\rho))C_t(r)C_t^T(r)C_t(\varepsilon_s(\rho)) - \delta_N^2 C_t^T(r)C_t(r)C_t^T(r)C_t(r) \leqslant 0 \\ \iff |\hat{\Phi}_{r\varepsilon_s}(\omega_k,\rho)| - \delta_N|\Phi_r(\omega_k)| \leqslant 0, \\ \omega_k = 2\pi k/N_p, \quad k = 0,\ldots,(N_p-1) \end{aligned} \qquad (3.30)$$

Using the Schur complement, the LMI (3.26) is obtained. ∎

Remark: Constraint (3.26) can be seen as a periodic version of the norm proposed in [31]. The direct use of the DFT instead of these circulant matrices has two advantages. First of all, the computational load is much smaller. Secondly, the frequencies considered can be chosen in a straightforward manner. For example, only frequencies where the signal-to-noise ratio is reasonable could be selected.

3.5 Guaranteeing stability for a finite number of data

In practice, the constraint $\hat{\delta}(\rho)$ used for controller tuning in the optimization problem of (3.10) is an estimation of $\delta(\rho)$. Consequently,

stability can only be guaranteed if the estimation errors are taken into account. Next, a stochastic approach that leads to a (conservative) probabilistic bound is considered.

In the following, $r(t)$ is assumed to satisfy **A5** and **A6**. The noise is assumed to satisfy **A1-A2**. Furthermore, assume that:

- there exists a finite pair of reals $\{A, \gamma\} \in \mathbb{R}, \gamma < 1$, such that $|d(k)| \leqslant A\gamma^k$, for $k \in \mathbb{Z}_+$, where $d(k)$ is the impulse response of Δ.

A and γ are in general not known beforehand and might need to be verified a posteriori.

Implementation using spectral estimates

The estimate (3.15) contains an error term due to the estimation error of $\Delta(e^{-j\omega_k})$ at the frequencies ω_k and a second error term due to the finite frequency grid.

Estimation error at ω_k. It follows from Assumption **A5** that the truncation error is zero and the error of $\Delta(e^{-j\omega_k})$ is entirely due to measurement noise.

Error due to finite frequency grid. The maximum of $|\Delta(e^{-j\omega})|$ might be situated in between two consecutive frequencies ω_k and ω_{k+1}. This error due to the finite frequency grid depends on the derivative of $|\Delta(e^{-j\omega})|$ with respect to ω, i.e. $\frac{d|\Delta(e^{-j\omega})|}{d\omega}$, and the distance between two consecutive frequencies.

If both errors are taken into account in the bound δ_N, stability is guaranteed also for finite data length. Define $\Phi_{r,min}$ as the minimal value of the spectrum $\Phi_r(\omega_k)$ at the frequencies $\omega_k = 2\pi k/N_p, k = 0 \ldots N_p - 1$.

Theorem 3.6 *The controller $K(\rho)$ stabilizes the plant G, with probability p, if*

$$\left| \frac{\hat{\Phi}_{r\varepsilon_s}(\omega_k, \rho)}{\Phi_r(\omega_k)} \right| < \delta_N, \text{ for } \omega_k = \frac{2\pi k}{N_p}, \quad k = 0 \ldots N_p - 1,$$

where

$$\delta_N = 1 - \frac{A\gamma}{(1-\gamma)^2}\frac{\pi}{N_p} - \|(1-M)K(\rho)\|_\infty \sqrt{-\ln(1-p)\frac{\|H_v\|_\infty^2 \sigma^2}{n_p \Phi_{r,min}}}.$$

Proof: See Appendix A.2 ∎

Note that the bound δ_N depends on the unknown parameters ρ. $\|(1-M)K(\rho)\|_\infty$ can be implemented using an LMI and (3.16) remains convex.

The bound presented in Theorem 3.6 represents a worst-case error in between frequencies. Furthermore, the error due to noise is based on inequalities. The bound is therefore conservative. Less conservative bounds can be formulated, based on the exact same data, if an FIR model is used that corresponds to the spectral estimates [14].

Implementation using finite impulse response model

Define the response of Δ to a periodic signal with period length N_p as:

$$d_{per}(t) = d(t) + \sum_{i=1}^{\infty} d(t + iN_p), \quad t = [0, \ldots, N_p - 1].$$

Define the vector

$$\bar{d}_{per} = [d_{per}(0), d_{per}(1) \ldots d_{per}(N_p - 1)]$$

An FIR estimate of $d(t)$ of length N_p is given by:

$$\hat{\theta} = [\Psi\Psi^T]^{-1}\Psi\bar{\varepsilon}_s \tag{3.31}$$

where

$$\begin{aligned}
\Psi &= [\psi(1), \psi(2), \ldots, \psi(N)] \\
\psi(t) &= [r(t), r(t-1) \ldots r(t - N_p + 1)]^T \\
\bar{\varepsilon}_s &= [\varepsilon_s(1) \ldots \varepsilon_s(N)]^T
\end{aligned}$$

$\varepsilon_s(t)$ is defined in (3.6) and can be written as

$$\varepsilon_s(t) = \Delta r(t) + (1-M)K(\rho)v(t).$$

The deterministic part of $\varepsilon_s(t)$ is given by $\Delta r(t) = \psi^T(t)\bar{d}_{per}$.

Since the noise is uncorrelated with the reference,

$$E\{\hat{\theta}\} = E\{[\Psi\Psi^T]^{-1}\Psi\bar{\varepsilon}_s\} = \bar{d}_{per}.$$

It is easily verified that

$$\Psi\bar{\varepsilon}_s = [\hat{R}_{r\varepsilon_s}(0), \ldots, \hat{R}_{r\varepsilon_s}(N_p - 1)],$$

and that the FIR estimate $\hat{\theta}$ is the deconvolution of $\hat{R}_{r\varepsilon_s}(\tau)$ and $R_r(\tau)$. This is the inverse Fourier transform of $\hat{\Delta}(e^{-j\omega_k}, \rho)$, for $\omega_k = 2\pi k/N_p, k = 0, \ldots, N_p - 1$. The estimate $\hat{\theta}$ is thus the time-domain equivalent of $\hat{\Delta}(e^{-j\omega_k}, \rho)$.

The estimate $\hat{\theta}$ can be used to define a constraint on the gain of the error function that is defined over all frequencies:

$$\hat{\Delta}(e^{-j\omega}, \rho) = \sum_{t=0}^{N_p-1} \hat{\theta}(t)e^{-j\omega t} = \Gamma^T(e^{-j\omega})\hat{\theta}, \tag{3.32}$$

where $\Gamma(e^{-j\omega}) = [1, e^{-j\omega}, e^{-j2\omega}, \ldots, e^{-j(N_p-1)\omega}]^T$. The constraint $\|\hat{\Delta}\|_\infty < 1$ can be implemented using an LMI based on a state-space representation of the FIR model ([8], chapter 2, bounded real lemma). This constraint is convex.

In [14], it is shown that the choice of the length of the FIR model introduces a trade-off between the bias and the noise error. The optimal length, for which the tightest bounds can be defined, depends on the system and the noise characteristics. The noise error is estimated using the data and the bias error also contains transition errors. In the following, a simplified bound is proposed. Only models with an FIR length equal to the period N_p are considered here. The results are based on a priori information on the system and noise, and the bounds are relatively simple to implement.

Theorem 3.7 *The controller $K(\rho)$ stabilizes the plant G with probability p, if*

$$\|\hat{\Delta}\|_\infty < \delta_N, \text{ for } \omega_k = \frac{2\pi k}{N_p}, k = 0 \ldots N_p - 1,$$

where

$$\delta_N = 1 - 2\left(\frac{A\gamma^{N_p}}{1-\gamma}\right) - \|(1-M)K(\rho)\|_\infty \sqrt{-\ln(1-p)\frac{\|H_v\|_\infty^2 \sigma^2}{n_p \Phi_{r,min}}}.$$

Proof: See Appendix A.3 ∎

This error bound is tighter that of Theorem 3.6 and is therefore less conservative. However, this approach uses the H_∞ norm based on an FIR model, which leads to a large LMI, for which the computational load is considerable.

3.6 Illustrative examples

3.6.1 Numerical example: delay system

A simple example was used in [31] to show that stability problems occur "for the class of identification-for-control methods that use arbitrary data in the identification". The same example will be used here to show that the method proposed in this thesis leads to stabilizing controllers.

The pure time-delay system $G(q^{-1}) = q^{-1}$ is considered. The proportional controller $K = \rho$ is used to control the plant. The controlled system is unstable for $|\rho| > 1$. The reference model is $M = 1-\alpha+\alpha q^{-1}$, where α is a parameter controlling the bandwidth. The model-reference control problem is minimized by $K(\rho_0) = \rho_0 = \frac{4\alpha-1}{6\alpha}$. For $0 < \alpha < 0.1$, $|\rho_0| > 1$, and the controlled system will be unstable.

The system is excited by a periodic PRBS with period $N_p = 63$ and $n_p = 4$ periods. The reference model is chosen as $M = 0.95 + 0.05q^{-1}$, i.e. with $\alpha = 0.05$ for which the optimal controller $K(\rho_0) = -2.67$ destabilizes the plant. Two controllers are calculated using noise-free simulation data. The first controller is calculated without the stability constraints in (3.16). The controller found is $K(\rho_1) = -2.67$, which destabilizes the system. The second controller is calculated using (3.16) with $\delta_N = 0.999$. This optimization is infeasible. A closer look at the bound shows that $\delta = \|M - K(1 - M)G\|_\infty = 1$ for all stabilizing controllers and the problem is indeed

infeasible. The controller design was poorly formulated through an inappropriate choice of M.

In order to show the effectiveness of the method in the presence of noise, the reference model used for the stability constraints is slightly altered, $M_s = 1 - \alpha + 0.95\alpha q^{-1}$. The reference model used in the control objective remains unchanged. For this problem $\delta = \|M_s - K(\rho)(1 - M_s)G\|_\infty < 1$ for a subset of the stabilizing controllers and the problem is thus feasible. The output of the system is perturbed by a white noise such that the signal-to-noise ratio is about 10 in terms of variance. The controller obtained without using the constraints in (3.16) is $K(\rho_1) = -2.34$, which again destabilizes the system. The second controller calculated using (3.16) is $K(\rho_2) = -0.33$. Clearly, since $|K(\rho_2)| < 1$, it stabilizes the system. The difference between $K(\rho_1)$ and $K(\rho_2)$ indicates a poor problem formulation.

The alternative implementation using circulant matrices leads to a large LMI, which becomes expensive to compute for large data length. The following comparison is found using Matlab V 7.4 on a Mac with a 3 GHz processor and 5 GB memory. The optimization is implemented using Yalmip [55] and SeDuMi [78]. The aforementioned problem for $N = 252$ leads to exactly the same result using both implementations. The DFT approach is more expensive to formulate but faster to run. The difference is small for small data lengths, e.g. for $N_p = 63, N = 252$ the DFT approach takes $0.7s$ vs. $2s$ for the LMI. For $N_p = 127, N = 1016$, the DFT approach takes $2.2s$ vs. $13s$ for the LMI. For $N_p = 255, N = 2040$, the LMI cannot be solved (memory problems) whereas the DFT approach takes only $3s$. When using the DFT approach, the data length can be increased to at least $N_p = 1023, N = 8184$, for which the optimization is solved within $10s$.

3.6.2 Numerical example: flexible transmission system

Consider the plant given by the discrete-time model $G(q^{-1})$:

$$G(q^{-1}) = \frac{0.7893q^{-3}}{1 - 1.418q^{-1} + 1.59q^{-2} - 1.316q^{-3} + 0.886q^{-4}}.$$

This corresponds to a stable minimum-phase model of the flexible transmission system proposed as a benchmark for digital control design in [49]. The control objective is defined by the reference model

$$M(q^{-1}) = \frac{q^{-3}(1-\alpha)^2}{(1-\alpha q^{-1})^2},$$

with $\alpha = 0.606$. The integral controller

$$K(\rho) = \frac{\rho_0 + \rho_1 q^{-1} + \rho_2 q^{-2} + \rho_3 q^{-3} + \rho_4 q^{-4} + \rho_5 q^{-5}}{1 - q^{-1}}$$

is chosen, with the unknown parameters $\rho_0, \ldots, \rho_5$. The reference model M has unity static gain, thus ensuring that $1 - M$ has a zero at 1, which makes Lemma 3.1 applicable.

A PRBS signal of 255 samples with unity amplitude is used as input to the system. Four periods of this signal are used for controller design, $N = n_p N_p = 1020$. The periodic output is disturbed by zero-mean white noise such that the signal-to-noise ratio is about 10 in terms of variance. The instrumental variables are defined according to (2.29), with $l_1 = 20$ in order to limit the bias due to the finite number of data. For the same reason, the bound in the stability condition is fixed to $\delta_N = 0.95$. The filter F is chosen as $F = 1$. The spectrum of the PRBS reference signal is known, $\Phi_r(\omega_k) = 1$ for all ω_k except for $\omega_k = 0$. The spectrum is therefore approximated in the weighting filter by 1 for all frequencies and, therefore $L = 1 - M$. The filter is implemented in the time domain. The constraints are implemented as in (3.16). A Monte Carlo simulation with 100 experiments is performed, using a different noise realization for each experiment.

Bode plots of the resulting closed-loop system for all 100 controllers are shown in Figure 3.2. All 100 controllers stabilize the system and achieve acceptable performance. The stability constraint is active for 4 controllers; however, the difference between the unconstrained and the constrained solution is small. A small bias at high frequencies can be observed as expected from (2.44). Since the reference model is chosen appropriately, the optimal controller minimizing $J(\rho)$ stabilizes the system. Furthermore, because the quality of the estimate found using the correlation approach is good, the addition of the stability constraints does not affect the results.

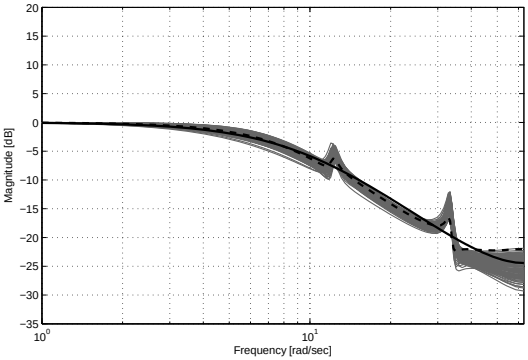

Fig. 3.2. Magnitude Bode plots of M (black line), achieved closed-loop performance in Monte Carlo simulation for the proposed approach (grey lines), and in the noise-free case (black dashed line).

Guaranteeing stability for VRFT

To show the effectiveness of the stability constraints, the same data are used to calculate controllers using the VRFT approach [9]. The goal is to show that, when the unconstrained problem has a destabilizing solution, addition of the stability constraints leads to stabilizing controllers. The VRFT approach that uses a second experiment to define the instrumental variables is used specifically to find these destabilizing controllers. This approach leads to an unbiased estimate, but it is well known that the use of noise-corrupted instrumental variables increases the variance of the estimate [72]. This variance might lead to instability even in the case of an appropriate reference model. It should be noted that this variance results from the choice of instrumental variables and is not inherent to VRFT. Other methods to deal with measurement noise are suggested in [9].

For each of the 100 simulations, a second experiment is simulated with a different noise realization. Hence, the VRFT controllers are calculated using 2040 samples. Two controllers are calculated for each set of data. The first controller is calculated using the VRFT approach as proposed in [9]. For the second controller, the stability constraints are added to the VRFT problem. The samples available

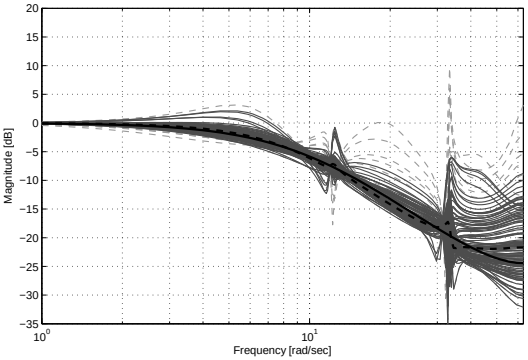

Fig. 3.3. Magnitude Bode plots of M (black line), achieved closed-loop performance without stability constraints for the 96 stabilizing VRFT controllers (grey dashed lines), with stability constraints for 100 stabilizing controllers (grey solid lines), and the noise-free case (black dashed line).

from both experiments are used in the constraints that are implemented as in (3.16).

Four of the controllers calculated using the unconstrained VRFT approach destabilize the system. All controllers calculated with the stability constraints stabilize the system. Note that, due to the conservatism in the stability criterion, 7 of the 96 stabilizing VRFT controllers do not satisfy the stability constraints. The optimum of the constrained optimization problem is therefore different from the VRFT solution. For these stabilizing controllers, the active constraints indicate poor closed-loop performance and the conservatism in the constraints actually leads to better performance. This can be seen in Figure 3.3, which shows the magnitude Bode plots of all stabilizing controllers (96 for the unconstrained problem and 100 for the constrained problem).

3.6.3 Experimental torsional setup

The effectiveness of the proposed approach is demonstrated experimentally on the torsional setup shown in Figure 3.4. The setup consists of three discs connected by a torsionally flexible shaft. Two masses are fixed to each disc. The shaft is driven by a brushless servo

Fig. 3.4. Torsional setup, ECP Model 205

motor. The angular displacement of the top disc is measured by an encoder and expressed in degrees. The plant contains an integrator and has two strong resonances. The sampling time is 60 ms. The sampled plant model is assumed to be minimum phase.

A set of periodic open-loop data is collected using a zero-mean PRBS input of 255 samples. Five periods of input and output measurements are used for controller design. The controller structure is fixed as a 7th-order FIR filter. The controllers are calculated using (3.16) with $F = 1$. The input spectrum is approximated as 1 for all frequencies, therefore $L = 1 - M$. $\zeta(t)$ is defined as (2.48) with $l_1 = 127$. The bound in the stability condition is fixed as $\delta_N = 0.8$. The reference model needs to have unity static gain since the plant contains an integrator. Two different reference models are considered. The first one reads:

$$M_1 = \frac{0.0765q^{-1}}{(1 - 0.7q^{-1})^2(1 - 0.15q^{-1})}.$$

The second reference model is chosen with a similar bandwidth but a high-frequency roll-off of only one:

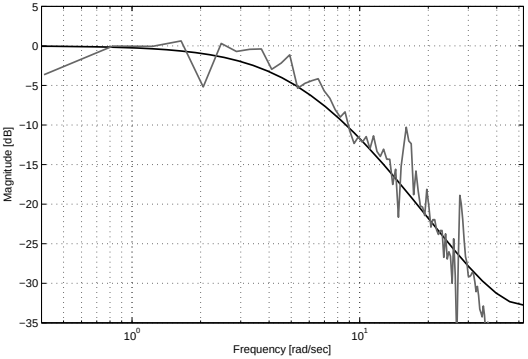

Fig. 3.5. Magnitude Bode plot of the reference model M_1 (black) and the estimated closed-loop plant controlled by K_1 (grey).

$$M_2 = \frac{0.3q^{-1}}{1 - 0.7q^{-1}}.$$

The stability constraints in the optimization problem for M_1 are not active. The resulting controller is denoted K_1. In contrast, the stability constraints are active in the optimization problem for M_2. Two controllers are calculated using M_2: controller K_2 is the unconstrained optimum, controller K_3 is the solution to the constrained problem.

When applied to the plant, controller K_2 leads to instability. Stability is obtained with K_1 and K_3, for which the closed-loop frequency-response can be identified. Four periods of the PRBS of 255 samples with amplitude 50 degrees are collected on the plant controlled by K_1. The frequency response estimated using DFT is shown in Figure 3.5. The reference model M_1 is appropriate, and the achieved closed-loop system resembles the reference model. The steady-state gain is smaller than one due to static friction. The plant controlled by K_3 is excited by a PRBS with a frequency divider of 2, 510 samples per period and amplitude 50 degrees. Three periods are used for the DFT estimate. The result is shown in Figure 3.6. The controller does stabilize the plant but the required closed-loop performance is not achieved. Reference model M_2 is inappropriate

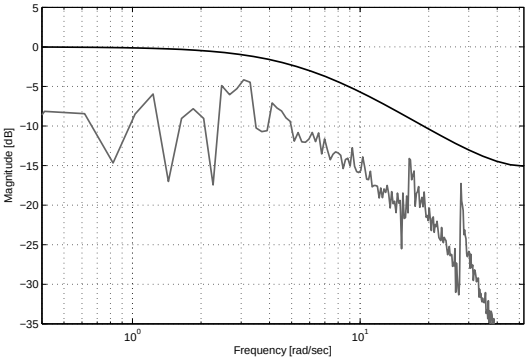

Fig. 3.6. Magnitude Bode plot of the reference model M_2 (black) and the estimated closed-loop plant controlled by K_3 (grey).

and cannot be achieved. The fact that the stability constraints are active actually indicates this problem.

Remark: In the numerical example of Section 3.6.2, addition of the stability constraints to VRFT improves the closed-loop performance. The reference model is appropriate and instability is the result of the variance of the estimated controller parameters. In contrast, for the experimental torsional setup, instability is due to an inappropriate reference model. Addition of the stability constraints leads to a stabilizing solution, but the closed-loop performance remains poor because it is not possible to achieve the required performance.

3.7 Conclusions

A sufficient condition for closed-loop stability is proposed and it is shown how an estimate of this condition can be used to guarantee stability in data-driven controller tuning. The resulting controller is guaranteed to stabilize the plant as the number of data tends to infinity. The asymptotic nature of this result might seem restrictive, but is equivalent to results for model-based approaches. If a model is used, stability can be guaranteed only if the model is perfect, or if the modeling errors are taken into account. Similarly, in the data-driven

approach, the estimation error affecting the stability constraint can be taken into account. Bounds are given for periodic data.

Note that two estimates are used in the constrained optimization that guarantees stability, one for the control criterion and one for the stability constraint. Since different characteristics of the plant are determining for the control criterion and the constraint, two different identification techniques are used. The correlation approach is used to estimate the control criterion whereas a spectral estimate or a finite impulse response model are proposed for the stability constraint.

In data-driven model reference control, the choice of an appropriate reference model is tricky. Since no model of the plant is available, it is difficult to know beforehand whether the control objective can be achieved or not. In the open-loop scheme proposed in this study, the fact that the stability constraint is active indicates this problem. In practice, the reference model can be adjusted until an adequate reference model is found, off-line, without the need for additional experiments.

In the closed-loop scheme, the stability constraint is defined with respect to the previously implemented stable controller. The conservatism of this solution is comparable to the conservatism introduced in some iterative identification and control procedures, where the allowed controller changes are small in order to maintain stability. An approach similar to the windsurfing approach can be imagined, where the performance of the reference model, and consequently the controller, is increased gradually and several iterations are needed to achieve the objective.

4

Data-driven stability test

The stability constraint proposed in Chapter 3 is conservative. As an alternative, stability can be verified a posteriori. Suppose that the controller $K(q^{-1})$ has been designed to control the linear SISO plant $G(q^{-1})$. The proposed stability test can then be used to verify, before implementation, whether this $K(q^{-1})$ actually stabilizes the plant.

The use of closed-loop experimental data to verify if controllers are stabilizing has been proposed for iterative control design methods [50]. In such methods, information from a closed-loop experiment is used to redesign a controller in order to increase the performance. In [50], a fundamental contradiction is pointed out for stability tests for such methods. Limited information from closed-loop experiments is used to obtain information for small controller changes that provide performance improvement. However, in order to guarantee stability, identification of the full dynamics of the plant is required.

An example of a stability test that requires identification of the full plant dynamics is the model-based approach proposed in [21]. A parametric plant model is identified and the uncertainty of the estimated parameters is described. Stability is then verified for all plants in the uncertainty set. In the model-based approach of [71], a method is proposed to identify the closed-loop system without actually implementing the controller. If the identified model is stable, the controller is validated. In practice, the choice of model order affects the reliability of the test, and it is not clear whether the re-

sult obtained with a high-order model is more reliable than with a low-order model or vice versa.

The stability test proposed in [50] uses phase information of some error function. It is argued that, since instability can only occur when the gain of some error function is bigger than unity, the phase information is important only at those frequencies where the gain of the error is large. Consequently, partial information of the plant is sufficient to guarantee stability for small controller changes. However, this approach indirectly implies that it is known up to which frequencies the gain might be larger than one. Furthermore, even though more data become available in consecutive iterations, the reliability of the test does not improve because the data are collected with different controllers in the loop and cannot be combined.

In the following, a stability test is proposed that assumes neither an iterative procedure, nor small changes in the controller. If the plant is stable, open-loop experiments can be used. If some a priori information on the plant and the disturbances is available, the estimation error can be taken into account and stability can be guaranteed also for a finite number of data. If the estimation error is not taken into account, the test provides a clear trade-off between conservatism and reliability. Furthermore, if closed-loop data are available from measurements with different controllers in the loop, the data can be combined. The tests are based on an extension of Theorem 3.1.

4.1 Conditions for closed-loop stability

In the following, Theorem 3.1 is extended to provide necessary and sufficient conditions for closed-loop stability. Consider the controller K_s, for which the closed-loop plant is given by (3.1). Define the error function $\Delta := M_s - KG(1 - M_s)$ and its infinity norm $\delta := \|\Delta\|_\infty$. In Theorem 3.1, K_s is assumed to be fixed and stabilizing, which also fixes M_s. Sufficient conditions for stability are then formulated with respect to this fixed M_s. In the following, M_s and K_s are variable, and an additional condition on K_s is needed.

Theorem 4.1 *The controller K stabilizes the plant G iff there exists a stable strictly proper transfer function M_s, and $0 \leqslant \delta_N < 1$ such that*

1. $K_s = \frac{M_s}{G(1-M_s)}$ *internally stabilizes the plant, i.e. $G(1-M_s)$ and M_s/G are stable,*
2. Δ *is stable,*
3. $\delta \leqslant \delta_N$.

Proof: *Sufficiency* can be shown using the small-gain theorem: When the interconnection of Figure 3.1 is opened at q, the resulting system is stable when Conditions 1 and 2 are satisfied. In this case, the small-gain theorem can be applied to define a sufficient condition for closed-loop stability: the interconnection is stable if $\delta < 1$. This is the H_∞-norm of the transfer function from q back to q.

In order to show *necessity*, consider a stabilizing controller K. If K stabilizes the plant, there exists an M_s such that

$$M_s = \frac{KG}{1+KG}$$

for which Condition 1 is clearly satisfied. For this specific M_s, the controller $K_s = K$ and $\Delta = 0$. It follows that Conditions 2 and 3 are satisfied. Combining this result with the sufficient condition following from the small-gain theorem leads to $0 \leqslant \delta_N \leqslant 1$. This completes the proof. ■

This theorem can now be used to verify closed-loop stability. The main idea is as follows: If an M_s exists that satisfies the conditions of Theorem 4.1, the controller is stabilizing. This M_s can be found as follows:

- The structure of M_s is chosen such that Conditions 1 and 2 are verified.
- Experiments are proposed to verify the Condition 3.
- A convex optimization is proposed to find an M_s that satisfies the conditions.

If the optimization is feasible, the controller is validated.

Note that there are no assumptions regarding the linear SISO plant G. Theorem 4.1 is applicable to stable, unstable, minimum-phase and nonminimum-phase plants. However, Conditions 1 and

2 imply that it is known whether or not some unknown controller K_s stabilizes the plant, which is a non-trivial question in the case of unstable or nonminimum-phase plants.

An appropriate choice of M_s for different types of plants and controllers is summarized in the following lemma. The stable filter X will be used to define a structure of M_s such that Conditions 1 and 2 are met. The lemma considers only stable controllers; however, the specific case of controllers with poles on the unit circle can also be handled. Although this does not cover all possible combinations of plants and controllers, it does cover the cases encountered in many control problems in practice.

Lemma 4.1 *Consider a stable filter X and let the structure of M_s depend on the type of plant G as follows:*

a) For stable minimum-phase plants:
$M_s = X$

b) For unstable minimum-phase plants:
$M_s = 1 - X(1 - M_0)$*, where M_0 is the closed-loop system of the plant controlled by a stable stabilizing controller K_0,*

$$M_0 = \frac{K_0 G}{1 + K_0 G}.$$

c) For stable nonminimum-phase plants:
$M_s = XG$

Then, the plant G is stabilized by the stable controller K iff there exists a filter X and $0 \leqslant \delta_N < 1$, such that $\delta \leqslant \delta_N$.

Proof: *Sufficiency:* Conditions 1 and 2 of Theorem 4.1 are satisfied if $M_s, G(1 - M_s), M_s/G$ and $KG(1 - M_s)$ are stable. Since M_s is stable by definition, only the stability of $G(1 - M_s), M_s/G$ and $KG(1 - M_s)$ remains to be verified.

a) If the plant G is stable minimum-phase and the controller K is stable, that is both G and K have no poles outside or on the unit circle, then these three transfer functions are stable for any stable M_s.
b) For an unstable minimum-phase plant G, instability might occur in $G(1 - M_s)$ or $KG(1 - M_s)$. The plant controlled by the

stabilizing controller K_0 is given by $M_0 = K_0G(1 + K_0G)^{-1}$, and M_0 clearly satisfies Conditions 1 and 2, i.e. $G(1 - M_0)$ and $KG(1 - M_0)$ are stable. For any stable transfer function X, $XG(1 - M_0)$ and $XKG(1 - M_0)$ are also stable. $M_s = 1 - (1 - M_0)X$ thus satisfies Conditions 1 and 2.

c) For a stable nonminimum-phase plant, controlled by a stable controller, instability might occur in M_s/G. This transfer function is stable iff M_s contains the unstable zeros of G, which is the case for $M_s = XG$.

If the structure of M_s is chosen as in Lemma 4.1, Conditions 1 and 2 are satisfied. According to Theorem 4.1, the remaining condition, $\delta \leqslant \delta_N$, is sufficient for closed-loop stability.

Necessity: Consider the stable stabilizing controller K.

a)
$$X = \frac{KG}{1 + KG}$$
is stable, satisfies Conditions 1 and 2 and achieves $\delta = 0$.

b)
$$X = \frac{1 + K_0G}{1 + KG} = \frac{1}{1 + KG} + K_0\frac{G}{1 + KG}$$
is stable since K is stabilizing and K_0 is stable. This X achieves $\delta = 0$ and Conditions 1 and 2 are satisfied.

c)
$$X = \frac{K}{1 + KG}$$
is stable, satisfies Conditions 1 and 2 and achieves $\delta = 0$.

It thus follows that for every stable stabilizing K, there exists a stable filter X that satisfies the conditions of Theorem 4.1. This completes the proof. ■

Note that for unstable minimum-phase plants sufficiency can be shown also if the controller K_0 is unstable. However, in this case necessity is lost and the stable controller K might stabilize the plant also if no stable X can be found that satisfies Condition 3.

For the specific case of a controller or plant that contains poles on the unit circle, for example an integrator, instability might occur in $G(1 - M_s)$ or $KG(1 - M_s)$. These transfer functions are stable iff

the unstable poles of G and K are zeros of $1 - M_s$. An appropriate choice for M_s is thus $M_s = X$, where the unstable poles of G and K are zeros of $1 - M_s$. In the specific case of a simple integrator in G or K, this is equivalent to requiring unity static gain for X.

4.2 Generating the error signal

According to Theorem 4.1, the controller K stabilizes the plant G iff a M_s exists that satisfies Conditions 1, 2 and 3. Lemma 4.1 introduces structures of M_s for which Condition 1 and 2 are satisfied, using a stable filter X. If a stable filter X can be found such that Condition 3 is satisfied, the controller stabilizes the system. In Section 4.3, a convex optimization is introduced to find an X that satisfies Condition 3. This requires parameterization of the stable filter X. Define $X(q^{-1}, \rho)$ as a linear combination of stable linear discrete-time orthogonal basis functions $\beta(q^{-1}) = [\beta_1(q^{-1}), \ldots, \beta_{n_\rho}(q^{-1})]$:

$$X(q^{-1}, \rho) = \beta^T(q^{-1})\rho, \quad \rho \in \mathcal{D}_X, \tag{4.1}$$

where the set $\mathcal{D}_X$ is compact. Note that $X(q^{-1}, \rho)$ is a subset of all stable filters X.

If the structure of M_s is chosen according to Lemma 4.1 and $X(q^{-1}, \rho)$ is defined as (4.1), Conditions 1 and 2 of Theorem 4.1 are satisfied, and only Condition 3, $\delta \leqslant \delta_N$, remains to be verified. δ is the H_∞-norm of some error function that depends on the unknown plant G and is therefore unknown. However, it can be estimated from measured data.

The basis of the data-driven stability test is therefore to generate an error signal $\varepsilon_s(t, \rho)$ corresponding to the error function Δ, for a specific reference signal $r(t)$. This error signal can be used to compute $\hat{\delta}$, an estimate of δ. In the case of a stable minimum-phase plant, the corresponding error signal can be generated using one open-loop experiment. The error signal for unstable plants can be generated using one closed-loop experiment. Generating the error signal for nonminimum-phase plants requires two open-loop experiments.

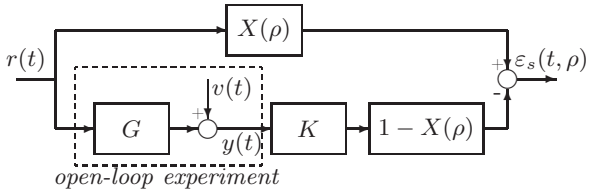

Fig. 4.1. Experimental scheme for closed-loop stability test using an open-loop experiment for stable, minimum-phase plants

For stable minimum-phase plants

Consider the scheme of Figure 4.1, which includes one open-loop experiment on the plant G. The reference signal $r(t)$ is applied to the plant. The resulting output $y(t) = Gr(t)+v(t)$ is measured. The measurement noise $v(t)$ satisfies **A1**. The error is given by:

$$\begin{aligned}\varepsilon_s(t,\rho) &= X(\rho)r(t) - (1 - X(\rho))\, Ky(t) \\ &= [X(\rho) - (1 - X(\rho))\, KG]\, r(t) - (1 - X(\rho))\, Kv(t) \quad (4.2)\end{aligned}$$

The transfer function between $r(t)$ and $\varepsilon_s(t,\rho)$ is precisely Δ, when M_s is chosen according to case a) of Lemma 4.1. A set of data obtained using the scheme of Figure 4.1 can thus be used to estimate δ and verify whether $\hat{\delta} \leqslant \delta_N$.

For unstable minimum-phase plants

Consider the closed-loop experiment where the unstable plant G is controlled by the stabilizing controller K_0. The excitation signal $r(t)$ is applied directly to the plant input, as illustrated in Figure 4.2. The data set consists of the excitation signal $r(t)$, the measured output of the controller K_0, $u_1(t)$, and the measured output of the closed-loop system $y(t)$. Define the error as:

$$\begin{aligned}\varepsilon_s(t,\rho) &= [1 - X(\rho)]\, r(t) - X(\rho)u_1(t) - X(\rho)Ky(t) \\ &= [1 - (1 - M_0)X(\rho) - X(\rho)KG(1 - M_0)]\, r(t) \\ &\quad + \left[\frac{X(\rho)M_0}{G} - X(\rho)K(1 - M_0)\right] v(t) \quad (4.3)\end{aligned}$$

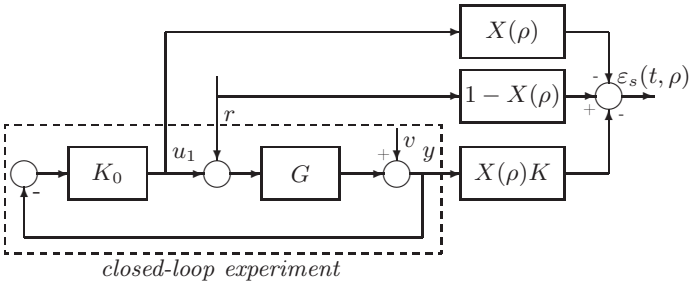

Fig. 4.2. Experimental scheme for unstable plants using one closed-loop experiment

The transfer function between $r(t)$ and $\varepsilon_s(t,\rho)$ is equal to Δ, when M_s is chosen according to case b) of Lemma 4.1. These two signals can be used to estimate δ. Note that the error corresponds to the error used by [50] in the specific case of a stable controller.

Only the data set $r(t), u_1(t)$ and $y(t)$ is needed. The controller K_0 does not need to be known, and there are no requirements on the performance of this controller other than the fact that it stabilizes the system. A closed-loop experiment can also be applied to a stable minimum-phase plant. In this case, the parameterization of M_s corresponds to the parameterization for unstable plants, $M_s = 1 - (1 - M_0)X(\rho)$.

For stable nonminimum-phase plants

Generating the error signal for nonminimum-phase plants requires two open-loop experiments. In the first experiment, the reference signal $r(t)$ is applied to the plant and the output $y_1(t) = Gr(t) + v_1(t)$ is measured. In the second experiment the plant is excited by $y_1(t)$ and gives $y_2(t) = Gy_1(t) + v_2(t)$. Note that a scaling can be used here if necessary. The error signal corresponding to Δ for M_s chosen according to case c) of Lemma 4.1 is then given by

$$\begin{aligned}\varepsilon_s(t,\rho) &= X(\rho)y_1(t) - Ky_1(t) + X(\rho)Ky_2(t)\\ &= [X(\rho)G - KG(1 - X(\rho)G)]r(t)\\ &\quad + [X(\rho) - K + X(\rho)KG]v_1(t) + X(\rho)Kv_2(t) \quad (4.4)\end{aligned}$$

4.3 Controller validation

In the following, a convex optimization problem is proposed, which uses the error signal $\varepsilon_s(t,\rho)$ introduced previously to compute $X(\rho)$ that minimizes $\hat{\delta}$. Since $\varepsilon_s(t,\rho)$ is affected by noise, this estimate is uncertain. In order to minimize the estimation error due to noise and leakage, a spectral estimate will be used [54]. If possible, a periodic reference signal should be used, for which the error due to leakage is zero.

An estimate of $\delta(\rho)$ for non-periodic data, based on spectral estimates, is given by (3.7),

$$\hat{\delta}(\rho) = \max_{\omega_k} \left| \hat{\Delta}(e^{-j\omega_k}) \right| = \max_{\omega_k} \left| \frac{\hat{\Phi}_{r\varepsilon_s}(\omega_k,\rho)}{\hat{\Phi}_r(\omega_k)} \right|.$$

For periodic data, the estimate is given by (3.15). Note that, due to the linear parameterization of $X(\rho)$, the error $\varepsilon_s(t,\rho)$ is linear in ρ for all the cases discussed in Section 4.2 and, consequently, $\hat{\Phi}_{r\varepsilon_s}(\omega_k,\rho)$ is a linear combination of ρ. The estimate of (3.7) (or (3.15) for periodic signals) can therefore be used to define a set of convex constraints such that $\hat{\delta}(\rho) \leqslant \delta_N$.

Proposition 4.1 (Controller validation) *Let $\varepsilon_s(t,\rho)$ be generated as discussed in Section 4.2. Let $\hat{\delta}(\rho)$ be defined as in (3.7) or (3.15) for non-periodic and periodic data, respectively. The controller K is validated if the minimizer $\hat{\gamma}$ of the following convex optimization problem satisfies $\hat{\gamma} \leqslant \delta_N < 1$:*

$$\begin{aligned} \hat{\gamma} &= \min \gamma, \\ \text{subject to } &\hat{\delta}(\rho) \leqslant \gamma, \quad \delta \in \mathcal{D}_X. \end{aligned} \tag{4.5}$$

Theorem 4.2 *Assume that **A1** is satisfied. For non-periodic signals satisfying **A3** and **A4**, let $N, l_2 \to \infty$ with $l_2/N \to 0$. For periodic signals satisfying **A5** and **A6**, let $N, N_p \to \infty$ with $N_p/N \to 0$. Then, a validated controller K is guaranteed to stabilize G.*

Proof: It follows from the proof of Theorem 3.2 that the estimate $\hat{\delta}(\rho)$ converges to δ and $\hat{\rho}$ converges to the minimizer of $\delta(\rho) \leqslant \gamma$.

If $\gamma \leqslant \delta_N$, the sufficient conditions for closed-loop stability given in Theorem 4.1 are met, and K is guaranteed to stabilize G. ■

Remark: Theorem 4.1 presents necessary and sufficient conditions for closed-loop stability. However, according to Theorem 4.2, the data-driven approach of (4.5) is only sufficient. Necessity of the stability conditions is lost due to the parameterization of X, which depends on the choice of the basis functions in β. This introduces a certain conservatism since the parameterization might not allow $\Delta = 0$.

Guaranteeing stability for a finite number of data

Theorem 4.2 states that, if the controller is validated, stability is guaranteed as the number of data tends to infinity. In practice, only a finite number of data is available and stability can be guaranteed only if the estimation errors on $\hat{\delta}(\rho)$ are taken into account in the bound δ_N.

δ_N can be defined using the approach of Section 3.5. Both the error due to the finite frequency grid and the error due to measurement noise and truncation need to be taken into account. The derivation of the bounds is analogous to the derivation in Appendix A.2 and is not detailed here. The error bound between frequencies presented in Section 3.5 represents a worst-case error. Tighter bounds can be formulated if an FIR model is used (see Appendix A.3), but the computational load of the resulting optimization problem is considerable.

Note that the H_∞-norm will, in general, be overestimated in the presence of noise. Even though (for periodic data) the estimate $\hat{\Delta}(e^{-j\omega_k})$ is consistent, its absolute value $|\hat{\Delta}(e^{-j\omega_k})|$ is biased and $E\{|\hat{\Delta}(e^{-j\omega_k})|\} > |E\{\hat{\Delta}(e^{-j\omega_k})\}|$, [54].

4.4 Combining information from different closed-loop experiments

The stability condition for closed-loop experiments (3.3) as well as the condition used in [50] are defined with respect to some stabilizing controller K_s. An error function is constructed using K_s, the plant

controlled by this K_s, and the controller to be verified K. If this error function satisfies the stability conditions, the controller K is guaranteed to stabilize the plant. An experiment is performed with the controller K_s in the loop and the conditions for stability are verified using an estimate of the error function.

If a set of data from a second experiment is available, but obtained with a different stabilizing controller (say K_2) in the loop, the stability conditions would be defined with respect to this controller K_2. Consequently, only the data available from this second experiment can be used to verify the condition. This situation is for example encountered in iterative identification and control [1] and in the windsurfing approach [3], and also in iterative data-driven approaches such as IFT [28]. Even though more data becomes available whenever a new controller is implemented, the effect of noise does not decrease because data from different experiments cannot be combined.

In Theorem 4.1, M_s and K_s are not fixed beforehand, the theorem is valid for any K_s that satisfies the conditions. Consequently, information from different experiments can be combined. In the following, a controller validation test is presented for iterative controller tuning methods.

Assume that the plant G is minimum phase and that n_c stabilizing controllers, $K_1, K_2, \ldots, K_{n_c}$, are available. Define $M_1, M_2, \ldots, M_{n_c}$ as the corresponding closed-loop systems, i.e.

$$M_1 = \frac{K_1 G}{1 + K_1 G}, M_2 = \frac{K_2 G}{1 + K_2 G}, \ldots, M_{n_c} = \frac{K_{n_c} G}{1 + K_{n_c} G}.$$

Sufficient conditions for closed-loop stability can then be formulated as follows.

Lemma 4.2 *Consider the stable filter X. Define $M_{s1} = 1 - X(1 - M_1), M_{s2} = 1 - X(1 - M_2), \ldots, M_{sn_c} = 1 - X(1 - M_{n_c})$. Let M_s be defined as*

$$M_s = \frac{M_{s1} + M_{s2} + \cdots + M_{sn_c}}{n_c} \tag{4.6}$$

Then, the plant G is stabilized by the stable controller K if there exists a filter X and $0 \leqslant \delta_N < 1$, such that $\delta \leqslant \delta_N$.

Proof: Conditions 1 and 2 of Theorem 4.1 are satisfied if $M_s, G(1-M_s), M_s/G$ and $KG(1-M_s)$ are stable. M_s is stable since $M_1, M_2, \ldots, M_{n_c}$ are stable.

$$G(1-M_s) = G\left(1 - \frac{(M_{s1} + M_{s2} + \cdots + M_{sn_c})}{n_c}\right) =$$
$$G\left(1 - \frac{1 - X(1-M_1) + 1 - X(1-M_2) + \cdots + 1 - X(1-M_{n_c})}{n_c}\right)$$
$$= G\left(\frac{X(1-M_1) + X(1-M_2) + \cdots + X(1-M_{n_c})}{n_c}\right)$$

$K_1, K_2 \ldots, K_{n_c}$ stabilize the plant, therefore $G(1-M_1), G(1-M_2)$, $\ldots, G(1-M_{n_c})$ are stable. X is stable by definition, therefore $G(1-M_s)$ is also stable. Since K is stable, $KG(1-M_s)$ is also stable. M_s/G is stable since G is minimum phase and M_s is stable. Conditions 1 and 2 are thus satisfied. According to Theorem 4.1, the remaining condition, $\delta \leqslant \delta_N$, is sufficient for closed-loop stability. ■

Note that this lemma defines sufficient conditions for stability, and can therefore be conservative. However, if this lemma is used for controller validation, data from different closed-loop experiments can be combined and the quality of the estimate can be improved as more data becomes available.

Assume that n_c experiments have been performed according to the scheme of Figure 4.2, with different controllers K_1 to K_{n_c} in the loop for each experiment. Assume that the excitation signal $r(t)$ was the same for all experiments. Let $X(q^{-1}, \rho)$ be parameterized as (4.1). Let the error for each experiment be defined according to (4.3), i.e. $\varepsilon_{s1}(t, \rho)$ is the error calculated according to (4.3) for the experiment with K_1 in the loop, $\varepsilon_{s2}(t, \rho)$ the error with K_2 in the loop, etc. The noise in the experiment with K_1 in the loop is denoted $v_1(t)$, in the experiment with K_2 by $v_2(t)$, etc. Define the error signal as

$$\varepsilon_s(t,\rho) = \frac{\varepsilon_{s1}(t,\rho) + \varepsilon_{s2}(t,\rho) + \cdots + \varepsilon_{sn_c}(t,\rho)}{n_c} =$$
$$[M_s - X(\rho)K(1-M_s)]r(t) + \left[\frac{X(\rho)M_1}{G} - X(\rho)K(1-M_1)\right]\frac{v_1(t)}{n_c}$$
$$+ \left[\frac{X(\rho)M_2}{G} - X(\rho)K(1-M_2)\right]\frac{v_2(t)}{n_c}$$
$$+ \cdots + \left[\frac{X(\rho)M_{n_c}}{G} - X(\rho)K(1-M_{n_c})\right]\frac{v_{n_c}(t)}{n_c}. \tag{4.7}$$

The transfer function from $r(t)$ to $\varepsilon_s(t,\rho)$ then corresponds to Δ, when M_s is chosen as in (4.6). Note that the stochastic properties of the noise change as the controller in the loop changes. The noise sequence of the consecutive experiments is therefore non-stationary. In the following theorem, convergence is shown for periodic input signals. This is a standard result for stationary stochastic sequences.

Theorem 4.3 *Assume that $r(t)$ satisfies **A5** and **A6**. Let $\varepsilon_s(t,\rho)$ be calculated according to (4.7), $\hat{\Phi}_{r\varepsilon_s}(\omega_k,\rho)$ according to (3.13) and $\hat{R}_{r\varepsilon_s}(\tau,\rho)$ according to (3.14). Assume that the noise in the n_c experiments is independent and satisfies **A1** and **A2**. Then, with probability 1, as the number of experiments n_c tends to infinity,*

$$\lim_{n_c\to\infty} \frac{\hat{\Phi}_{r\varepsilon_s}(\omega_k,\rho)}{\Phi_r(\omega_k)} = \Delta(e^{-j\omega_k}).$$

Proof: The proof is given in Appendix A.4. ∎

Theorem 4.3 states that, as the number of experiments tends to infinity, the estimate

$$\frac{\hat{\Phi}_{r\varepsilon_s}(\omega_k,\rho)}{\Phi_r(\omega_k)}$$

converges to the noise-free value $\Delta(e^{-j\omega_k})$. If this estimate is used in the controller validation of Proposition 4.1, the reliability of the test increases as the number of experiments increases. Since $r(t)$ is periodic, $\Delta(e^{-j\omega_k})$ can be estimated only on a finite frequency grid and the inter-frequency error needs to be taken into account. If the bound δ_N is formulated similar to the bounds of Section 3.5, the conservatism decreases as the number of experiments increases.

If a burst excitation is used, where $r(t) = 0, \forall t \neq [1, T_b]$ and the output is measured until the transient is zero, $\Delta(e^{-j\omega})$ can be estimated for all frequencies ω and not just on a finite frequency grid ω_k. This estimate is statistically less efficient than an estimate based on a periodic input, when only one experiment is available. If data of different experiments are combined, the estimate $\hat{\delta}$ converges to δ and, asymptotically as $n_c \to \infty$, a validated controller is guaranteed to stabilize the plant.

4.5 Numerical example

Consider the plant given by the discrete-time model $G(q^{-1})$:

$$G(q^{-1}) = \frac{0.7893q^{-3}}{1 - 1.418q^{-1} + 1.59q^{-2} - 1.316q^{-3} + 0.886q^{-4}}$$

This corresponds to a stable minimum-phase model of the flexible transmission system proposed as a benchmark for digital control design in [49]. This example is also used in Section 3.6.2. Eight different controllers are available, out of which four stabilize the plant and four destabilize it. All controllers have the same structure and contain an integrator:

$$K = \frac{k_0 + k_1q^{-1} + k_2q^{-2} + k_3q^{-3} + k_4q^{-4} + k_5q^{-5}}{1 - q^{-1}}.$$

The parameters of the controllers are given in Table 4.1: K_1 to K_4 stabilize the plant, K_5 to K_8 do not.

An open-loop experiment on G is simulated. The plant is excited by a periodic pseudo-randon binary signal (PRBS) with period $N_p = 127$, length $N = 4N_p = 508$ and amplitude 1. The output is periodic and disturbed by a zero-mean white noise, such that the signal-to-noise ratio on the output of the plant is about 10 in terms of variance. Since $r(t)$ is periodic, $\hat{\delta}(\rho)$ is calculated according to (3.15). The bound is fixed to $\delta_N = 0.9$ to compensate for the finite frequency grid and the estimation error due to noise.

The filter $X(q^{-1}, \rho)$ is defined as an FIR filter of order $(n_\rho - 1)$. An additional linear constraint $\sum \rho = 1$ is added to ensure unity static

Table 4.1. Controllers used in the illustrative example

	k_0	k_1	k_2	k_3	k_4	k_5
K_1	0.17	−0.18	0.17	−0.12	0.07	0.05
K_2	0.27	−0.43	0.50	−0.45	0.32	−0.05
K_3	0.21	−0.28	0.29	−0.24	0.16	0.01
K_4	0.17	−0.18	0.17	−0.11	0.07	0.05
K_5	−2.77	7.76	−11.01	11.19	−8.07	3.06
K_6	−1.23	3.56	−5.01	5.07	−3.68	1.45
K_7	−0.96	2.87	−4.10	4.23	−3.12	1.26
K_8	0.88	−2.10	2.81	−2.74	1.97	−0.67

gain, which is required since the controllers contain an integrator. A Monte-Carlo simulation with 100 experiments is performed, using a different noise realization for each experiment.

For $n_\rho = 4$, all four destabilizing controllers fail the validation test, for all 100 experiments. The stabilizing controllers K_1 and K_4 are validated in 98 experiments, K_2 is validated in 91 experiments, K_3 in 97. If n_ρ is increased to 8, K_1, K_3 and K_4 are validated in all 100 experiments and K_2 in 96. If n_ρ is increased further, K_2 is also validated in all 100 experiments. When the order of X is increased to 20, all destabilizing controllers are still discarded correctly.

Due to the system gain, a signal-to-noise ratio of about 10 with respect to the output signal corresponds to a ratio of $r/v \approx 1.3$ in terms of variance. The stable controllers are rejected as a result of the bias in the estimate due to noise. The effect of noise can be reduced by increasing the number of periods in the reference signal. When the same experiment is performed with a reference signal of length $N = 8N_p = 1016$, all stabilizing controllers are validated for all 100 experiments for $n_\rho = 3$.

4.6 Conclusions

In all stability tests, detailed information regarding the plant is needed to guarantee closed-loop stability. If only partial information is available, stability can be guaranteed only if bounds on the lacking information can be formulated. Definition of such bounds

often introduces conservatism, but without these bounds the test is not reliable. The test proposed in this chapter is no exception, and stability is guaranteed as the number of data tends to infinity. For a finite number of data, the estimation error needs to be taken into account, and error bounds are in general conservative. However, the proposed approach offers an intuitive trade-off between conservatism and reliability, if tight error bounds cannot be formulated.

In the proposed test, the bound δ_N and the number of basis functions in X need to be chosen by the user. The trade-off between conservatism and reliability introduced by these parameters is clear. Since the optimization is convex, the conservatism of the test decreases if more basis functions are added to X. If the bound δ_N is increased, the conservatism also decreases, but the reliability decreases since smaller estimation errors are accounted for. If data are available from closed-loop experiments with different controllers in the loop, the data can be combined to improve the quality of the estimate and reduce the conservatism.

5

Accuracy of non-iterative model reference control

One of the main features of the non-iterative data-driven controller tuning approach treated in this thesis is the possibility to fix the order of the controller and minimize the control criterion for this class of controllers. In common terms of system identification, this situation leads to undermodeling of the controller. In the case of undermodeling, bias shaping is essential for the control performance that can be achieved [20]. This bias shaping is complicated by the way the noise enters the controller identification problem. In Chapter 2, the use of the correlation approach has been proposed to deal with the noise.

The problems encountered in non-iterative data-driven controller tuning have been treated in several publications, [9, 71]. In Section 5.1, the accuracy of the solutions proposed in the literature as well as that of the correlation approach is studied. For the case of no undermodeling, variance expressions for the different approaches are derived. For the case of undermodeling, convergence to the optimal solution is investigated. In addition to these approaches, application of the method presented in [73] to the controller tuning problem is presented. This method is developed for errors-in-variables problems and uses periodicity of the data. It is shown that this method can also be used in the case of undermodeling. The performance of the different approaches is compared in Section 5.2 for the cases with undermodeling and without undermodeling. The results are illustrated by a simulation example.

According to [29], non-iterative data-driven model reference control can be interpreted as the identification of a plant model that is parameterized directly in terms of the controller parameters. In this case the resulting controller tuning approach is direct. The results of Section 5.1 are therefore also applicable for identification using a direct parameterization.

The advantage of directly minimizing the control objective with respect to the controller parameters is that undermodeling is circumvented that might occur in an intermediate modeling step. However, this leads to a non-standard identification problem. Furthermore, the lack of a plant model complicates the robustness analysis of the resulting controller. A legitimate question is therefore: why would one prefer such a direct approach over an indirect (model-based) method? If an intermediate model is used, results from system identification apply directly to the plant model, and robustness can be analyzed using well-known methods.

Clearly, many different model-based approaches have been developed. In many model-based approaches, the controller order depends on the model order. Such approaches cannot be compared directly to the data-driven approach presented in this thesis. Furthermore, the achieved performance depends on the identification procedure used to identify the plant model. In order to provide a fair comparison between an indirect approach and the proposed direct (data-driven) solution, the results of Section 5.1 are compared to an asymptotically efficient indirect method, based on results from system identification.

It is argued in [29] that, in the context of system identification, the problem of undermodeling can be avoided when a full-order model is estimated using a statistically efficient estimator. This full-order model can then be used for further calculations, without the loss of statistical accuracy. In Section 5.3, a model-based approach is presented that uses this idea to solve the approximate model reference problem for a fixed-order controller. The accuracy of this approach is compared to direct (data-driven) solutions. The results are illustrated by a simulation example.

In the approximate model reference control problem, the main objective is to minimize the approximate model reference criterion. However, in this chapter the asymptotic variance of the controller parameters is studied. Since the approximate model reference crite-

rion is a quadratic function of these controller parameters, the performance is directly related to the accuracy of the parameters and smaller parameter variance implies better performance.

5.1 Accuracy of data-driven approaches

In the following, only stable systems and open-loop measurements are considered. The filter $F = 1$ and $L = 1 - M$ are chosen as in Section 2.3. Assume that **A1** and **A2** are satisfied and that **A7** is satisfied in Case **C1** and **A8** in Case **C2**. Consistency and accuracy of the different estimates is analyzed for Case **C1**. Asymptotic convergence is analyzed for Case **C2**.

5.1.1 Prediction error methods

In Section 2.3, the controller identification problem was analyzed in the prediction error framework. It was shown that, in Case **C1**, a tailor-made noise model is required. If such a tailor-made parametrization is used, where $H(\eta, \rho) = K(\rho)H_p(\eta)$, the estimation error is asymptotically Gaussian distributed [54], i.e. $\sqrt{N}(\hat{\rho} - \rho_0) \overset{dist}{\rightarrow} \mathcal{N}(0, P_p)$. The variance of the parameters, which is equal to the Cramér-Rao bound, is given by:

$$P_p = \sigma^2 C_1^{-1}, \tag{5.1}$$

where

$$C_1 = \lim_{N\to\infty} \frac{1}{N} \sum_{t=1}^{N} \left[\frac{1}{H^*}\phi_0(t)\right] \left[\frac{1}{H^*}\phi_0(t)\right]^T. \tag{5.2}$$

$\phi_0(t)$ is defined in (2.20) and

$$H^* = K^* H_{\tilde{y}}. \tag{5.3}$$

In Case **C2**, the estimate does not converge to the optimal controller $K(\rho_0)$.

5.1.2 Instrumental variables

In [9], the use of instrumental variables (IV) is proposed to deal with the measurement noise. The IV solution is given by:

$$\hat{\rho} = \left[\frac{1}{N} \sum_{t=1}^{N} \zeta(t)\phi(t)^T \right]^{-1} \frac{1}{N} \sum_{t=1}^{N} \zeta(t)s(t), \tag{5.4}$$

where $\zeta(t)$ is a vector of length n_ρ that is not correlated with $\tilde{y}_c(t)$. The regression vector $\phi(t)$ is defined in (2.20).

Case C1, $K^* \in \{K(\rho)\}$

Two different choices for the instruments $\zeta(t)$ are discussed in [9] .

Repeated experiment: Perform a second experiment with the same input $r(t)$. The instrumental variable vector is then defined as:

$$\zeta(t) = \beta(q^{-1})y_{k2}(t) = \phi_2(t) \triangleq \phi_0(t) + \tilde{\phi}_2(t).$$

where $\beta(q^{-1})$ is defined in (2.8). The noise in the second experiment is not correlated with the noise in the first experiment, therefore

$$\lim_{N\to\infty} (\hat{\rho} - \rho_0) =$$
$$\lim_{N\to\infty} \left[\frac{1}{N} \sum_{t=1}^{N} \phi_2(t)\phi(t)^T \right]^{-1} \lim_{N\to\infty} \frac{1}{N} \sum_{t=1}^{N} \tilde{\phi}_2(t)K(\rho_0)\tilde{y}_c(t) = 0$$

This estimate is thus consistent.

Identification of the plant: Identify a model of the plant $\hat{G}$, generate the simulated output $\hat{y}(t) = \hat{G}r(t)$ and define the instruments as $\zeta(t) = \beta(1-M)^2\hat{y}(t)$. The estimate is consistent, but the variance depends on the quality of the model [75].

The instruments generated by a second experiment are analyzed in [73]. The estimation error $\sqrt{N}(\hat{\rho} - \rho_0)$ is asymptotically Gaussian distributed and the asymptotic covariance matrix is given by:

$$P_{IV} = \sigma^2 R_0^{-1}(C_2 + C_3)R_0^{-1}, \tag{5.5}$$

where

$$
\begin{aligned}
R_0 &= \lim_{N\to\infty} \frac{1}{N} \sum_{t=1}^{N} \phi_0(t)\phi_0^T(t) \\
C_2 &= \lim_{N\to\infty} \frac{1}{N} \sum_{t=1}^{N} [H^*\phi_0(t)][H^*\phi_0(t)]^T \\
C_3 &= E\left\{ [H^*\tilde{\phi}_2(t)][H^*\tilde{\phi}_2(t)]^T \right\}
\end{aligned}
\tag{5.6}
$$

and H^* is defined in (5.3).

Using a second experiment, $2N$ data points are needed for an estimate with a covariance matrix of approximately $\frac{1}{N}P_{IV}$. Theoretically, optimal variance can be achieved by using an optimal instrumental variable [75]. Such optimal instruments depend on the unknown controller parameters. An iterative algorithm can be used to improve the accuracy: in the first iteration, a controller is identified with a non-optimal IV, then, in the second iteration, a better IV is constructed based on the controller from the first iteration. This procedure can be continued to improve the accuracy of the estimates.

Case C2, $K^* \notin \{K(\rho)\}$

In contrast to prediction error methods, no identification criterion is minimized in an instrumental variable approach. The parameter estimate is defined directly as (5.4). However, for the specific choice of IV suggested in [9], where the instrumental variables are generated by a second experiment, a corresponding quadratic identification criterion exists asymptotically. This specific choice of instrumental variables can therefore be used for bias shaping and 2-norm minimization as shown next. Assume that the instruments are generated using a second experiment. The IV solution is then given by:

$$
\hat{\rho} = \left[\frac{1}{N} \sum_{t=1}^{N} \phi_2(t)\phi(t)^T \right]^{-1} \frac{1}{N} \sum_{t=1}^{N} \phi_2(t)s(t). \tag{5.7}
$$

Since the noise in the second experiment is not correlated with the noise in the first experiment, the estimate converges to

$$
\lim_{N\to\infty} \hat{\rho} = \lim_{N\to\infty} \left[\frac{1}{N} \sum_{t=1}^{N} \phi_0(t)\phi_0(t)^T \right]^{-1} \lim_{N\to\infty} \frac{1}{N} \sum_{t=1}^{N} \phi_0(t)s(t).
$$

This is the least squares minimum of:

$$J_{IV}(\rho) = \lim_{N\to\infty} \frac{1}{N}\sum_{t=1}^{N}[s(t) - \phi_0(t)\rho]^2$$
$$= \lim_{N\to\infty} \frac{1}{N}\sum_{t=1}^{N}\left[\left((1-M)M - (1-M)^2GK(\rho)\right)r(t)\right]^2. \quad (5.8)$$

Since $r(t)$ is white, the frequency domain equivalent by Parseval's theorem is given by:

$$J_{IV}(\rho) = \frac{1}{2\pi}\int_{-\pi}^{\pi}\left|(1-M)M - (1-M)^2GK(\rho)\right|^2 d\omega, \quad (5.9)$$

where, for the ease of notation, $e^{-j\omega}$ has been omitted from the arguments of M, G and $K(\rho)$. It is clear that $J_{IV}(\rho)$ is equivalent to $J(\rho)$ in (2.6).

If the instruments are generated using a second experiment, the estimate is consistent. However, the variance of this estimate is relatively large. In order to reduce the variance, it is suggested in [9] to generate the instruments by simulating an identified model. In case **C1**, this does not affect the consistency. In case **C2** it does affect convergence. The IV solution in (5.7) is the minimizer of $J_{IV}(\rho)$ only if the model is identified correctly, i.e. $\hat{G} = G$. If this is not the case, the resulting estimate does not converge to ρ_0.

5.1.3 Identifying the inverse of the controller using PEM

Since the output $s(t)$ is not affected by noise, identification of the inverse of the controller, $K^{-1}(\rho)$, is a standard identification problem. In [71], the use of PEM methods to identify $K^{-1}(\rho)$ is proposed. The error is constructed using the VRFT scheme and given by:

$$\varepsilon_i(t,\rho) = \frac{L_i}{M(1-M)}\left(K^{-1}(\rho)s(t) - y_c(t)\right)$$
$$= L_i\left(K^{-1}(\rho) - (K^*)^{-1}\right)r(t) - \frac{L_i}{M(1-M)}\tilde{y}_c(t), \quad (5.10)$$

where L_i is an appropriate filter. The noise filter is thus given by

$$H_i^* = \frac{L_i}{M(1-M)} H_{\tilde{y}} \tag{5.11}$$

Case C1, $K^* \in \{K(\rho)\}$

The gradient of $\varepsilon_i(t,\rho)$ is given by:

$$\psi(t) = \frac{d\varepsilon_i(t,\rho)}{d\rho} = -\frac{L_i \beta(q^{-1})}{K(\rho)^2} r(t), \tag{5.12}$$

where $\beta(q^{-1})$ is defined in (2.8). If a model structure is used that identifies a noise model $H(\eta)$ such that $H_i^* \in \{H(\eta)\}$, the covariance matrix is given by [54]:

$$P_i = \sigma^2 \left[\lim_{N\to\infty} \frac{1}{N} \sum_{t=1}^{N} \left[\frac{1}{H_i^*} \psi(t) \right] \left[\frac{1}{H_i^*} \psi(t) \right]^T \right]^{-1} \tag{5.13}$$

Replacing H_i^* and $\psi(t)$ by the expressions of (5.11) and (5.12) gives:

$$P_i = \sigma^2 C_1^{-1} = P_p \tag{5.14}$$

where P_p defined in (5.1) corresponds to the Cramér-Rao bound.

Remarks:

- The linear controller structure defined in (2.7) now leads to a non-convex optimization problem.
- The inverse of the controller $K^{-1}(\rho)$ needs to be stable.

Case C2, $K^* \notin \{K(\rho)\}$

In this case, *bias shaping* is again essential for the quality of the controller. The following analysis follows the analysis of Section 2.3. Let the identification criterion for estimation of the inverse of the controller be defined as

$$J_i(\rho) = \frac{1}{N} \sum_{t=1}^{N} [H^{-1}(\eta,\rho)\varepsilon_i(t,\rho)]^2, \tag{5.15}$$

where $\varepsilon_i(t,\rho)$ is defined as (5.10) and $H(\eta,\rho)$ is the noise model. If no measurement noise is present, the identification criterion is given by:

$$J_i(\rho) = \frac{1}{N}\sum_{t=1}^{N}\left[H^{-1}(\eta,\rho)L_i\left(\frac{1}{K(\rho)} - \frac{1}{K^*}\right)r(t)\right]^2. \qquad (5.16)$$

This corresponds to the transfer function in $J(\rho)$ of (2.6) if

$$H(\eta,\rho)^{-1}L_i = K(\rho)M(1-M).$$

However, if the measurements are affected by noise, substitution of $H(\eta,\rho)^{-1}L_i$ by $K(\rho)M(1-M)$ gives

$$J_i(\rho) = \frac{1}{N}\sum_{t=1}^{N}\left[K(\rho)M(1-M)\left(\frac{1}{K(\rho)} - \frac{1}{K^*}\right)r(t) - K(\rho)(1-M)^2 v(t)\right]^2.$$

In this case, the controller parameters appear in the noise term, as was the case for the PEM in Section 2.3 and $\lim_{N\to\infty}\hat{\rho} \neq \rho_0$.

In [71], the use of a different filter $L_i = M^2/G$ that depends on the unknown plant G is proposed. Clearly L_i is unknown and only an estimate can be used. The resulting criterion, if G is available, would be

$$J_i(\rho) = \left\|(1-M)M\left[\frac{K^*}{K(\rho)} - 1\right]\right\|_2^2.$$

This criterion does not correspond to $J(\rho)$. In [9], the quality of the approximation $J(\rho)$ is established, the quality of $J_i(\rho)$ remains an open question.

Remark: According to [29], VRFT can be interpreted as identification of a directly parameterized plant model using a prefiltering approach. In this direct parameterization, the plant model is parameterized as

$$G(\rho) = \frac{M}{(1-M)K(\rho)}.$$

The corresponding prediction error is given by

$$\begin{aligned}\varepsilon_g(t,\rho) &= L_g\left(\frac{M}{(1-M)K(\rho)}r(t) - y(t)\right)\\ &= \frac{L_g}{(1-M)^2}\left(K^{-1}(\rho)s(t) - y_c(t)\right).\end{aligned}$$

If this error is compared to $\varepsilon_i(t,\rho)$ in (5.10), it is easily seen that both errors are equivalent if

$$L_g = L_i \frac{1-M}{M}.$$

Estimating a directly parameterized plant model is thus equivalent to estimating the inverse of the controller. Consequently, the Cramér-Rao bound can be reached in Case **C1**. If, in Case **C2**, the parameters are estimated using a PEM, the estimates do not converge to the optimal parameters.

5.1.4 Correlation approach

The use of the correlation approach to deal with the effect of noise has been proposed in Chapter 2. It is shown that the correlation criterion $J_{N,l_1}(\rho)$ of (2.31) converges asymptotically to $J(\rho)$. The estimate is therefore consistent in Case **C1** and converges asymptotically to ρ_0 in Case **C2**.

In Case **C1**, the accuracy of the estimate follows from standard results for extended instrumental variable methods [75]. The covariance matrix for the correlation approach is given by:

$$P_c = \sigma^2 (Q^T Q)^{-1} Q^T S Q (Q^T Q)^{-1} \tag{5.17}$$

where

$$Q = \lim_{N\to\infty} \frac{1}{N} \sum_{t=1}^{N} E\{\zeta(t)\phi^T(t)\} = \lim_{N\to\infty} \frac{1}{N} \sum_{t=1}^{N} \zeta(t)\phi_0^T(t)$$

$$S = \lim_{N\to\infty} \frac{1}{N} \sum_{t=1}^{N} [H^*\zeta(t)][H^*\zeta(t)]^T.$$

The estimate is consistent, but a bias exists when a finite number of data is used for the estimate, as shown in Section 2.4.3. The bias is given by (2.44). For a finite number of data, the design variable l_1 leads to a trade-off between the bias due to noise and the difference $\tilde{J}_{N,l_1}(\rho) - J(\rho)$.

5.1.5 Periodic errors-in-variables approach

The identification problem shown in Figure 2.4 can be seen as a specific case of an errors-in-variables problem. There is no fundamental identifiability problem, and the identification is a lot simpler than the standard errors-in-variables (EIV) problem, but techniques developed for EIV problems can be applied to deal with the measurement noise. In particular, the method proposed in [73] is considered, which takes advantage of the periodicity of the reference signal. The method uses an extended IV method.

Assume that $r(t)$ satisfies **A5**. The regression vector $\phi_j(t)$ in period j is defined as :

$$\phi_j(t) = \phi_0(t) + \tilde{\phi}_j(t), \quad t = 1, \ldots, N_p, \tag{5.18}$$

where $1 \leqslant j \leqslant n_p$ and $\tilde{\phi}_j(t)$ is the noise contribution to the regression vector in period j. $\zeta_j(t)$ denotes the instrumental vector for period j, defined as:

$$\begin{aligned}
\zeta_1(t) &= [\phi_2^T(t) \ldots \phi_{n_p}^T(t)]^T \\
\zeta_2(t) &= [\phi_3^T(t) \ldots \phi_{n_p}^T(t)\, \phi_1^T(t)]^T \\
&\vdots \\
\zeta_j(t) &= [\phi_{j+1}^T(t) \ldots \phi_{n_p}^T(t)\, \phi_1^T(t) \ldots \phi_{j-1}^T(t)]^T
\end{aligned} \tag{5.19}$$

Define the matrices:

$$\begin{aligned}
\bar{\zeta}(t) &= [\zeta_1(t) \ldots \zeta_{n_p}(t)] \\
\bar{\phi}(t) &= [\phi_1(t) \ldots \phi_{n_p}(t)]
\end{aligned} \tag{5.20}$$

and the vector

$$\bar{s}(t) = [s_1(t) \ldots s_{n_p}(t)]^T \tag{5.21}$$

where $s_j(t)$ is the output of K^* at time t within period j:

$$s_j(t) = s(t + (j-1)N_p).$$

The solution of the extended IV method proposed in [73] is then given by:

$$\hat{\rho} = (\hat{R}^T \hat{R})^{-1} \hat{R}^T \hat{r} \tag{5.22}$$

where

$$\begin{aligned}\hat{R} &= \frac{1}{N}\sum_{t=1}^{N_p}\bar{\zeta}(t)\bar{\phi}^T(t) = \frac{1}{N}\sum_{j=1}^{n_p}\sum_{t=1}^{N_p}\zeta_j(t)\phi_j^T(t)\\ \hat{r} &= \frac{1}{N}\sum_{t=1}^{N_p}\bar{\zeta}(t)\bar{s}^T(t) = \frac{1}{N}\sum_{j=1}^{n_p}\sum_{t=1}^{N_p}\zeta_j(t)s_j(t)\end{aligned} \tag{5.23}$$

Case C1, $K^* \in \{K(\rho)\}$

In [73], it is assumed that the measurement noise within different periods is uncorrelated. If the scheme of Figure 2.4 is used to generate $s(t)$ and $\phi(t)$, if the input is periodic and **A1-A2** are valid, then this assumption is not met. Even if the measurement noise $v(t)$ is white, i.e. $H_v = 1$, $\tilde{y}_c(t)$ is not white since $H_{\tilde{y}} = (1-M)^2 H_v$. Consequently, the measurement noise within different periods is correlated. The following theorem is an extension of the results of [73].

Theorem 5.1 *Assume that **A1,A2** and **A5** are satisfied and that $r(t)$ is persistently exciting of order n_ρ. Then, the estimate $\hat{\rho}$ of (5.22) converges w.p.1 to ρ_0 as $N_p \to \infty$ and the asymptotic covariance matrix of the estimation error $\sqrt{N}(\hat{\rho} - \rho_0)$ for (5.22) is given by:*

$$P_{eiv} = \sigma^2 R_0^{-1}\left(C_2 + \frac{C_3}{n_p - 1}\right)R_0^{-1}, \tag{5.24}$$

where C_2 is defined as in (5.6) and

$$C_3 = E\left\{[H^*\tilde{\phi}_j(t)][H^*\tilde{\phi}_j(t)]^T\right\}. \tag{5.25}$$

Proof: The main idea of the proof is that, as $N_p \to \infty$, the noise within different periods is uncorrelated. The proof is given in Appendix A.5. ■

Note that the definition of C_3 corresponds to the definition in (5.6), with $\tilde{\phi}_2$ replaced by $\tilde{\phi}_j$ and, if the characteristics of the noise are the same, these matrices are equivalent. It is shown in [73] that the achieved variance P_{eiv} is optimal in the class of extended IV methods. As the number of periods $n_p \to \infty$, $P_{eiv} \to \sigma^2 R_0^{-1} C_2 R_0^{-1}$. This

variance corresponds to the optimal variance that can be achieved when no noise model is identified, $P_{opt} = \sigma^2 R_0^{-1} C_2 R_0^{-1}$. Note that in standard identification problems, if the input is noise free and the output is affected by white noise filtered by H^* defined in (5.3), this variance would be achieved for the output error structure [54]. As the number of periods $n_p \to \infty$, the variance thus converges to this optimal variance, $P_{eiv} \to P_{opt}$.

Case C2, $K^* \notin \{K(\rho)\}$

The estimate in (5.22) is the optimum of

$$J_{eiv}(\rho) = \|\hat{r} - \hat{R}\rho\|_2^2. \tag{5.26}$$

Define

$$r_0 = \lim_{N_p \to \infty} \frac{1}{N_p} \sum_{t=1}^{N_p} \phi_0(t) s(t), \tag{5.27}$$

and note that, for periodic data, R_0 is equivalent to

$$R_0 = \lim_{N_p \to \infty} \frac{1}{N_p} \sum_{t=1}^{N_p} \phi_0(t) \phi_0^T(t). \tag{5.28}$$

The matrix $\hat{R}$ converges to

$$\lim_{N_p \to \infty} \hat{R} = [R_0 \dots R_0]^T. \tag{5.29}$$

Equivalently

$$\lim_{N_p \to \infty} \hat{r} = [r_0 \dots r_0]^T, \tag{5.30}$$

and

$$\lim_{N_p \to \infty} J_{eiv}(\rho) = \left\| \begin{bmatrix} r_0 \\ \vdots \\ r_0 \end{bmatrix} - \begin{bmatrix} R_0 \\ \vdots \\ R_0 \end{bmatrix} \rho \right\|_2^2 = (n_p - 1) \|r_0 - R_0 \rho\|_2^2. \tag{5.31}$$

Assume **A1, A2, A5** and $\Phi_r(\omega_k) = 1$ for $\omega_k = 2\pi k/N_p$ and $k = 0, \dots, N_p - 1$. Note that this signal can be generated as a multi-sine,

or as a PRBS signal with an offset. Since R_0 is square and has full rank, the optimum of this criterion is given by

$$\lim_{N_p \to \infty} \hat{\rho} = R_0^{-1} r_0. \tag{5.32}$$

This is the solution of the following least-squares criterion

$$R_0^{-1} r_0 = \arg \min_{\rho \in \mathcal{D}_K} \lim_{N_p \to \infty} \frac{1}{N_p} \sum_{t=1}^{N_p} (s(t) - \phi_0(t)\rho)^2.$$

It then follows from (5.8) and (5.9) that the minimizer of $J_{eiv}(\rho)$ converges to ρ_0 in case **C2**.

5.2 Comparison of data-driven approaches

5.2.1 Asymptotic accuracy

Case C1, $K^* \in \{K(\rho)\}$

Under assumption **C1**, the following can be concluded:

- The Cramér-Rao bound can be achieved with a PEM when a tailor-made parameterization is used. The noise-model needs to be identified correctly for consistency, in contrast to the standard identification problem.
- The Cramér-Rao bound can also be achieved when identifying the inverse of the controller. In this case, the noise-model does not affect consistency.
- The Cramér-Rao bound can also be achieved by using optimal instrumental variables.

These methods lead to a non-convex optimization problem (also for a linearly parameterized controller). Convergence to the global optimum cannot in general be guaranteed. Furthermore, the inverse of the controller needs to be stable.

The correlation approach and the errors-in-variables approach lead to a *convex* optimization when the controller is parameterized as in (2.7). No noise model is identified.

- The errors-in-variables approach is optimal, as the number of periods $n_p \to \infty$, i.e. $P_{eiv} \to P_{opt}$.
- The variance expression for the correlation method is difficult to analyze. It can be shown, under some specific hypotheses, that the variance of an extended IV tends to the optimal variance [75], but this is not the case for the general identification problem. The design parameter l_1 affects the bias with respect to noise for a finite number of data.

To conclude, under assumption **C1**, the Cramér-Rao bound can be achieved. Since the noise model does not affect consistency when the inverse of the controller is identified, identifying the inverse of the controller should be prefered over the use of a PEM approach to identify the controller itself. If the inverse of the controller is unstable, the best variance achievable, P_{opt}, is achieved using the errors-in-variables approach, when $n_p \to \infty$.

Case C2, $K^* \notin \{K(\rho)\}$

Assumption **C1** is not compatible with one of the main motivations for direct controller tuning, namely the tuning of controllers of limited order. If the order of the controller is fixed beforehand, and the controller minimizing a 2-norm is sought, **C1** is violated per definition and case **C2** needs to be considered. It is shown in Section 2.3 that, in this case, the estimate by PEM does not converge asymptotically to ρ_0. In Section 5.1.3, it is shown that identification of the inverse of the controller also does not converge to the optimal solution. It is thus necessary to resort to the statistically less efficient methods using (extended) instrumental variables.

In Case **C2**, frequency weighting is essential. Since the identification of a noise model affects the frequency weighting, no noise model can be used when bias shaping is required. If the reference signal $r(t)$ can be chosen, a periodic signal with many periods can be applied and the EIV method of the correlation approach can be used to identify the controller parameters. If the reference signal cannot be chosen arbitrarily and non-periodic data or only a few periods of periodic data are available, the correlation approach can be used.

To conclude, in case **C2**, the price to pay for convergence is the use of statistically less efficient methods, since no noise model can be

used to improve the estimate. The achieved control objective $J(\hat{\rho})$ depends on both the variance and the bias error, and this mean-square-error of the criterion depends strongly on the nature of the problem, i.e. the reference signal $r(t)$, the noise spectrum and the distance between K^* and $K(\rho)$.

5.2.2 Numerical example

The different methods discussed above are tested in simulation on the flexible transmission system proposed as benchmark in [49]. This example was used in [9,71] to illustrate the direct data-driven controller tuning approach. In Section 3.6.2, a minimum-phase model of this same plant was used.

The plant is given by the discrete-time model $G(q^{-1})$

$$G(q^{-1}) = \frac{0.283q^{-3} + 0.507q^{-4}}{1 - 1.418q^{-1} + 1.589q^{-2} - 1.316q^{-3} + 0.886q^{-4}}.$$

The controller structure is given as

$$K(\rho) = \frac{\rho_1 + \rho_2 q^{-1} + \rho_3 q^{-2} + \rho_4 q^{-3} + \rho_5 q^{-4} + \rho_6 q^{-5}}{1 - q^{-1}}$$

PRBS signals with unity amplitude are used as input to the system, $r(t)$. The output of the plant is disturbed by zero-mean white noise. The first periods, i.e. from zero initial state, are used in the PEM method and when identifying the inverse of the controller. For the correlation approach and the errors-in-variables method, a periodic signal of the same length is used. Since $r(t)$ is a PRBS signal, the extended instruments of (2.29) can be taken as $\zeta(t) = [r(t), r(t-1), \ldots, r(t-l_1)]^T$. In the following, $l_1 = 25$, for which $\tilde{J}_{N,l_1}(\rho)$ is a good approximation of $J(\rho)$.

Results are given for different period lengths N_p and an increasing number of periods n_p. A Monte-Carlo simulation with 100 experiments is performed, using a different noise realization for each experiment, for a signal-to-noise ratio (SNR) of 100 and of 10 in terms of variance. The noise realizations are the same for all methods.

Table 5.1. Mean values for the achieved performance $J(\rho)$, for M_1, different period lengths N_p and different number of periods n_p.

	$N_p = 63, n_p = 16$		$N_p = 127, n_p = 8$		$N_p = 127, n_p = 12$	
SNR	100	10	100	10	100	10
PEM	0.01240	0.3008	0.00730	0.2629	0.00729	0.2645
Inv	0.00466	0.2929	0.00324	0.0255	0.00227	0.0110
CbT	0.00784	0.0295	0.00643	0.0244	0.00545	0.0202
EIV	0.00676	0.0643	0.00558	0.0499	0.00472	0.0405

Case C1, $K^* \in \{K(\rho)\}$

The reference model is defined as

$$M_1(q^{-1}) = \frac{K(\rho_0)G}{1 + K(\rho_0)G} \tag{5.33}$$

with

$$\rho_0 = [0.2045 \quad -0.2715 \quad 0.2931 \quad -0.2396 \quad 0.1643 \quad 0.0084]^T$$

The optimal controller $K(\rho_0) \in \{K(\rho)\}$ and the objective can be achieved. The PEM approach with a tailor-made parameterization has not been implemented. Instead, the Box-Jenkins structure is used, which should theoretically be consistent if the order of the noise model is sufficiently large. The inverse of the controller is identified using the Box-Jenkins structure (Inv).

The results are given in Table 5.1. For a SNR of 100 and $N > 1000$, the asymptotic variance expressions of Sections 5.1.1-5.1.5 are assumed to be applicable. For this SNR, estimation of the inverse is efficient, as expected. The error for the correlation approach (CbT) and the periodic errors-in-variables approach (EIV) is about 2 times larger than that of the identification of the inverse of the controller. However, the PEM does not perform as expected. The estimate of the noise model is not accurate, therefore the estimate of the controller is biased. Although this method is consistent, it is not efficient for a finite number of data. A tailor-made parameterization would probably perform better. The EIV approach is more efficient than the correlation approach.

For a smaller SNR of 10, estimation of the inverse of the controller is not as efficient as expected. For such an important noise level, the non-convex optimization does not always converge to the global optimum. CbT is more efficient than EIV, which was not the case for a SNR of 100. For a finite number of data, both the CbT and the EIV estimates are biased. The bias depends on the signal-to-noise ratio and, for CbT, on l_1 as shown in (2.44). It can be shown that the bias of the EIV estimate depends on the number of periods n_p. In this example, EIV is more efficient for low noise levels. For a SNR of 10, the bias of the EIV estimate is larger than the bias of the CbT estimate and CbT is more efficient.

Case C2, $K^* \notin \{K(\rho)\}$

The control objective is defined by the closed-loop reference model

$$M_2(q^{-1}) = \frac{q^{-3}(1-\alpha)^2}{(1-\alpha q^{-1})^2},$$

with $\alpha = 0.606$. In this case $K^* \notin \{K(\rho)\}$ and the objective cannot be achieved. However, this problem can be considered well-defined. Even though the optimal controller cannot be found, the error $M - K(\rho)G(1-M)$ can be made small, and the optimal fixed-order controller $K(\rho_0)$ achieves good closed-loop performance. The results are given in Table 5.2.

The results for the estimation of the inverse are not acceptable, even though the distance between $K(\rho)$ and K^* can be made relatively small. It seems that using standard PEM algorithms a local optimum is found for this specific problem. The estimate of the controller using PEM does not converge asymptotically to the optimal controller, and the performance of the converging estimates CbT and EIV is better. CbT and EIV give again similar performance.

5.3 Model-based versus data-driven model reference control

In Section 1.2, model-based approaches are defined as a controller design approach where two optimizations are used, one in the identification step and a second one in the controller design. According

Table 5.2. Mean values for the achieved performance $J(\rho)$, for M_2.

	$N_p = 63, n_p = 16$		$N_p = 127, n_p = 8$		$N_p = 127, n_p = 12$	
SNR	100	10	100	10	100	10
PEM	0.1587	0.2948	0.0791	0.2807	0.0793	0.2808
Inv	30.96	61.74	32.97	17.98	32.08	20.27
CbT	0.0754	0.0940	0.0744	0.0852	0.0742	0.0817
EIV	0.0748	0.1493	0.0743	0.1280	0.0741	0.1129

to this definition such techniques can be regarded as *indirect*. Data-driven approaches are defined in Section 1.2 as techniques where the data is used to *directly* minimize a control criterion. Such approaches thus use only one optimization.

The use of only one optimization is expected to be advantageous firstly because no information of the plant is lost in the intermediate optimization. Secondly, a direct estimate is expected to be more accurate for a finite number of data. Assume that a parameter estimator is available, which achieves the Cramér-Rao bound for a finite number of data. If this estimator is used to directly estimate the controller, the accuracy of the controller parameters is equal to the Cramér-Rao bound. If this same estimator is used to estimate a plant model, the accuracy of the model parameters is equal to the Cramér-Rao bound. The controller parameters calculated using this model will achieve the Cramér-Rao bound asymptotically, but the finite-data-length estimate achieves this bound only if the mapping from the model to the controller is linear. Examples where the indirect approach is not optimal are easily constructed, see for example [45]. A model-based approach can thus at best achieve the same performance as an optimal direct approach.

Clearly, this result holds only if the data-driven approach is optimal for finite data length, and none of the methods discussed in this thesis is claimed to be optimal for a finite number of data. In this section, non-iterative data-driven controller tuning is compared to an indirect method. The characteristics of the data-driven approaches as presented in Section 5.1 and Section 5.2 are compared to a model-based approach that uses two distinct optimization steps. Unfortunately, analysis for finite data length is not possible with the

existing tools, and the accuracy analysis presented in this chapter is asymptotic.

Many different model-based techniques have been developed. If a parametric model is used, the order of the controller depends in general on the order of this model. Furthermore, the achieved performance depends strongly on the identification approach that is used and the resulting characteristics and amount of undermodeling. In this section, a model-based solution for fixed-order controllers is proposed, which is directly comparable to the data-driven approach treated in this thesis. The proposed approach is based on the invariance principle for maximum-likelihood estimators. Undermodeling is avoided by identifying a full-order model, which is then used for controller design. It has been shown that this specific indirect approach is optimal in the context of system identification [80]. Note that this approach, which is not a standard model-based approach, is based on the results of Chapters 2 and 3.

It is shown that the model-based approach achieves the same asymptotic accuracy as some of the data-driven methods described in Section 5.1. It is also shown that, even though the data-driven approaches are not optimal for a finite number of data, the achieved accuracy for finite data length can be better than the accuracy of an optimal model-based approach. A numerical example is included to illustrate these finite-sample properties.

5.3.1 Model-based model reference control

If a model $\hat{G}$ of the plant G is available, the approximate model reference problem with guaranteed stability, as defined in Definition 3.1, can be approximated using this model. If, for example, the plant G is stable and minimum phase, (3.5) can be approximated by:

$$\begin{aligned} \hat{\rho} = \arg\min_{\rho} & \left\| F(1-M)[M - K(\rho)(1-M)\hat{G} \right\| \\ & \text{subject to} \\ & \|M - K(\rho)(1-M)\hat{G}\|_\infty \leqslant \delta_N \end{aligned} \tag{5.34}$$

As with the data-driven case, stability can be guaranteed only if the modeling errors are taken into account.

In the following, accuracy of the unconstrained problem is studied. Assume that the plant G is stable. The user-defined filter is fixed as $F = 1$ and the structure of the controller is fixed as $K(\rho)$, according to (2.7).

In many standard techniques for model reference control, the order of the controller depends on the order of the model and these techniques can therefore not be used to calculate a fixed-order controller with a predefined structure. For the design of fixed-order controllers, the use of non-parametric frequency models has been proposed, for example in [34]. If a parametric model is available, a simulated output sequence can be generated. This sequence can then be used to approximate $J(\rho)$. This approach has also been used in model reduction [79, 80].

In the following, a high-order parametric model with an FIR structure is used and an output sequence is simulated to calculate the optimal controller. The data is assumed to be periodic. In this case an FIR model of order N_p can be considered as a full-order model. It will be shown that the resulting estimate of the controller parameters is indeed consistent. Furthermore, an FIR estimator is a maximum-likelihood estimator if the noise is white and, according to [29], the use of this model in further calculations does not jeopardize the statistical efficiency.

5.3.2 Controller tuning using a full-order FIR model

Assume that the plant G is stable and that an open-loop experiment has been performed, where the data satisfies **A1-A2** and **A5-A6**. The signals $r(t)$ and $y(t) = Gr(t) + v(t)$ are available (note that the exact same signals are used in the data-driven approach for stable system, see Section 2.4.1). Define the response of the plant G to a periodic signal with a period of length N_p as

$$g_{per}(t) = g(t) + \sum_{i=1}^{\infty} g(t + iN_p), \quad t = [0, \ldots, N_p - 1].$$

where $g(t)$ is the impulse response of G. Define

$$\theta_0 = [g_{per}(0) \ldots g_{per}(N_p - 1)]^T$$

and note that $y(t) = \psi_\theta^T(t)\theta_0 + v(t)$, where

$$\psi_\theta(t) = [r(t) \dots r(t - N_p + 1)]^T.$$

An FIR estimate of G of length N_p is given by:

$$\begin{aligned}
\hat{\theta} &= \left[\frac{1}{N}\sum_{t=1}^{N}\psi_\theta(t)\psi_\theta^T(t)\right]^{-1}\frac{1}{N}\sum_{t=1}^{N}\psi_\theta(t)y(t) \\
&= \left[\frac{1}{N}\sum_{t=1}^{N}\psi_\theta(t)\psi_\theta^T(t)\right]^{-1}\frac{1}{N}\sum_{t=1}^{N}\psi_\theta(t)\left(\psi_\theta^T(t)\theta_0(k) + v(t)\right) \\
&= \theta_0 + \left[\frac{1}{N}\sum_{t=1}^{N}\psi_\theta(t)\psi_\theta^T(t)\right]^{-1}\frac{1}{N}\sum_{t=1}^{N}\psi_\theta(t)v(t)
\end{aligned} \tag{5.35}$$

Note that due to periodicity

$$\begin{aligned}
\hat{\theta} &= \theta_0 + \left[\frac{1}{N}\sum_{t=1}^{N}\psi_\theta(t)\psi_\theta^T(t)\right]^{-1}\frac{1}{N}\sum_{t=1}^{N}\psi_\theta(t)v(t) \\
&= \theta_0 + \left[\frac{1}{N_p}\sum_{t=1}^{N_p}\psi_\theta(t)\psi_\theta^T(t)\right]^{-1} \\
&\quad \frac{1}{N_p}\sum_{t=1}^{N_p}\psi_\theta(t)\frac{v(t) + v(t+N_p)\cdots + v(t+(p-1)N_p)}{n_p}
\end{aligned} \tag{5.36}$$

Define

$$v_m(t) = \frac{v(t) + v(t+N_p)\cdots + v(t+(p-1)N_p)}{n_p}. \tag{5.37}$$

Clearly $v_m(t) \to 0$ as $n_p \to \infty$, and as the number of periods tends to infinity, $\lim_{n_p\to\infty}\hat{\theta} = \theta_0$.

The excitation signal $r(t)$ and the model $\hat{G}$ are now used to generate a simulated output sequence, $\hat{y}(t) = \hat{G}r(t)$:

$$\hat{y}_\theta(t) = \psi_\theta(t)^T\hat{\theta}$$
$$= \psi_\theta(t)^T\theta_0 + \psi_\theta^T(t)\left[\frac{1}{N_p}\sum_{t=1}^{N_p}\psi_\theta(t)\psi_\theta^T(t)\right]^{-1}\frac{1}{N_p}\sum_{t=1}^{N_p}\psi_\theta(t)v_m(t)$$
$$= Gr(t) + \tilde{y}_\theta(t) \quad (5.38)$$

Define the following vectors

$$\begin{aligned}\overline{\tilde{y}_\theta} &= [\tilde{y}_\theta(1)\dots\tilde{y}_\theta(N_p)]^T,\\ \overline{v} &= [v_m(1)\dots v_m(N_p)]^T\end{aligned} \quad (5.39)$$

and the matrix

$$\Psi = [\psi_\theta(1)\dots\psi_\theta(N_p)]. \quad (5.40)$$

The noise contribution of the simulated output $\hat{y}_\theta(t)$ can then be written as

$$\overline{\tilde{y}_\theta} = \Psi^T\left[\Psi\Psi^T\right]^{-1}\Psi\overline{v} \quad (5.41)$$

If Assumption **A6** is satisfied, Ψ is a square invertible matrix and consequently

$$\overline{\tilde{y}_\theta} = \Psi^T\Psi^{-T}\Psi^{-1}\Psi\overline{v} = \overline{v} \quad (5.42)$$

This simulated output can be used to minimize the approximate model reference criterion:

$$\hat{\rho}_\theta = \arg\min_\rho \frac{1}{N_p}\sum_{t=1}^{N_p}\left(s(t) - K(\rho)(1-M)^2\hat{y}_\theta(t)\right)^2$$
$$= \arg\min_\rho J_m(\rho) \quad (5.43)$$

Note that the sum over only one period is taken. Since the model is defined on N_p FIR coefficients, the simulated output of consecutive periods is identical. The error can be written as:

$$s(t) - K(\rho)(1-M)^2\hat{y}_\theta(t) = s(t) - \phi_\theta^T(t)\rho, \quad (5.44)$$

where the regression vector $\phi_\theta(t)$ is given by:

$$\phi_\theta(t) = \beta(1-M)^2\hat{y}_\theta(t) = \beta(1-M)^2Gr(t) + \beta(1-M)^2v_m(t)$$
$$\triangleq \phi_0(t) + \tilde{\phi}_\theta(t). \quad (5.45)$$

The minimizer of (5.43) is given by

$$\hat{\rho}_\theta = \left[\frac{1}{N_p}\sum_{t=1}^{N_p}\phi_\theta(t)\phi_\theta^T(t)\right]^{-1}\frac{1}{N_p}\sum_{t=1}^{N_p}\phi_\theta(t)s(t) \tag{5.46}$$

Theorem 5.2 *Assume that* ***A1, A5*** *and* ***A6*** *are satisfied, that* $N_p \geqslant n_\rho$*, the number of controller parameters, and that* $(1-M)^2G$ *has no zero on the imaginary axis. Then, if* $\hat{\theta}$ *is estimated according to (5.35) and* $\hat{\rho}_\theta$ *according to (5.46),*

$$\lim_{n_p\to\infty}\hat{\rho}_\theta = \rho_0, w.p.1$$

Proof: In Case **C1**, the noise-free signal $s(t)$ can be written as $s(t) = \phi_\theta^T(t)\rho_0 - \tilde{\phi}_\theta(t)\rho_0$ and the estimation error is given by

$$\hat{\rho}_\theta - \rho_0 = -\left[\frac{1}{N_p}\sum_{t=1}^{N_p}\phi_\theta(t)\phi_\theta^T(t)\right]^{-1}\frac{1}{N_p}\sum_{t=1}^{N_p}\phi_\theta(t)\tilde{\phi}_\theta^T(t)\rho_0 \tag{5.47}$$

It follows from (5.36) that $\lim_{n_p\to\infty}\hat{\theta} = \theta_0$, w.p.1 [54]. A continuous function of this variable $f(\hat{\theta})$ converges w.p.1 to $f(\theta_0)$ ([63], page 450). Consequently

$$\lim_{n_p\to\infty}\tilde{\phi}_\theta(t) = 0, \quad \text{w.p.1},$$

the regressor converges to the noise-free regressor,

$$\lim_{n_p\to\infty}\phi_\theta(t) = \phi_0(t), \quad \text{w.p.1},$$

and

$$\lim_{n_p\to\infty}\frac{1}{N_p}\sum_{t=1}^{N_p}\phi_\theta(t)\phi_\theta^T(t) = R_0, \quad \text{w.p.1}, \tag{5.48}$$

with R_0 defined as in (5.28). This matrix has full rank since **A6** is satisfied and $N_p \geqslant n_\rho$. It follows that $\lim_{n_p\to\infty}(\hat{\rho}_\theta - \rho_0) = 0$, w.p.1., which completes the proof. ■

Theorem 5.2 states that the model-based estimate $\hat{\rho}_\theta$ is consistent. However, for a finite number of data, $E\{\hat{\rho}_\theta - \rho_0\} \neq 0$, i.e. the estimate based on a finite number of data is biased. Note that this is also the case for the data-driven EIV and CbT estimates.

5.3.3 Asymptotic accuracy

The accuracy of the model-based estimate $\hat{\rho}_\theta$ of (5.46) clearly depends on the accuracy of the estimate $\hat{\theta}$ defined in (5.35). According to the invariance principle of maximum-likelihood estimation, see Section 1.2, $\hat{\rho}_\theta$ is a maximum likelihood estimator of ρ_0 if $\hat{\theta}$ is a maximum likelihood estimator of θ_0. In the following, it is therefore assumed that the measurement noise satisfies:

A9 The measurement noise $v(t)$ is white, i.e. $H_v = 1$.

If the measurement noise satisfies **A9**, the FIR estimate $\hat{\theta}$ is a maximum likelihood estimator, whose variance corresponds to the Cramér-Rao bound.

The estimate $\hat{\rho}_\theta$ is thus a ML estimate if **A9** is satisfied. This estimate achieves asymptotically the Cramér-Rao bound. The Cramér-Rao bound for the function $g(\theta)$ of the ML estimate θ is given by

$$\frac{\partial g(\theta)}{\partial \theta} P_\theta \frac{\partial g(\theta)}{\partial \theta},$$

where P_θ is the Cramér-Rao bound for the estimate $\hat{\theta}$ [45]. The best variance that can be achieved thus depends on the function $g(\theta)$. Results from asymptotic analysis in system identification can be used to calculate the Cramér-Rao bound for the function $g(\theta)$ as defined in (5.43).

Proposition 5.1 *Assume that **A1, A2, A5, A6** and **A9** are satisfied, that $N_p > n_\rho$ and that $(1-M)^2 G$ has no zero on the imaginary axis. Then, if $\hat{\theta}$ is estimated according to (5.35) and $\hat{\rho}_\theta$ according to (5.46), $\sqrt{N}(\hat{\rho}_\theta - \rho_0)$ is asymptotically normally distributed with covariance matrix P_m:*

$$P_m = \sigma^2 R_0^{-1} C_2 R_0^{-1}, \tag{5.49}$$

where C_2 is defined in (5.6).

Proof: In Appendix A.6 it is shown that the estimate $\hat{\rho}_\theta$ satisfies the assumptions of theorem 9.1 of [54]. The asymptotic variance is then calculated according to theorem 9.1 of [54]. ■

The function $g(\theta)$ as defined in (5.43) corresponds to the filtering of the error by a unity noise filter, which is comparable to the EIV and CbT estimates minimizing this same criterion. The asymptotic variance of the model-based method is equal to the optimal variance P_{opt} if no noise model is estimated. The asymptotic accuracy of the estimate using a full-order FIR model is thus equal to the variance achieved by a data-driven method, if, for example, the errors-in-variables method of Section 5.1.5 is used and the number of periods $n_p \to \infty$.

If another function $g(\theta)$ is used, which corresponds to minimizing $J_i(\rho)$ of (5.16), the Cramér-Rao bound changes accordingly. In this case the optimization is non-convex and the variance is given by P_i (5.14). The model-based approach is again asymptotically equivalent to the data-driven approach.

5.3.4 Numerical example

In the previous section it is shown that the asymptotic accuracy of the proposed model-based approach is equivalent to that of data-driven approaches, if the assumptions in Theorem 5.1 are satisfied. In practice, only a finite number of data is available and expressions for asymptotic variance are not necessarily accurate for finite data length. Analysis of the accuracy of estimators for a finite number of data remains a challenging topic for research. Interesting results have appeared recently [12, 17], but these results cannot be used to compare the estimators considered here. A numerical example is therefore used to compare the different approaches.

In practice, not only a finite number of data, but also Case **C2** should be considered, where $K^* \notin \{K(\rho)\}$. However, in Theorem 5.1 Case **C1** is assumed, and asymptotic equivalence has been shown in this case. Case **C1** is therefore considered in this numerical example as well. The model-based estimate of (5.46) is compared to the EIV and CbT estimates. Asymptotically, these estimates minimize the same criterion and are therefore comparable. The example of the flexible transmission system of Section 5.2.2 is used. The model, reference model and data sets are described in Section 5.2.2. The results are given in Table 5.3.

Table 5.3. Mean values for the achieved performance $J(\rho)$, for M_1.

	$N_p = 63, n_p = 16$		$N_p = 127, n_p = 8$		$N_p = 127, n_p = 12$	
SNR	100	10	100	10	100	10
CbT	0.00784	0.0295	0.00643	0.0244	0.00545	0.0202
EIV	0.00676	0.0643	0.00558	0.0499	0.00472	0.0405
MB	0.01042	0.0407	0.01069	0.0438	0.00828	0.0364

For a SNR of 100, the EIV estimate is the most accurate. For a SNR of 10, CbT is the most efficient. CbT performs better than the model-based approach (MB) for both noise levels.

In this numerical example, the accuracy achieved with a data-driven approach is higher than that achieved with the model-based approach. This result is specific for this example, the plant considered, the noise levels and the choice of input signal. For other examples the result might be different. This example simply shows that a data-driven solution can outperform an optimal model-based solution.

5.4 Conclusions

Different identification methods that have been proposed for non-iterative data-driven controller tuning are compared. Two distinctive cases are considered. In the first case, it is assumed that perfect matching of the reference model is possible, i.e. there is no undermodeling of the controller. In this case, the Cramér-Rao bound can be attained when the inverse of the controller is identified. In practice, however, perfect matching of the reference model is not possible and undermodeling of the controller needs to be considered. In this case, only less efficient instrumental variable approaches guarantee convergence of the estimate to the optimal controller parameters.

The data-driven approach is compared to a model-based approach that uses two distinct optimizations. A model-based solution for fixed-order controllers is proposed for comparison. A high-order FIR model is identified to avoid undermodeling. This model is then used to calculate the controller. This approach is asymptotically efficient. In the case without undermodeling, the asymptotic accuracy that

can be achieved by data-driven approaches is the same as that of this model-based solution. However, in practice, undermodeling of the controller should be considered, and the properties of the estimate should be compared for a finite number of data. Unfortunately, analysis is not possible in this situation. A numerical example shows that, for finite data length, a data-driven approach can achieve better performance than an asymptotically efficient model-based approach.

6

Conclusions

Summary

This thesis has investigated a non-iterative data-driven model reference control approach, which is extended with a constraint that guarantees closed-loop stability. A set of measured open-loop or closed-loop data is used directly to minimize an approximation of the model-reference criterion. Straighforward tuning schemes are proposed that generate an error signal that can be used to identify the optimal, fixed-order controller. In the resulting identification problem, the noise affects the input of the controller to be identified rather than the output as in standard identification problems. The use of the correlation approach is proposed to deal with the effect of noise.

Other identification approaches have been proposed in literature to deal with noise in this specific controller identification problem. The accuracy of these methods is compared to that of the correlation approach. It is shown that, if the order of the controller is fixed and a bias exists between the ideal controller and the optimal controller in the controller set, (extended) instrumental variable methods provide convergence to the optimal solution. For comparison, a statistically efficient indirect model-based approach for fixed-order controllers is presented. In this method, an optimization is used to identify a plant model. The controller is then designed using a second optimization step. The asymptotic properties of this approach are equivalent to

those of data-driven solutions, which use only one optimization. In a numerical example, it is shown that a data-driven approach can achieve better performance than the model-based solution for finite data length.

Closed-loop stability is guaranteed through the addition of a set of constraints based on a sufficient condition for stability. These constraints use an estimate of the infinity norm of an error function. Stability is guaranteed as the number of data tends to infinity. For a finite number of data, the estimation error needs to be taken into account. A non-conservative a posteriori data-driven stability test is proposed based on similar stability conditions. Again, the infinity norm of an error function is estimated from the data. If it is not possible to formulate a bound on the estimation error, the test provides a clear trade-of between reliability and conservatism.

Conclusions

The method presented in this thesis provides a *stabilizing solution* for data-driven controller tuning, thereby eliminating one of the main drawbacks of such techniques. The proposed stability condition is applied to correlation-based controller tuning. Note that the stability condition can be used in model-based model reference control as well and it can be added to other data-driven approaches, as illustrated in the example in Chapter 3, where the constraints are integrated in VRFT.

The proposed constrained optimization guarantees a stabilizing solution as the number of data tends to infinity. In practice, the number of available data will be limited, and stability can be guaranteed only if the estimation error is taken into account. This might seem restrictive, but the result is equivalent to model-based approaches. In robust control, stability can be guaranteed only if the plant dynamics are contained in the uncertainty set. Clearly, quantification of the estimation error of the stability constraints remains a challenging problem. The bounds proposed in Section 3.5 use a priori information on the noise and on the quantity that is estimated, and these hypotheses need to be validated.

Data-driven controller tuning approaches have been developed to avoid the problem of undermodeling encountered in practice in

model-based approaches. It is expected that a data-driven approach can achieve better performance than a model-based approach, if only a finite number of data is available. However, most of the data-driven approaches proposed in literature only consider consistency. The analysis in this thesis shows that asymptotically optimal variance can be achieved in a data-driven approach. As expected, this asymptotic accuracy is equivalent to the asymptotic accuracy achieved by an optimal model-based approach. However, for finite data length data-driven approaches can achieve better performance than an optimal model-based approach. This has been demonstrated by a simulation example.

One can argue whether the proposed data-driven approach is model-free or not. One can for example argue that the proposed constraints for stability use an implicit frequency-domain model of the plant. One can also argue whether frequency-domain methods can be considered data-driven or not. The terms model-based and data-driven are ambiguous. The definitions used throughout this thesis distinguish data-driven methods, which use one optimization to calculate the optimal controller parameters directly from data, from model-based methods, which are indirect. This distinction between *direct* and *indirect* approaches might be more valuable than the distinction between data-driven and model-based methods, even though the terms direct and indirect can also be considered ambiguous. Under certain hypotheses, optimal direct and indirect approaches are asymptotically equivalent. However, a direct approach can outperform an indirect approach if only a finite number of data is available.

This thesis has only considered the accuracy of the control criterion. However, for stability, the accuracy of the estimate of the stability condition should be optimized. In the proposed direct data-driven approach, the different requirements for performance and stability appear naturally. Both the control criterion and the stability condition are a function of the control parameters and the accuracy of each of these estimates can be optimized separately. In practice, other control criteria or constraints can be of interest. In a direct approach, the quality of the estimate needed for each objective can be optimized separately, *directly* with respect to the controller parameters.

Perspectives

Model-based approaches have been developed for years, and solutions exist for many different control objectives, physical constraints and robustness issues. This is not the case for data-driven approaches. The stability constraints proposed in this thesis are a first and necessary step towards the development of reliable data-driven approaches. Solutions that can deal with input constraints, robustness issues or performance guarantees would be valuable.

The comparison between model-based (indirect) and data-driven (direct) approaches in this thesis considers a simple case and this comparison is obviously limited. A more complete comparison requires accurate expressions for variance and bias, also for a finite number of data. Progress has been made in this field, but many questions remain unanswered.

Recently, much attention has been given to the design of experiments in the context of system identification. It is shown that the control performance can be improved when the experiment for system identification is designed specifically for the intended control objective. An identification objective is defined to estimate the model parameters, but this intermediate objective is linked to the end objective, which is control performance. Study of the design of experiments in a direct setting would be interesting.

The approach presented in this thesis is compatible with frequency-domain methods. The constraints proposed in [39] can for example be used to impose robustness margins in a data-driven approach. Only linear SISO systems are treated in this thesis. Extensions to MIMO systems can be considered. The stability constraint for closed-loop experiments in Chapter 3 remains valid for MIMO systems.

A

Appendix

A.1 Bias in correlation approach for finite data length

Equation (2.44) can be derived as follows: $e_{D_s}(t)$ can be written as

$$e_{D_s}(t) = \sum_{k=0}^{\infty} d_k e(t-k),$$

with d_k the impulse response of D_s. The vector of random variables:

$$X_N = \frac{1}{\sqrt{N}} \sum_{t=1}^{N} \zeta(t) e_{D_s}(t)$$

converges in distribution to a normal distribution with zero mean and variance P [54]:

$$P = \lim_{N\to\infty} E\left\{X_N X_N^T\right\} = \sigma^2 \lim_{N\to\infty} \frac{1}{N} \sum_{t=1}^{N} E\left\{\tilde{\zeta}(t)\tilde{\zeta}^T(t)\right\},$$

where

$$\begin{aligned}\tilde{\zeta}(t) &= \sum_{k=0}^{\infty} d_k \zeta(t+k) \\ &= D_s(q)[r(t+l_1), r(t+l_1-1), \ldots r(t), r(t-1), \ldots, r(t-l_1)]^T\end{aligned}$$

The diagonal elements of P are equal to $\sigma^2 R_{r_{D_s}}(0)$, where $R_{r_{D_s}}(\tau)$ is the auto-correlation function of $D_s(q)r(t)$. The expected value $E\{J_{N,l_1}(\rho)\}$ can then be expressed as:

$$\begin{aligned}
&E\{J_{N,l_1}(\rho)\} = \\
&\quad E\left\{\frac{1}{N^2}\sum_{t=1}^{N}\zeta^T(t)[r_{D_d}(t)-e_{D_s}(t)]\sum_{s=1}^{N}\zeta(s)[r_{D_d}(s)-e_{D_s}(s)]\right\} \\
&\qquad = E\left\{\frac{1}{N^2}\sum_{t=1}^{N}\zeta^T(t)r_{D_d}(t)\sum_{s=1}^{N}\zeta(s)r_{D_d}(s)\right\} \\
&\qquad - 2E\left\{\frac{1}{N^2}\sum_{t=1}^{N}\zeta^T(t)r_{D_d}(t)\sum_{s=1}^{N}\zeta(s)e_{D_s}(s)\right\} \\
&\qquad + E\left\{\frac{1}{N^2}\sum_{t=1}^{N}\zeta^T(t)e_{D_s}(t)\sum_{s=1}^{N}\zeta(s)e_{D_s}(s)\right\} \\
&\qquad\qquad = \tilde{J}_{N,l_1}(\rho) - 0 + \frac{1}{N}E\left\{X_N^T X_N\right\}
\end{aligned}$$

For large N, the distribution of X_N is well approximated by P, and $E\{J_{N,l_1}(\rho)\}$ can be approximated using this asymptotic distribution:

$$\begin{aligned}
E\{J_{N,l_1}(\rho)\} &= \tilde{J}_{N,l_1}(\rho) + \frac{1}{N}E\left\{X_N^T X_N\right\} \\
&\approx \tilde{J}_{N,l_1}(\rho) + \frac{1}{N}\mathrm{trace}(P) = \tilde{J}_{N,l_1}(\rho) + \frac{2l_1+1}{N}\sigma^2 R_{r_{D_s}}(0)
\end{aligned}$$

Using Parseval's theorem, this can be expressed as:

$$\begin{aligned}
E\{J_{N,l_1}(\rho)\} &\approx \tilde{J}_{N,l_1}(\rho) + \frac{2l_1+1}{N}\sigma^2\frac{1}{2\pi}\int_{-\pi}^{\pi}\Phi_{r_{D_s}}(\omega)d\omega \\
&= \tilde{J}_{N,l_1}(\rho) + \frac{\sigma^2(2l_1+1)}{2\pi N}\int_{-\pi}^{\pi}|D_s(e^{-j\omega})|^2\Phi_r(\omega)d\omega
\end{aligned}$$

Replacing D_s by $L(1-M)K(\rho)H_v$ and L by (2.33) gives (2.44).

A.2 Proof of Theorem 3.6

The estimation error is given by

$$\max_{\omega_k} \left| \frac{\hat{\Phi}_{r\varepsilon_s}(\omega_k, \rho)}{\Phi_r(\omega_k)} \right| - \delta(\rho)$$

$$= \max_{\omega_k} \left| \frac{\hat{\Phi}_{r\varepsilon_s}(\omega_k, \rho)}{\Phi_r(\omega_k)} \right| - \max_{\omega_k} |\Delta(e^{-j\omega_k}, \rho)| + \max_{\omega_k} |\Delta(e^{-j\omega_k}, \rho)| - \delta(\rho)$$

$$\leqslant \left| \max_{\omega_k} \left| \frac{\hat{\Phi}_{r\varepsilon_s}(\omega_k, \rho)}{\Phi_r(\omega_k)} \right| - \max_{\omega_k} |\Delta(e^{-j\omega_k}, \rho)| \right|$$

$$+ \left| \max_{\omega_k} |\Delta(e^{-j\omega_k}, \rho)| - \delta(\rho) \right|$$

The second part of this error is due to the finite frequency grid, the first part is due to measurement noise.

Error due to finite frequency grid

The error due to the finite frequency grid can be bounded by

$$\left| \max_{\omega_k} |\Delta(e^{-j\omega_k}, \rho)| - \delta(\rho) \right| \leqslant \max_{\omega} \frac{d|\Delta(e^{-j\omega}, \rho)|}{d\omega} \frac{\omega_{k+1} - \omega_k}{2}$$

$$\leqslant \max_{\omega} \left| \frac{d\Delta(e^{-j\omega}, \rho)}{d\omega} \right| \frac{\omega_{k+1} - \omega_k}{2},$$

i.e. the error is smaller than the maximal value of the derivative times half of the distance between two frequency points.

The derivative of Δ can be bounded as follows, using series convergence results:

$$\left\| \frac{d\Delta(e^{-j\omega})}{d\omega} \right\|_\infty \leqslant \frac{A\gamma}{(1-\gamma)^2}$$

and

$$|\max_{\omega_k} |\Delta(e^{-j\omega_k})| - \delta_0| \leqslant \frac{A\gamma}{(1-\gamma)^2} \frac{\pi}{N_p}.$$

Estimation error due to measurement noise

If assumption **A5** and **A6** are satisfied, the spectral estimate of (3.15) is equivalent to the empirical transfer function estimate (ETFE):

$$\hat{\Delta}(\omega_k,\rho) = \frac{\hat{\Phi}_{r\varepsilon_s}(\omega_k,\rho)}{\Phi_r(\omega_k)} = \frac{\sum_{\tau=0}^{N_p-1}\frac{1}{N}\sum_{t=1}^{N} r(t-\tau)\varepsilon_s(t,\rho)e^{-j\tau\omega_k}}{\sum_{\tau=0}^{N_p-1}\frac{1}{N}\sum_{t=1}^{N} r(t-\tau)r(t)e^{-j\tau\omega_k}}$$

(due to periodicity)

$$= \frac{\frac{1}{N}\sum_{t=1}^{N}(\Delta r(t) + (1-M)K(\rho)v(t))e^{-jt\omega_k}}{\frac{1}{N}\sum_{t=1}^{N} r(t)e^{-jt\omega_k}}$$

$$= \sum_{n=0}^{\infty} d(n)e^{-jn\omega_k} + \frac{\sum_{t=1}^{N}(1-M)K(\rho)v(t)e^{-jt\omega_k}}{\sum_{t=1}^{N} r(t)e^{-jt\omega_k}}$$

Well known results for the ETFE are therefore applicable to the estimate $\hat{\Delta}(\omega_k,\rho)$ [54]:

- The estimate $\hat{\Delta}(\omega_k,\rho)$ is consistent at the frequencies $\omega_k = 2\pi k/N_p, k = 0,\ldots,N_p-1$.
- Asymptotically the variance of $\hat{\Delta}(\omega_k,\rho)$ is given by

$$\sigma_\Delta^2 = E\left|\hat{\Delta}(\omega_k,\rho) - E\hat{\Delta}(\omega_k,\rho)\right|^2 = \frac{|(1-M(e^{-j\omega_k}))K(e^{-j\omega_k},\rho)|^2\Phi_v(\omega_k)}{n_p\Phi_r(\omega_k)} \quad \text{(A.1)}$$

- The estimates $Re\hat{\Delta}(\omega_k,\rho)$ and $Im\hat{\Delta}(\omega_k,\rho)$ are asymptotically uncorrelated.
- The estimates $Re\hat{\Delta}(\omega_k,\rho)$ and $Im\hat{\Delta}(\omega_k,\rho)$ are asymptotically jointly normally distributed with variance equal to half of that in (A.1)

The variance of (A.1) can be bounded as:

$$\sigma_\Delta^2 \leqslant \frac{\|(1-M)K(\rho)\|_\infty^2\,\Phi_{v,max}}{n_p\Phi_{r,min}} \quad \text{(A.2)}$$

The estimate $\hat{\Delta}(\omega_k,\rho) = Re\hat{\Delta}(\omega_k,\rho) + jIm\hat{\Delta}(\omega_k,\rho)$ is unbiased. However, the constraint in (3.16) is based on its absolute value $|\hat{\Delta}(\omega_k,\rho)|$. According to [61], page 194,

$$\left|\hat{\Delta}(\omega_k,\rho)\right| \sim \text{Rice}(\frac{1}{\sqrt{2}}\sigma_\Delta, |\Delta(\omega_k,\rho)|).$$

Unlike the estimate of Δ, the estimate of its absolute value $|\Delta(\omega_k,\rho)|$ is biased. The distribution function of the Rice distribution depends on the unknown $|\Delta(\omega_k,\rho)|$, and cannot be implemented in the convex stability constraints. However, a (conservative) result can be used based on a bound on the error $|\hat{\Delta}(\omega_k,\rho)-\Delta(\omega_k,\rho)|$: $Re\hat{\Delta}(\omega_k,\rho)$ and $Im\hat{\Delta}(\omega_k,\rho)$ are asymptotically uncorrelated, therefore $|\hat{\Delta}(\omega_k,\rho)-\Delta(\omega_k,\rho)|$ has a Rayleigh distribution. The cumulative distribution function of the Rayleigh distribution of two uncorrelated normally distributed variables with variance $\frac{1}{2}\sigma_\Delta^2$ is given by:

$$\mathcal{F}(x) = 1 - e^{-\frac{x^2}{2\frac{1}{2}\sigma_\Delta^2}} = 1 - e^{-\frac{x^2}{\sigma_\Delta^2}}$$

With probability $\mathcal{F}(x)$, the error $|\hat{\Delta}(\omega_k,\rho)-\Delta(\omega_k,\rho)| < x$ and therefore $|\Delta(\omega_k,\rho)| < |\hat{\Delta}(\omega_k,\rho)|+x$ with probability $p > \mathcal{F}(x)$. Note that this last step is conservative.

$$|\Delta(\omega_k,\rho)| < |\hat{\Delta}(\omega_k,\rho)| + x < 1 \rightarrow |\hat{\Delta}(\omega_k,\rho)| < 1 - x$$

Define $\Phi_{v,max}$ as the maximal value of the spectrum $\Phi_v(\omega_k)$ at the frequencies ω_k, which can be bounded as $\Phi_{v,max} \leqslant \|H_v\|_\infty^2 \sigma^2$. In order to assure that the constraint is satisfied with probability p,

$$\begin{aligned} 1 - p &= e^{-\frac{x^2}{\sigma_\Delta^2}} \\ x &= \sqrt{-\ln(1-p)\sigma_\Delta^2} \\ &= \sqrt{-\ln(1-p)\frac{\|(1-M)K(\rho)\|_\infty^2 \Phi_{v,max}}{n_p \Phi_{r,min}}} \\ &\leqslant \|(1-M)K(\rho)\|_\infty \sqrt{-\ln(1-p)\frac{\|H_v\|_\infty^2 \sigma^2}{n_p \Phi_{r,min}}} \end{aligned} \tag{A.3}$$

This completes the proof.

A.3 Proof of Theorem 3.7

The FIR estimation is given by (3.31):

$$\hat{\theta} = [\Psi\Psi^T]^{-1}\Psi\bar{\varepsilon}_s$$

Define

$$\bar{v}_\Delta = [(1-M)K(\rho)v(t)\dots(1-M)K(\rho)v(t+N)]^T.$$

$\hat{\theta}$ can then be written as

$$\hat{\theta} = \bar{d}_{per} + [\Psi\Psi^T]^{-1}\Psi\bar{v}_\Delta$$

The error in the estimation the H_∞ norm is given by

$$\begin{aligned}
&\|\hat{\Delta}\|_\infty - \|\Delta\|_\infty \leqslant \|\hat{\Delta} - \Delta\|_\infty = \max_\omega |\hat{\Delta}(e^{-j\omega}) - \Delta(e^{-j\omega})| \\
&= \max_\omega \left| \sum_{t=0}^{N_p-1} d_{per}(t)e^{-j\omega t} + \Gamma^T(e^{-j\omega})[\Psi\Psi^T]^{-1}\Psi\bar{v}_\Delta - \sum_{t=0}^{\infty} d(t)e^{-j\omega t} \right| \\
&\qquad \leqslant \max_\omega \left| \sum_{t=0}^{N_p-1} d_{per}(t)e^{-j\omega t} - \sum_{t=0}^{\infty} d(t)e^{-j\omega t} \right| \\
&\qquad\qquad + \max_\omega \left| \Gamma^T(e^{-j\omega})[\Psi\Psi^T]^{-1}\Psi\bar{v}_\Delta \right|
\end{aligned} \tag{A.4}$$

The last term in this inequality is the error due to measurement noise. The first part is due to undermodeling.

Estimation error due to undermodeling

The error due to undermodeling can be bounded by

$$\begin{aligned}
&\max_\omega \left| \sum_{t=0}^{N_p-1} d_{per}(t)e^{-j\omega t} - \sum_{t=0}^{\infty} d(t)e^{-j\omega t} \right| \\
&\quad = \max_\omega \left| \sum_{t=0}^{N_p-1} (d(t) + \sum_{i=1}^{\infty} d(t+iN_p))e^{-j\omega t} - \sum_{t=0}^{\infty} d(t)e^{-j\omega t} \right| \\
&\quad = \max_\omega \left| \sum_{t=0}^{N_p-1} \sum_{i=1}^{\infty} d(t+iN_p))e^{-j\omega t} - \sum_{m=N_p}^{\infty} d(m)e^{-j\omega m} \right|
\end{aligned} \tag{A.5}$$

This error can be bounded using series convergence results:

$$\max_{\omega} \left| \sum_{t=0}^{N_p-1} \sum_{i=1}^{\infty} d(t+iN_p))e^{-j\omega t} - \sum_{m=N_p}^{\infty} d(m)e^{-j\omega m} \right| \leqslant 2 \sum_{t=N_p}^{\infty} |d(t)| \leqslant 2 \left(\frac{A\gamma^{N_p}}{1-\gamma} \right) \quad \text{(A.6)}$$

Error due to measurement noise

In the following, the equivalence of the ETFE and the FIR estimate will be exploited. First of all, a bound is established for the DFT frequencies. It is then shown that the maximal error over all frequencies is achieved at one of these DFT frequencies, and that consequently the bound is valid for all frequencies.

In Appendix A.2, it was established that for the frequencies ω_k, with probability p, the estimation error due to noise error is smaller than x, where x is defined in (A.3):

At intermediate frequencies the error is given by

$$\hat{\Delta}(e^{-j\omega}) - E\{\hat{\Delta}(e^{-j\omega})\} = \Gamma^T(e^{-j\omega})[\Psi\Psi^T]^{-1}\Psi\bar{v}_{\Delta}.$$

This is a linear (complex) function of the estimation error $\hat{\theta} - \bar{d}_{per}$. Following the reasoning of [32], the variance of the frequency response function is given by:

$$Var\{\hat{\Delta}(e^{-j\omega})\} = \frac{\sigma^2}{N}\Gamma^T(e^{-j\omega})P\Gamma(e^{j\omega}), \quad \text{(A.7)}$$

where P is the covariance of the estimate $\hat{\theta}$. The FIR estimate is normally distributed, with zero mean and variance P, where P is given by [54]

$$P = [\Psi\Psi^T]^{-1}S_{\theta}[\Psi\Psi^T]^{-1},$$

where

$$S_{\theta} = (1 - M(q))K(q,\rho)H_v(q)\Psi(1 - M(q^{-1}))K(q^{-1},\rho)H_v(q^{-1})\Psi^T.$$

Evaluation of this expression requires the noise model H_v to be known and bounds that use this expression will be difficult to calculate in practice. In the following, a simpler upper bound is defined, which requires only $\|H_v\|_\infty$ to be known.

A closer look at the variance expression (A.7) shows that the variance for a specific frequency ω depends on the gain of the matrix P is the direction of $\Gamma(e^{-j\omega})$, and the 2-norm of this $\Gamma(e^{-j\omega})$. This 2-norm of $\Gamma(e^{-j\omega})$ is the same for all ω. The variance of the estimate is thus bounded by the maximal gain of the matrix P, i.e. its maximum singular value.

The expression for P for periodic signals and an FIR estimate of length N_p is highly structured. The matrices $[\Psi\Psi^T]$ and S_θ are circulant matrices. This is easily verified. Consider for example a periodic signal with period length $N_p = 3$. Ψ is then given by:

$$\Psi = \begin{bmatrix} r(1) & r(2) & r(3) \\ r(0) & r(1) & r(2) \\ r(-1) & r(0) & r(1) \end{bmatrix}$$

Due to periodicity $r(0) = r(3), r(-1) = r(2)$, and

$$\Psi = \begin{bmatrix} r(1) & r(2) & r(3) \\ r(3) & r(1) & r(2) \\ r(2) & r(3) & r(1) \end{bmatrix}$$

It follows from the characteristic of circulant matrices that, since Ψ is circulant $[\Psi\Psi^T]$ is circulant, and that $[\Psi\Psi^T]^{-1}$ and P are also circulant, see Section 3.4.

The eigenvalues and eigenvectors of the circulant matrix P are given by (3.22) and (3.23) respectively, see Section 3.4. Furthermore, since multiplications of circulant matrices are also circulant, the eigenvectors of P^TP are also given by (3.23). Since the eigenvectors of P^TP and P are the same, the maximal gain of P is achieved in the direction of one of the eigenvectors, which are the DFT vectors. Note that the DFT vectors are equivalent to $\Gamma(e^{-j\omega_k})$, $\omega_k = 2\pi k/N_p, k = 0, \ldots, N_p - 1$. The singular values are thus achieved at the frequencies ω_k. The maximal gain is thus achieved at one of these frequencies:

$$\max_{\omega} Var\{\hat{\Delta}(e^{-j\omega})\} = \max_{\omega} \frac{\sigma^2}{N} \Gamma^T(e^{-j\omega}) P \Gamma(e^{j\omega})$$
$$= \max_{\omega_k} \frac{\sigma^2}{N} \Gamma^T(e^{-j\omega_k}) P \Gamma(e^{j\omega_k}) \quad \text{(A.8)}$$

A value for this bound is known through the ETFE and given by (A.2). The rest of the proof then follows from Appendix A.2.

Remark: According to [14], section 5.4.3, the estimate $Re\hat{\Delta}(\omega, \rho)$ is correlated with the estimate $Im\hat{\Delta}(\omega, \rho)$, when calculated using the FIR approach. If these two estimates are correlated, the distribution of the absolute value does not follow the Rayleigh distribution, used in the probabilistic bound of (A.3). However, (A.3) is based on the asymptotic result, which states that the two estimates are asymptotically uncorrelated. The use of the Rayleigh distribution thus introduces an approximation.

A.4 Proof of Theorem 4.3

The proof uses the following lemma.

Lemma A.1 ([77] p. 253) *Let $X(n)$ be an independent random sequence with constant mean μ_x and variance $\sigma_x^2(n)$, defined for $n \leqslant 1$. Then, if*

$$\sum_{n=1}^{\infty} \frac{\sigma_x^2(n)}{n^2} < \infty,$$

$$\frac{1}{n} \sum_{k=1}^{n} X(k) \to \mu_x, \ \ as\ n \to \infty, w.p.1$$

The estimate

$$\frac{\hat{\Phi}_{r\varepsilon_s}(\omega_k, \rho)}{\Phi_r(\omega_k)}$$

can be written as a combination of the spectral estimates of the n_c experiments.

$$\begin{aligned}\frac{\hat{\Phi}_{r\varepsilon_s}(\omega_k,\rho)}{\Phi_r(\omega_k)} &= \frac{\sum_{\tau=0}^{N_p-1}\frac{1}{N}\sum_{t=1}^{N} r(t-\tau)\varepsilon_s(t,\rho)e^{-j\tau\omega_k}}{\Phi_r(\omega_k)} \\ &= \frac{\sum_{\tau=0}^{N_p-1}\frac{1}{N}\sum_{t=1}^{N} r(t-\tau)\varepsilon_{s1}(t,\rho)e^{-j\tau\omega_k}}{n_c\Phi_r(\omega_k)} + \dots \\ &\quad + \frac{\sum_{\tau=0}^{N_p-1}\frac{1}{N}\sum_{t=1}^{N} r(t-\tau)\varepsilon_{sn_c}(t,\rho)e^{-j\tau\omega_k}}{n_c\Phi_r(\omega_k)} \\ &= \frac{1}{n_c}\left(\frac{\hat{\Phi}_{r\varepsilon_{s1}}(\omega_k,\rho)}{\Phi_r(\omega_k)} + \frac{\hat{\Phi}_{r\varepsilon_{s2}}(\omega_k,\rho)}{\Phi_r(\omega_k)} + \dots + \frac{\hat{\Phi}_{r\varepsilon_{sn_c}}(\omega_k,\rho)}{\Phi_r(\omega_k)}\right)\end{aligned}$$

Since the noise within different experiments is independent, the estimates

$$\frac{\hat{\Phi}_{r\varepsilon_{s1}}(\omega_k,\rho)}{\Phi_r(\omega_k)},\dots,\frac{\hat{\Phi}_{r\varepsilon_{sn_c}}(\omega_k,\rho)}{\Phi_r(\omega_k)}$$

are also independent. If Assumptions **A1** and **A2** are satisfied,

$$E\left\{\frac{\hat{\Phi}_{r\varepsilon_{s1}}(\omega_k,\rho)}{\Phi_r(\omega_k)}\right\} = \dots = E\left\{\frac{\hat{\Phi}_{r\varepsilon_{sn_c}}(\omega_k,\rho)}{\Phi_r(\omega_k)}\right\} = \Delta(e^{-j\omega_k})$$

and the variance of the estimate from each experiment n out of the n_c experiments is bounded and given by (see (A.1)),

$$\begin{aligned}\sigma_\Delta^2(n) &= E\left|\frac{\hat{\Phi}_{r\varepsilon_{sn}}(\omega_k,\rho)}{\Phi_r(\omega_k)} - \Delta(e^{-j\omega_k})\right|^2 \\ &= \frac{\left(\frac{X(\rho)M_n}{G} - X(\rho)K(1-M_n)\right)^2\Phi_{v_n}(\omega_k)}{\Phi_r(\omega_k)}.\end{aligned}$$

Define

$$\bar{\sigma}_\Delta^2 \triangleq \max(\sigma_\Delta^2(1),\sigma_\Delta^2(2),\dots,\sigma_\Delta^2(n_c)).$$

Then,

$$\sum_{n=1}^{\infty}\frac{\sigma_\Delta^2(n)}{n^2} \leqslant \sum_{n=1}^{\infty}\frac{\bar{\sigma}_\Delta^2}{n^2} = \bar{\sigma}_\Delta^2\sum_{n=1}^{\infty}\frac{1}{n^2} = \bar{\sigma}_\Delta^2\frac{\pi}{6} < \infty,$$

and according to Lemma A.1, the estimate $\frac{\hat{\Phi}_{r\varepsilon_s}(\omega_k,\rho)}{\Phi_r(\omega_k)}$ converges w.p. 1 to its expected value, $\Delta(e^{-j\omega_k})$. This completes the proof.

A.5 Proof of Theorem 5.1

The estimate of equation (5.22) is consistent if $\lim_{N_p\to\infty}\hat{\rho} = \rho_0$, w.p.1, where $K(\rho_0) = K^*$. Using (2.19) and (2.20), $s(t)$ can be written as

$$s(t) = \phi^T(t)\rho_0 - K(\rho_0)\tilde{y}_c(t),$$

where $\tilde{y}_c(t)$ is defined in (2.18). Define

$$\hat{q} = -\frac{1}{N_p n_p}\sum_{j=1}^{n_p}\sum_{t=1}^{N_p}\zeta_j(t)K(\rho_0)\tilde{y}_{c_j}(t),$$

where $\zeta_j(t)$ is defined in (5.19). The error $\hat{\rho} - \rho_0$ is then given by:

$$\hat{\rho} - \rho_0 = (\hat{R}^T\hat{R})^{-1}\hat{R}^T\hat{q}$$

Consistency is guaranteed if $\lim_{N_p\to\infty}\hat{q} = 0$ and $\lim_{N_p\to\infty}\hat{R} = e_{n_p-1}\otimes R_0$, where $e_{n_p-1} = (1\ldots1)^T$ has dimension $(n_p-1)\times 1$ and $\otimes$ denotes Kronecker product [73]. Convergence of $\lim_{N_p\to\infty}\hat{q}\to 0$, w.p.1 is shown next. Substituting $\zeta_j(t)$ by (5.19) gives:

$$\begin{aligned}
&\lim_{N_p\to\infty}\hat{q}\\
&= \lim_{N_p\to\infty}\left(-\frac{1}{N_p n_p}\sum_{j=1}^{n_p}\sum_{t=1}^{N_p}[\phi_{j+1}^T(t)\ldots\phi_{n_p}^T(t)\,\phi_1^T(t)\right.\\
&\qquad\left.\ldots\phi_{j-1}^T(t)]^T K(\rho_0)\tilde{y}_{c_j}(t)\right)\\
&= \lim_{N_p\to\infty}\left(-\frac{1}{N_p n_p}\sum_{j=1}^{n_p}\sum_{t=1}^{N_p}[\tilde{\phi}_{j+1}^T(t)\ldots\tilde{\phi}_{n_p}^T(t)\,\tilde{\phi}_1^T(t)\right.\\
&\qquad\left.\ldots\tilde{\phi}_{j-1}^T(t)]^T K(\rho_0)\tilde{y}_{c_j}(t)\right)\\
&= \lim_{N_p\to\infty}\left(-\frac{1}{N_p n_p}\sum_{j=1}^{n_p}\sum_{t=1}^{N_p}[(\beta\tilde{y}_{c(j+1)}(t))^T\ldots(\beta\tilde{y}_{cn_p}(t))^T(\beta\tilde{y}_1(t))^T\right.\\
&\qquad\left.\ldots(\beta\tilde{y}_{c(j-1)}(t))^T]^T K(\rho_0)\tilde{y}_{c_j}(t)\right). \qquad \text{(A.9)}
\end{aligned}$$

According to (A.9), $\hat{q}$ consists of cross-correlations between $\beta\tilde{y}_c(t)$ and $K(\rho_0)\tilde{y}_c(t-\tau)$, with $\tau = N_p(j-n), n = [1 \dots j-1, j+1 \dots n_p]$. Note that, if $j = 1$, $n = [j+1 \dots n_p] = [2 \dots n_p]$ and if $j = n_p$, $n = [1 \dots n_p - 1]$. The minimal value for τ that appears in $\hat{q}$ is thus $\tau = N_p$. Under assumption **A2**,

$$\lim_{N_p \to \infty} \frac{1}{N_p} \sum_{t=1}^{N_p} \beta(q^{-1})\tilde{y}_c(t)K(q^{-1}, \rho_0)\tilde{y}_c(t-\tau) = \beta(q^{-1})H_{\tilde{y}}(q^{-1})K(q, \rho_0)H_{\tilde{y}}(q)\mathrm{X}_e(\tau), \quad \text{w.p.1}, \quad \text{(A.10)}$$

where

$$\mathrm{X}_e(\tau) = \lim_{N_p \to \infty} \frac{1}{N_p} \sum_{t=1}^{N_p} e(t)e(t-\tau) = E\{e(t)e(t-\tau)\},$$

the autocorrelation of $e(t)$. Note that, throughout this thesis, the backward shift operator q^{-1} is used and omitted for convenience. In (A.10), the shift operator is mentioned explicitly, because both q^{-1} and q appear. Under assumption **A2**, $\mathrm{X}_e(\tau) = \sigma^2$, for $\tau = 0$ and $\mathrm{X}_e(\tau) = 0$, for $\tau \neq 0$. By definition, $K(q^{-1}, \rho_0)$ and $K(q, \rho_0)$ are stable. $H_{\tilde{y}}(q)$, $H_{\tilde{y}}(q^{-1})$ and $\beta(q^{-1})$ are also stable, therefore

$$\lim_{N_p \to \infty} \frac{1}{N_p} \sum_{t=1}^{N_p} \beta\tilde{y}_c(t)K(\rho_0)\tilde{y}_c^T(t-\tau) \to 0, |\tau| \to \infty, \quad \text{w.p.1}.$$

Consequently, $\lim_{N_p \to \infty} \hat{q} \to 0$, w.p.1.

Convergence of $\lim_{N_p \to \infty} \hat{R}$ can be shown using similar reasoning and is omitted here. Validity of (5.24) follows from applying the proof above to the results of [73], i.e. asymptotically the results of [73] hold.

A.6 Proof of Proposition 5.1

$K(\rho)$ is linear and uniformly stable on $\mathcal{D}_K$ and the data set satisfies condition D1 of [54], p. 249.

Define $J'_m(\rho)$ and $J''_m(\rho)$ as the first and second derivative with respect to ρ of $J_m(\rho)$ defined in (5.43). Using (5.43) and (5.44), the derivatives of $J_m(\rho)$ can be written as

$$\begin{aligned} J'_m(\rho) &= -\frac{1}{N_p}\sum_{t=1}^{N_p}\phi_\theta(t)(s(t)-\phi_\theta^T(t)\rho) \\ J''_m(\rho) &= \frac{1}{N_p}\sum_{t=1}^{N_p}\phi_\theta(t)\phi_\theta^T(t). \end{aligned}$$

According to [54] theorem 9.1, if the estimate $\hat{\rho}_\theta$ is consistent, if $\lim_{N\to\infty} E\{J''_m(\rho_0)\}$ is positive definite, and if

$$\begin{aligned} \lim_{N\to\infty}\sqrt{N}E\Bigg\{\frac{1}{N_p}\sum_{t=1}^{N_p}\big[\phi_\theta(t)(s(t)-\phi_\theta^T(t)\rho_0) \\ -\lim_{N\to\infty}\frac{1}{N_p}\sum_{t=1}^{N_p}E\{\phi_\theta(t)(s(t)-\phi_\theta^T(t)\rho_0))\}\big]\Bigg\}=0, \end{aligned} \quad \text{(A.11)}$$

then

$$\sqrt{N}(\hat{\rho}_\theta-\rho_0)\in AsN(0,P_m),$$

with

$$P_m=[\lim_{N\to\infty}E\{J''_m(\rho_0)\}]^{-1}Q[\lim_{N\to\infty}E\{J''_m(\rho_0)\}]^{-1},$$

where Q is defined as

$$Q=\lim_{N\to\infty}N\cdot E\{[J'_m(\rho_0)][J'_m(\rho_0)]^T\}.$$

The estimate $\hat{\rho}_\theta$ is consistent according to Theorem 5.2.

It follows from (5.48) that $\lim_{N\to\infty}E\{J''_m(\rho_0)\}=R_0>0$. Condition (A.11) remains to be verified.

$$\lim_{N\to\infty}\sqrt{N}E\Bigg\{\frac{1}{N_p}\sum_{t=1}^{N_p}\big[\phi_\theta(t)(s(t)-\phi_\theta^T(t)\rho_0) - \lim_{N\to\infty}\frac{1}{N_p}\sum_{t=1}^{N_p}E\{\phi_\theta(t)(s(t)-\phi_\theta^T(t)\rho_0))\}\big]\Bigg\}$$
$$= \lim_{N\to\infty}\sqrt{N}E\Bigg\{\frac{1}{N_p}\sum_{t=1}^{N_p}\phi_\theta(t)(s(t)-\phi_\theta^T(t)\rho_0)\Bigg\} \tag{A.12}$$

Equality follows since the second term in (A.11) is zero by definition, that is $\lim_{N\to\infty} J'_m(\rho_0) = 0$. The limit can then be written as:

$$\lim_{N\to\infty}\sqrt{N}E\Bigg\{\frac{1}{N_p}\sum_{t=1}^{N_p}\phi_\theta(t)(s(t)-\phi_\theta^T(t)\rho_0)\Bigg\}$$
$$= \lim_{N\to\infty}\sqrt{N}E\Bigg\{\frac{1}{N_p}\sum_{t=1}^{N_p}(\phi_0(t)+\tilde{\phi}_\theta(t))\left(s(t)-(\phi_0(t)+\tilde{\phi}_\theta(t))^T\rho_0\right)\Bigg\}$$
$$= \lim_{N\to\infty}\sqrt{N}E\Bigg\{\frac{1}{N_p}\sum_{t=1}^{N_p}\tilde{\phi}_\theta(t)\tilde{\phi}_\theta^T(t)\rho_0\Bigg\}$$
$$= \lim_{n_p\to\infty}\sqrt{N_p n_p}E\Bigg\{\frac{1}{N_p}\sum_{t=1}^{N_p}\beta(1-M)^2 v_m(t)K(\rho_0)(1-M)^2 v_m(t)\Bigg\}. \tag{A.13}$$

According to (5.37) and **A9**, $v_m(t)$ is a white noise signal with variance σ^2/n_p and it follows that

$$\lim_{n_p\to\infty}\sqrt{N_p n_p}E\Bigg\{\frac{1}{N_p}\sum_{t=1}^{N_p}\beta(1-M)^2 v_m(t)K(\rho_0)(1-M)^2 v_m(t)\Bigg\}$$
$$= \lim_{n_p\to\infty}\frac{\sqrt{N_p n_p}}{n_p}R_{v_\beta}(0) = 0,$$

where $R_{v_\beta}(0)$ is the cross-correlation between $\beta(1-M)^2 v(t)$ and $K(\rho_0)(1-M)^2 v(t)$ at lag $\tau = 0$. Convergence follows since this value is bounded as $R_{v_\beta}(0) < C\sigma^2$, where C is a constant.

The asymptotic variance of the estimate is thus given by P_m. Using some of the simplifications introduced in (A.13), Q is given by

$$
\begin{aligned}
Q &= \lim_{N\to\infty} N \cdot E\Bigg\{ \left[\frac{1}{N_p}\sum_{t=1}^{N_p}(\phi_0(t)+\tilde{\phi}_\theta(t))\tilde{\phi}_\theta^T(t)\rho_0\right] \\
&\qquad\qquad \left[\frac{1}{N_p}\sum_{s=1}^{N_p}(\phi_0(s)+\tilde{\phi}_\theta(s))\tilde{\phi}_\theta^T(s)\rho_0\right]^T\Bigg\} \\
&= \lim_{N\to\infty} N \cdot E\left\{ \left[\frac{1}{N_p}\sum_{t=1}^{N_p}\phi_0(t)\tilde{\phi}_\theta^T(t)\rho_0\right]\left[\frac{1}{N_p}\sum_{s=1}^{N_p}\phi_0(s)\tilde{\phi}_\theta^T(s)\rho_0\right]^T\right\} \\
&= \lim_{N\to\infty} N \cdot E\left\{ \left[\frac{1}{N_p}\sum_{t=1}^{N_p}H^*\phi_0(t)v_m(t)\right]\left[\frac{1}{N_p}\sum_{s=1}^{N_p}H^*\phi_0(s)v_m(s)\right]^T\right\} \\
&= \lim_{n_p\to\infty} \frac{N_p n_p}{N_p^2}\sum_{t=1}^{N_p}H^*\phi_0(t)E\{v_m(t)v_m(t)\}H^*\phi_0^T(t) \\
&= \lim_{n_p\to\infty} \frac{N_p n_p}{N_p^2}\frac{N_p\sigma^2}{n_p}C_2 = \sigma^2 C_2
\end{aligned}
$$

C_2 is defined in (5.6), H^* in (5.3). The first equality follows from condition (A.11), which implies that the other terms of Q tend to zero as $n_p \to \infty$. The fourth equality follows from the variance of the white noise signal $v_m(t)$, which is given by σ^2/n_p. P_m is thus given by $P_m = \sigma^2 R_0^{-1} C_2 R_0^{-1}$.

References

[1] P. Albertos and A. Sala, editors. *Iterative Identification and Control: Advances in Theory and Applications,*. Springer-Verlag, Berlin, 2002.

[2] B. D. O. Anderson. Adaptive systems, lack of persistency of excitation and bursting phenomena. *Automatica*, 21(3):247 – 258, 1985.

[3] B. D. O. Anderson. Windsurfing approach to iterative control design. In P. Albertos and A. Sala, editors, *Iterative Identification and Control: Advances in Theory and Applications,*. Springer-Verlag, Berlin, 2002.

[4] B. D. O. Anderson and A. Dehghani. Challenges of adaptive control - past, permanent and future. *Annual Reviews in Control*, 32(2):123 – 135, 2008.

[5] B. D. O. Anderson and Y. Liu. Controller reduction: Concepts and approaches. *IEEE Transactions on Automatic Control*, 34(8):802–812, August 1989.

[6] K. J. Åström and B. Wittenmark. *Adaptive Control*. Addison-Wesley, 1989.

[7] R. R. Bitmead. Iterative optimal control design. In P. Albertos and A. Sala, editors, *Iterative Identification and Control: Advances in Theory and Applications,*. Springer-Verlag, Berlin, 2002.

[8] S. P. Boyd, L. El Ghaoui, E. Feron, and V. Balakrishnan. *Linear Matrix Inequalities in System and Control Theory*. SIAM, 1994.

[9] M. C. Campi, A. Lecchini, and S. M. Savaresi. Virtual reference feedback tuning: A direct method for the design of feedback controllers. *Automatica*, 38:1337–1346, 2002.

[10] M. C. Campi, A. Lecchini, and S. M. Savaresi. Tuning of the controller for a benchmark active suspension system through VRFT. *European Journal of Control*, 9(1):66–76, January 2003.

[11] M. C. Campi and S. M. Savaresi. Direct nonlinear control design: The virtual reference feedback tuning (VRFT) approach. *IEEE Transactions on Automatic Control*, 51(1):14–27, 2006.

[12] M.C. Campi, S. Ko, and E. Weyer. Non-asymptotic confidence regions for model parameters in the presence of unmodelled dynamics. *Automatica*, 45(10):2175 – 2186, 2009.

[13] B. Chachuat. *Nonlinear and Dynamic Optimization: From Theory to Practice*. Lecture notes, url: http://lawww.epfl.ch/page4234.html, 2007.

[14] D. de Vries. *Identification of model uncertainty for control design*. PhD thesis, Delft University of Technology, Delft, The Netherlands, 1994.

[15] A. Dehghani, B. D. O. Anderson, and A. Lanzon. Unfalsified adaptive control: A new controller implementation and some remarks. In *European Control Conference*, pages 709–716, July 2007.

[16] A. Dehghani, A. Lecchini-Visintini, A. Lanzon, and B. Anderson. Validating controllers for internal stability utilizing closed-loop data. *Automatic Control, IEEE Transactions on*, 54(11):2719–2725, Nov. 2009.

[17] A.J. den Dekker, X. Bombois, and P.M.J. Van den Hof. Finite sample confidence regions for parameters in prediction error identification using output error models. In *17th IFAC World Congress*, pages 5024–5029, Seoul, Korea, July 2008.

[18] A.J. den Hamer, M. Steinbuch, S. Weiland, and G.Z. Angelis. Non-parametric h_∞ control synthesis with suboptimal controller sets. In *17th IFAC World Congress*, pages 6319–6324, Seoul, Korea, July 2008.

[19] U. Forssell and L. Ljung. Closed-loop identification revisited. *Automatica*, 35(7):1215 – 1241, 1999.

[20] M. Gevers. Identification for control: from the early achievements to the revival of experiment design. In *44th IEEE Con-*

ference on Decision and Control and European Control Conference, Seville, Spain, December 2005.

[21] M. Gevers, X. Bombois, B. Codrons, G. Scorletti, and B. D. O. Anderson. Model validation for control and controller validation in a prediction error identification framework – Part I: theory. *Automatica*, 39:403–415, 2003.

[22] R. M. Gray. Toeplitz and circulant matrices: A review. *Foundations and Trends in Communications and Information Theory*, 2(3):155–239, 2006.

[23] G. O. Guardabassi and S. M. Savaresi. Virtual reference direct design method: an off-line approach to data-based control system design. *IEEE Transactions on Automatic Control*, 45(5):954–959, 2000.

[24] R. Hildebrand, A. Lecchini, G. Solari, and M. Gevers. Prefiltering in iterative feedback tuning: optimization of the prefilter for accuracy. *IEEE Transactions on Automatic Control*, 49(10):1801–1806, 2004.

[25] R. Hildebrand, A. Lecchini, G. Solari, and M. Gevers. Asymptotic accuracy of iterative feedback tuning. *IEEE Transactions on Automatic Control*, 50(8):1182–1185, 2005.

[26] H. Hjalmarsson. Control of nonlinear systems using iterative feedback tuning. In *IEEE American Control Conference*, pages 2083–2087, Jun 1998.

[27] H. Hjalmarsson. Efficient tuning of linear multivariable controllers using iterative feedback tuning. *International Journal of Adaptive Control and Signal Processing*, 13(8):553–572, 1999.

[28] H. Hjalmarsson. Iterative feedback tuning - an overview. *International Journal of Adaptive Control and Signal Processing*, 16:373–395, 2002.

[29] H. Hjalmarsson. From experiment design to closed-loop control. *Automatica*, 41(3):393–438, 2005.

[30] H. Hjalmarsson, S. Gunnarsson, and M. Gevers. A convergent iterative restricted complexity control design scheme. In *33rd IEEE Conference on Decision and Control*, volume 2, pages 1735–1740, December 1994.

[31] H. Hjalmarsson and K. Lindqvist. Identification for control: l_2 and l_∞ methods. In *40th IEEE Conference on Decision and Control*, volume 3, pages 2701–2706, 2001.

[32] H. Hjalmarsson and B. Ninness. Least-squares estimation of a class of frequency functions: A finite sample variance expression. *Automatica*, 42(4):589 – 600, 2006.

[33] H. Hjalmarsson and S. M. Veres. Robust loopshaping using iterative feedback tuning. In *European Control Conference*, pages 2046–2051, Porto, Portugal, September 2001.

[34] M. Holzel, S. Lacy, and V. Babuska. Direct optimal controller identification for uncertain systems using frequency response function data. In *Proceedings of the 15th IFAC Symposium on System Identification*, pages 1056–1061, Saint-Malo, France, July 2009.

[35] J. K. Huusom, N. K. Poulsen, and S. B. Jørgensen. Improving convergence of iterative feedback tuning. *Journal of Process Control*, 19(4):570 – 578, 2009.

[36] L. C. Kammer. Stability assessment for cautious iterative controller tuning. *Automatica*, 41(10):1829 – 1834, 2005.

[37] L. C. Kammer, R. R. Bitmead, and P. L. Bartlett. Direct iterative tuning via spectral analysis. *Automatica*, 36(9):1301–1307, 2000.

[38] A. Karimi, M. Butcher, and R. Longchamp. Model-free precompensator tuning based on the correlation approach. *IEEE Transactions on Control Systems Technology*, 16(5):1013–1020, September 2008.

[39] A. Karimi, G. Galdos, and R. Longchamp. Robust fixed-order H_∞ controller design for spectral models by convex optimization. In *47th IEEE Conference on Decision and Control*, Cancun, Mexico, 2008.

[40] A. Karimi, M. Kunze, and R. Longchamp. Robust controller design by linear programming with application to a double-axis positioning system. *Control Engineering Practice*, 15(2):197–208, February 2007.

[41] A. Karimi, L. Mišković, and D. Bonvin. Iterative correlation-based controller tuning - Frequency domain analysis. In *41st IEEE Conference on Decision and Control*, Las Vegas, USA, December 2002.

[42] A. Karimi, L. Mišković, and D. Bonvin. Iterative correlation-based controller tuning: Application to a magnetic suspension system. *Control Engineering Practice*, 11(9):1069–1087, 2003.

[43] A. Karimi, L. Mišković, and D. Bonvin. Iterative correlation-based controller tuning. *International Journal of Adaptive Control and Signal Processing*, 18(8):645–664, 2004.

[44] A. Karimi, K. van Heusden, and D. Bonvin. Non-iterative data-driven controller tuning using the correlation approach. In *European Control Conference*, pages 5189–5195, Kos, Greece, 2007.

[45] S.M. Kay. *Fundamentals of Statistical Signal Processing: Estimation Theory*. Prentice-Hall, New Jersey, 1993.

[46] D. Kostić, B. De Jager, and M. Steinbuch. Data-based design of high-performance motion controllers. In *IEEE American Control Conference*, volume 1, pages 722–727, 2004.

[47] R. L. Kosut. Uncertainty model unfalsification for robust adaptive control. *Annual Reviews in Control*, 25:65–76, 2001.

[48] I. D. Landau, R. Lozano, and M. M'Saad. *Adaptive Control*. Springer-Verlag, London, 1997.

[49] I. D. Landau, D. Rey, A. Karimi, A. Voda, and A. Franco. A flexible transmission system as a benchmark for robust digital control. *European Journal of Control*, 1(2):77–96, 1995.

[50] A. Lanzon, A. Lecchini, A. Dehghani, and B. D. O. Anderson. Checking if controllers are stabilizing using closed-loop data. In *45th IEEE Conference on Decision and Control*, pages 3660–3665, San Diego, CA, USA, 2006.

[51] A. Lecchini, M. C. Campi, and S. M. Savaresi. Virtual reference feedback tuning for two degree of freedom controllers. *International Journal of Adaptive Control and Signal Processing*, 16:355–371, 2002.

[52] A. Lecchini and M. Gevers. On iterative feedback tuning for non-minimum phase plants. In *41st IEEE Conference on Decision and Control*, pages 4658–4663, 2002.

[53] A. Lecchini, A. Lanzon, and B. D. O. Anderson. A model reference approach to safe controller changes in iterative identification and control. *Automatica*, 42(2):193–203, 2006.

[54] L. Ljung. *System Identification - Theory for the User*. Prentice Hall, NJ, USA, second edition, 1999.

[55] J. Löfberg. Yalmip : A toolbox for modeling and optimization in MATLAB. In *Proceedings of the CACSD Conference*, Taipei, Taiwan, 2004.

[56] I. Markovsky and P. Rapisarda. On the linear quadratic data-driven control. In *European Control Conference*, pages 5313–5318, July 2007.

[57] L. Mišković, A. Karimi, and D. Bonvin. Correlation-based tuning of a restricted-complexity controller for an active suspension system. *European Journal of Control*, 9(1):77–83, January 2003.

[58] L. Mišković, A. Karimi, and D. Bonvin. Iterative controller tuning by minimization of a generalized decorrelation criterion. In *13th IFAC Symposium on System Identification - SYSID 2003*, pages 1177–1182, August 2003.

[59] L. Mišković, A. Karimi, D. Bonvin, and M. Gevers. Correlation-based tuning of decoupling multivariable controllers. *Automatica*, 43(9):1481–1494, 2007.

[60] P.V. Osborn, H.P. Whitaker, and A. Kezer. New developments in the design of model reference adaptive control systems. *Institute of Aeronautical Sevices, Paper 61-39*, 1961.

[61] A. Papoulis. *Probability, Random Variables and Stochastic Processes*. McGraw-Hill, 1965.

[62] J. Park and R. R. Bitmead. Controller certification. *Automatica*, 44(1):167 – 176, 2008.

[63] R. Pintelon and J. Schoukens. *System Identification: A Frequency Domain Approach*. IEEE Press, New York, USA, 2001.

[64] K. Poolla, P. Khargonekar, A. Tikku, J. Krause, and K. Nagpal. A time-domain approach to model validation. *IEEE Transactions on Automatic Control*, 39(5):951–959, May 1994.

[65] F. Previdi, T. Schauer, S.M. Savaresi, and K.J. Hunt. Data-driven control design for neuroprotheses: a virtual reference feedback tuning (VRFT) approach. *Control Systems Technology, IEEE Transactions on*, 12(1):176–182, Jan. 2004.

[66] H. Prochazka, M. Gevers, B.D.O. Anderson, and C. Ferrera. Iterative feedback tuning for robust controller design and optimization. In *44th IEEE Conference on Decision and Control and European Control Conference*, pages 3602–3607, 2005.

[67] D. E. Rivera and M. Morari. Control-relevant model reduction problems for SISO H_2, H_∞, and μ-controller synthesis. *International Journal of Control*, 46(2):505 – 527, 1987.

[68] D. E. Rivera and M. Morari. Low-order SISO controller tuning methods for the H_2, H_∞, and μ objective functions. *Automatica*, 26(2):361–369, 1990.

[69] R.T. Rockafellar. *Convex Analysis*. Princeton University Press, Princeton, N. J., USA, 1970.

[70] M. G. Safonov and T. C. Tsao. The unfalsified control concept and learning. *IEEE Transactions on Automatic Control*, 42(6), 1997.

[71] A. Sala and A. Esparza. Extensions to "virtual reference feedback tuning: A direct method for the design of feedback controllers". *Automatica*, 41(8):1473–1476, 2005.

[72] T. Söderström. Errors-in-variables methods in system identification. In *14th IFAC Symposium on System Identification*, pages 1–19, Newcastle, Australia, 2006.

[73] T. Söderström and M. Hong. Identification of dynamic errors-in-variables systems with periodic data. In *16th IFAC World Congress*, Prague, Czech Republic, 2005.

[74] T. Söderström and P. Stoica. Instrumental variable methods for system identification. In A. V. Balakrishnan and M. Thoma, editors, *Lecture Notes in Control and Information Science*. Springer-Verlag, Berlin, 1983.

[75] T. Söderström and P. Stoica. *System Identification*. Prentice-Hall, U.K., 1989.

[76] H. M. J. R. Soemers. The design of high performance manipulators. In *IEEE/ASME International Conference on Advanced Intelligent Mechatronics, 2001*, volume 1, pages 26–31 vol.1, 2001.

[77] H. Stark and J. W. Woods. *Probability, Random Processes and Estimation Theory for Engineers*. Prentice-Hall, New Jersey, U.S.A., 1986.

[78] J. F. Sturm. Using SeDuMi 1.02, a Matlab toolbox for optimization over symmetric cones. *Optimization Methods and Software*, 11:625–653, 1999.

[79] F. Tjärnström. Variance analysis of l2 model reduction when undermodeling - the output error case. *Automatica*, 39(10):1809–1815, 2003.

[80] F. Tjärnström and L. Ljung. L2 model reduction and variance reduction. *Automatica*, 38(9):1517–1530, 2002.

[81] J. van Helvoort, B. de Jager, and M. Steinbuch. Direct data-driven recursive controller unfalsification with analytic update. *Automatica*, 43(12):2034 – 2046, 2007.

[82] K. van Heusden, A. Karimi, and D. Bonvin. Data-driven estimation of the infinity norm of a dynamical system. In *46th IEEE Conference on Decision and Control*, pages 4889–4894, New Orleans, USA, 2007.

[83] S. M. Veres. Convergence of control performance by unfalsification of models - levels of confidence. *International Journal of Adaptive Control and Signal Processing*, 15(5):471–502, 2001.

[84] S. Zacks. *The Theory of Statistical Inference*. John Wiley, New York, 1979.

[85] K. Zhou. *Essentials of Robust Control*. Prentice Hall, New Jersey, 1998.

[86] K. Zhou, J.C. Doyle, and K. Glover. *Robust and optimal control*. Prentice Hall, New Jersey, 1996.

Curriculum Vitae

Personal details

Family name	van Heusden
First name	Klaske
Email	KlaskevanHeusden@yahoo.com
Date of birth	30-12-1979
Nationality	Dutch
Gender	Female

Education

Oct 2005 - Now	PhD, Laboratoire d'Automatique *EPFL, Lausanne, CH*
1998 - Aug 2004	MSc, Mechanical Engineering *Delft University of Technology, NL*
1997 - 1998	High school exchange program *Hillcrest High, Hamilton, New Zealand*
1991 - 1997	VWO (High School) *Ommelander college, Appingedam, NL*

Internships and work experience

Oct 2005 - Now	Assistant, Laboratoire d'Automatique *EPFL, Lausanne, CH*
Sept 2004 - Dec 2004	Researcher, Department of physiology *AMC, University of Amsterdam, NL*
Apr 2003 - Aug 2004	MSc Thesis, Department of physiology *AMC, University of Amsterdam, NL*

Publications

Journal articles

1. K. van Heusden, A. Karimi and T. Söderström. "On identification methods for direct data-driven controller tuning." *Submitted to International Journal of Adaptive Control and Signal Processing.*
2. K. van Heusden, A. Karimi and D. Bonvin. "Data-driven model reference control with guaranteed stability." *Submitted to International Journal of Adaptive Control and Signal Processing.*
3. K. van Heusden, J. Gisolf, W.J. Stok, S. Dijkstra and J.M. Karemaker. "Mathematical modeling of gravitational effects on the circulation: importance of the time course of venous pooling and blood volume changes in the lungs." *Am J Physiol Heart Circ Physiol.* 2006 Nov;291(5):H2152-6
4. J. Gisolf, J.J. van Lieshout, K. van Heusden, F. Pott, W.J. Stok and J.M Karemaker. "Human cerebral venous outflow pathway depends on posture and central venous pressure." *J Physiol.* 2004 Oct 1;560(Pt 1):317-27.

Conference papers

1. K. van Heusden, A. Karimi, D. Bonvin, A.J. den Hamer and M. Steinbuch. "Non-iterative data-driven controller tuning with guaranteed stability: Application to direct-drive pick-and-place robot." *Submitted to IEEE Conference on Control Applications*, Yokohama, Japan, 2010.
2. K. van Heusden, A. Karimi and D. Bonvin. "Data-driven controller validation." *In 15th IFAC Symposium on System Identification*, St Malo, France, 2009.
3. K. van Heusden, A. Karimi and D. Bonvin. "Data-driven controller tuning with integrated stability constraint." *In 47th IEEE Conference on Decision and Control*, Cancun, Mexico, 2008.
4. K. Van Heusden, A. Karimi and D. Bonvin. "Data-Driven Estimation of the Infinity Norm of a Dynamical System." *In 46th IEEE Conference on Decision and Control*, New Orleans, LA, 2007.

5. A. Karimi, K. van Heusden and D. Bonvin. "Noniterative Data-driven Controller Tuning Using the Correlation Approach." *In European Control Conference*, Kos, Greece, 2007.